Immunoglobulin-based strategies for half-life extension of recombinant proteins

Immunglobulin-basierte Strategien zur Verlängerung der Halbwertszeit rekombinanter Proteine

Von der Fakultät Energie-, Verfahrens- und Biotechnik der Universität Stuttgart zur Erlangung der Würde eines Doktors der Naturwissenschaften (Dr. rer. nat.) genehmigte Abhandlung

Vorgelegt von

Felix Unverdorben

aus Immenstadt

Hauptberichter: Prof. Dr. Roland Kontermann

Mitberichter: Prof. Dr. Klaus Pfizenmaier

Tag der mündlichen Prüfung:

06. August 2015

Institut für Zellbiologie und Immunologie, Universität Stuttgart

2015

Summary

With numerous small recombinant proteins being developed for treatment of various diseases, half-life extension strategies are becoming increasingly vital for the creation of long lasting and efficient biotherapeutics. Because of their small size, these proteins are rapidly cleared from plasma circulation and lose a lot of their potential as therapeutic. Using immunoglobulin-binding domains (IgBD), in particular domain C3 from *Streptococcus* protein G (SpG_{C3}), can substantially increase the half-life by forming transient complexes with endogenous IgG molecules. This complex formation needs to occur at neutral pH to prevent rapid renal clearance, but also under acidic conditions, facilitating the salvage from lysosomal degradation via the neonatal Fc receptor (FcRn). In order to enable FcRn recycling, the major binding site of SpG_{C3} to the IgG-Fc part was eliminated, since it is overlapping with the FcRn binding site, generating the C_H1 specific domain SpG_{C3Fab}. Affinity maturation towards the Fab fragment resulted in domains SpG_{C3Fab}RR and SpG_{C3Fab}RR,E15V showing significantly increased terminal half-lives as scDb-IgBD fusion proteins.

Since the IgBDs originate from bacterial proteins, they might provoke immunogenic reactions and the production of anti-drug antibodies. For deimmunization, possible T-cell epitopes were identified by sequence and structure-based analysis and eliminated by combination of single amino acid substitutions. This resulted in deimmunized IgBDs that were able to strongly increase the terminal half-life as scDb fusion proteins.

The application of SpG_{C3Fab}RR to recombinant human erythropoietin (huEPO) resulted in a roughly 5-fold increased terminal half-life compared to the unmodified huEPO that also translated into increased hemoglobin concentration after one single intravenous injection.

Furthermore, a comparative study of various Fc fusion proteins revealed that a multitude of factors is jointly responsible for the long half-life of full-length IgG molecules. Although possessing an identical huIgG1 Fc part and affinity to the moFcRn, neither an scFv-Fc nor an scDb-Fc or a single-chain version of the IgG molecule (scFv-scCLCH1-Fc) could reach the pharmacokinetic properties of the IgG molecule, not fully explainable by factors like size, isoelectric point and stability.

All in all, the utilization of immunoglobulins and FcRn-mediated salvage via IgBDs and Fc fusion proteins is a powerful tool for the generation of recombinant fusion proteins with favorable pharmacokinetic properties.

Zusammenfassung

Angesichts der Entwicklung einer Vielzahl kleiner rekombinanter Proteine, die für die Behandlung verschiedenster Krankheiten eingesetzt werden, nimmt das Interesse an Strategien zur Halbwertszeitverlängerung zu, um lang zirkulierende und effiziente Biotherapeutika zu entwerfen. Aufgrund ihrer geringen Größe werden diese Proteine schnell aus dem Blutkreislauf eliminiert und verlieren einen Großteil ihrer therapeutischen Wirksamkeit. Die Verwendung von Immunglobulin-bindenden Domänen (IgBD), insbesondere Domäne C3 von Protein G aus *Streptococcus* (SpG_{C3}), führt zu einer deutlichen Erhöhung der Halbwertszeit rekombinanter Proteine, indem sie transiente Komplexe mit körpereigenen IgG Molekülen bildet. Diese Komplexbildung muss sowohl bei neutralem als auch saurem pH im Endosom auftreten und kann eine schnelle Ausscheidung in der Niere sowie den lysosomalen Abbau durch Recycling über den neonatalen Fc Rezeptor (FcRn) verhindern. Da die Bindestelle von SpG_{C3} und FcRn am IgG-Fc Teil überlappen, wurde diese bei der IgBD beseitigt und die C_H1 spezifische Domäne SpG_{C3Fab} generiert, um besseres FcRn Recycling zu ermöglichen. Die Domänen SpG_{C3Fab}RR und SpG_{C3Fab}RR,E15V, die durch C_H1-gerichtete Affinitätsreifungen entstanden, zeigten signifikant erhöhte terminale Halbwertszeiten als scDb-IgBD Fusionsproteine.

Da die IgBDs aus bakteriellen Proteinen hervorgingen, ist das Einsetzen einer Immunantwort und die damit verbundene Produktion von Antikörpern gegen das Medikament möglich. Für eine Deimmunisierung wurden daher mögliche T-Zell Epitope mittels sequenz- und strukturbasierter Untersuchung identifiziert und durch eine Kombination einzelner Aminosäureaustausche beseitigt. Die so entstandenen deimmunisierten IgBDs konnten die terminale Halbwertszeit als scDb Fusionsproteine deutlich steigern.

Die Fusion von SpG_{C3Fab}RR mit rekombinantem humanem Erythropoietin (huEPO) erhöhte dessen Halbwertszeit ungefähr 5-fach, verglichen mit nicht modifiziertem huEPO. Diese verbesserte Pharmakokinetik spiegelte sich auch in einer erhöhten Hämoglobin Konzentration nach einmaliger intravenöser Gabe wieder.

Außerdem zeigte eine vergleichende Studie verschiedener Fc Fusionsproteine, dass eine Vielzahl von Faktoren für die lange Halbwertszeit von ganzen IgG Molekülen mitverantwortlich ist. Obwohl alle Fusionsproteine einen identischen huIgG1 Fc Teil mit gleicher Affinität zum FcRn besaßen, konnten weder ein scFv-Fc, noch ein scDb-Fc oder eine einzelkettige Version des IgG Moleküls (scFv-scCLCH1-Fc) die

pharmakokinetischen Eigenschaften des IgG Moleküls erreichen. Faktoren wie Größe, isoelektischer Punkt und Stabilität sind nicht in der Lage dies hinreichend zu erklären.

Zusammenfassend kann gesagt werden, dass die Verwendung von Immunglobulinen und FcRn-abhängigem Recycling durch IgBDs und Fc Fusionsproteine rekombinante Fusionsproteine mit vorteilhaften pharmakokinetischen Eigenschaften schaffen kann.

Table of contents

Summary **3**

Zusammenfassung **4**

Table of contents **6**

Abbreviations **9**

1 Introduction **10**

1.1 Small therapeutic proteins with poor pharmacokinetics **10**

1.2 Strategies for half-life extension **12**

1.3 Immunoglobulin-binding domains **15**

1.4 Deimmunization **17**

1.5 Recombinant human erythropoietin **20**

1.6 IgG derivates **22**

1.7 Goal of this study **24**

2 Materials and methods **26**

2.1 Materials **26**

2.1.1 Instruments 26

2.1.2 Implements 26

2.1.3 Chemicals 27

2.1.4 Bacterial culture and phage display 27

2.1.5 Cell culture 27

2.1.6 Solutions 28

2.1.7 Enzymes 28

2.1.8 Antibodies and immobilized proteins 29

2.1.9 Kits and markers 29

2.1.10 Bacteria and phages 29

2.1.11 Cell lines 30

2.1.12 Plasmids 30

2.1.13 Primers 30

2.1.14 Programs and online tools 32

2.2 Cloning **32**

2.2.1 Cloning of antibody fragment-IgBD fusion proteins 32

2.2.2 Cloning of huEPO-IgBD fusion proteins 33

2.2.3 Cloning strategy for phage display 33

2.2.4 Cloning of Fc fusion proteins 33

2.2.5 Polymerase chain reaction 34

2.2.6 Error prone PCR 34

2.2.7 DNA electrophoresis and gel extraction ... 35
2.2.8 Restriction digestion ... 35
2.2.9 Ligation and heat shock transformation ... 35
2.2.10 Plasmid DNA isolation and sequence analysis ... 36
2.3 Phage display ... 36
2.3.1 Preparation of electrocompetent cells ... 36
2.3.2 Ethanol precipitation of DNA ... 36
2.3.3 Electroporation ... 37
2.3.4 Phage rescue ... 37
2.3.5 Immunotube selection ... 37
2.3.6 Selection with biotinylated antigen ... 38
2.4 Cell culture and transfection ... 38
2.5 Expression and purification of recombinant proteins ... 39
2.5.1 Periplasmic protein expression in *E.coli* TG1 ... 39
2.5.2 Protein expression in mammalian cells ... 39
2.5.3 Immobilized metal affinity chromatography ... 40
2.5.4 Protein A chromatography ... 40
2.6 Biochemical characterization ... 40
2.6.1 Protein concentration ... 40
2.6.2 SDS-PAGE ... 41
2.6.3 Deglycosylation of proteins ... 41
2.6.4 Size exclusion chromatography ... 41
2.6.5 Thermal stability ... 42
2.7 Quartz crystal microbalance ... 42
2.8 Enzyme-linked immunosorbent assay ... 43
2.9 Flow cytometry ... 43
2.9.1 Flow cytometry ... 43
2.9.2 Purification of peripheral blood mononuclear cells ... 44
2.10 Serum stability ... 44
2.11 Interleukin release ... 44
2.12 EPO dependent proliferation ... 45
2.13 Pharmacokinetics ... 45
2.14 Pharmacodynamics ... 46
2.15 Statistical analysis ... 46

3 Results ... 47
3.1 New domains from *Streptococcus* Protein G ... 47
3.1.1 Generation of a Fab and Fc fragment specific IgBD ... 47
3.1.2 *In vitro* characterization of new IgBDs ... 49
3.1.3 *In vivo* characterization of new scDb-IgBDs ... 53
3.2 Affinity maturation of SpG_{C3Fab} ... 54
3.2.1 Phage display selection of affinity maturated SpG_{C3Fab} variants ... 54
3.2.2 *In vitro* characterization of affinity maturated SpG_{C3Fab} mutants ... 57
3.2.3 *In vitro* characterization of scFv-IgBD fusion proteins ... 59
3.2.4 *In vivo* characterization of affinity maturated scFv and scDb-IgBDs ... 60
3.3 Deimmunization of SpG_{C3Fab} ... 63
3.3.1 Identification and elimination of possible T-cell epitopes ... 63
3.3.2 Characterization of deimmunized IgBD variants *in vitro* ... 65
3.3.3 Pharmacokinetic behavior of deimmunized scDb-IgBD fusion proteins ... 69
3.4 Half-life extension of recombinant human erythropoietin ... 71
3.4.1 Characterization of huEPO-IgBD fusion proteins ... 71
3.4.2 Pharmacokinetics of huEPO-IgBD fusion proteins ... 73
3.4.3 Pharmacodynamic study with huEPO-IgBDs ... 74
3.5 Pharmacokinetic properties of Fc fusion proteins ... 76
3.5.1 Characterization of various Fc fusion proteins ... 76
3.5.2 Stability determination ... 80
3.5.3 Neonatal Fc receptor binding ... 82
3.5.4 Pharmacokinetics of Fc fusion proteins ... 83
4 Discussion ... 85
4.1 Immunoglobulin binding domains ... 85
4.2 Novel immunoglobulin binding domains ... 86
4.3 Affinity maturation towards the C_H1 domain ... 87
4.4 Deimmunization of SpG_{C3Fab} ... 89
4.5 Half-life extension of recombinant human erythropoietin ... 92
4.6 Fc fusion proteins ... 95
4.7 Translation of animal results ... 98
4.8 Conclusion and outlook ... 98
5 Bibliography ... 100
6 Sequences ... 113
Acknowledgements ... 124
Declaration ... 125
Curriculum vitae ... 126

Abbreviations

ABD	Albumin-binding domain
ADA	Anti-drug antibody
ADCC	Antibody dependent cellular cytotoxicity
APC	Antigen presenting cell
AUC	Area under the curve
BiTE	Bispecific T-cell engager
CD	Cluster of differentiation
CDR	Complementarity determining region
CEA	Carcinoembryonic antigen
C_H	Constant region of the heavy chain
C_L	Constant region of the light chain
CTLA-4	Cytotoxic T lymphocyte associated molecule-4
DMSO	Dimethyl sulfoxide
DNA	Desoxyribonucleic acid
dNTP	Desoxy nucleotide triphosphate
EC_{50}	Half maximal effective concentration
EDTA	Ethylendiamtetraacetic acid
ELISA	Enzyme linked immunosorbent assay
EpCAM	Epithelial cell adhesion molecule
EPO	Erythropoietin
Fab	Fragment antigen binding
FAP	Fibroblast activation protein
FACS	Fluorescence activated cell sorting
Fc	Fragment crystallizable
FcRn	Neonatal Fc receptor
FCS	Fetal calf serum
HEK	Human embryonic kidney
His6	Hexahistidyl-tag
HLA	Human leukocyte antigen
HPLC	High pressure liquid chromatography
HRP	Horse radish peroxidase
hu	Human
IFN	Interferon
IgBD	Immunoglobulin-binding domain
IgG	Immunoglobulin G
IL	Interleukin
kcps	Kilo counts per second
kDa	Kilo Dalton
MFI	Mean fluorescence intensity
MHC	Major histocompatibility complex
mo	Mouse
MW	Molecular weight
n.d.	Not determined
NTA	Nitrilotriacetic acid
OD	Optical density
PAA	Polyacrylamide
PBMC	Peripheral blood mononuclear cell
PBS	Phosphate buffered saline
PCR	Polymerase chain reaction
PDB	Protein data bank
PE	Phycoerythrin
pI	Isoelectric point
S_r	Stokes radius
sc	Single-chain
scDb	Single-chain diabody
scFv	Single-chain variable fragment
SDS	Sodium dodecylsulfate
SEC	Size exclusion chromatography
SpA_B	Staphylococcal protein A domain B
SpG_{C3}	Streptococcal protein G domain C3
$t_{1/2\alpha}$	Initial half-life
$t_{1/2\beta}$	Terminal half-life time
TAE	Tris-acetate EDTA
TCR	T-cell receptor
TEMED	Tetramethylethylenediamine
TMB	3,3’,5,5’-Tetramethylbenzidine
TNF	Tumor necrosis factor
v/v	Volume per volume
V_H	Variable part of the heavy chain
V_L	Variable part of the light chain
w/v	Weight per volume
w/w	Weight per weight

1 Introduction

A prognosis for protein-based pharmaceuticals in 2020 projects a worldwide sale of more than $300 billion (Baeuerle and Murry 2014). A huge part thereof will be derived from monoclonal antibodies or other Fc constructs, but growing interest is placed into small recombinant fusion proteins. Although many of these proteins exhibit an extraordinary potential, most suffer from a rapid elimination, which requires frequent applications or even infusions to maintain a therapeutically effective concentration (Enever et al. 2009; Melder et al. 2005; Szlachcic, Zakrzewska, and Otlewski 2011). Therefore, half-life extension strategies gain an increasing interest to improve pharmacokinetic and pharmacodynamic properties.

1.1 Small therapeutic proteins with poor pharmacokinetics

Proteins broadly used for human therapies include hormones, growth factors, chemokines, coagulation factors, antibody fragments and many others (Kontermann 2012) (Table 1-1). The majority of them have a short half-life in common, ranging from several hours down to just a few minutes. In order to maintain a therapeutically effective dose over a prolonged period of time, frequent injections or even infusions are necessary (Kontermann 2011). For instance, the recently approved BiTE molecule Blinatumomab requires repeated continuous infusion with mini-pimps over several weeks (Topp et al. 2015), denoting a high burden for the patients. Differing from IgG molecules and Fc fusion proteins, many of these proteins possess a molecular mass below 50 - 60,000 Dalton and do not interact with the neonatal Fc receptor.

Table 1-1: Half-life of therapeutic proteins

Protein	Indication	M [kDa]	Terminal half-life
Insulin	Diabetes	6	4 – 6 min
Erythropoietin	Anemia	34	2 – 13 h
IFNα	Hepatitis C (and B)	20	2 – 3 h
IFNβ	Multiple sclerosis	23	5 – 10 h
IL-2	Renal cell carcinoma	16	5 – 7 min
Factor VIIa	Hemophilia	50	2 – 3 h
Tissue plasminogen activator	Myocardial infarction	65	2 – 12 min
IgG	Various	150	Days to weeks
TNFR2-Fc	Rheumatoid arthritis	150	3 – 6 d
Fab	Age-related macular degeneration	50	30 min
BiTE	Non-Hodgkin's lymphoma	55	Few hours *

Data adapted from (Kontermann 2012); * from (Baeuerle 2009); M: molecular mass

The single-chain diabody (scDb) and the single-chain fragment variable (scFv) used in this study fit well into this set of small recombinant proteins with a molecular mass of 28 and 53 kDa, respectively. Due to their size and missing salvage from lysosomal degradation via the FcRn, they exhibit terminal half-lives of only 0.6 and 1.3 h, representing good properties to be exploited as model molecules for half-life extension (Hutt et al. 2012).

One of the main elimination routes from the bloodstream is the filtration of small proteins in the glomeruli of the kidney. Luminal fenestrations of about 4 - 5 nm diameter decorated with negatively charged extracellular matrix proteins function as a filter for proteins with a molecular mass below 60 kDa (Haraldsson and Sörensson 2004; Tryggvason and Wartiovaara 2005) (Figure 1-1). Proteins that exhibit hydrodynamic radii above that threshold are less subject to renal clearance and therefore continue to circulate in the blood for a longer period of time. Due to electrostatic repulsion, proteins with negative net charge, like serum albumin, are also retained, although their size would just allow them to pass through the vessel walls (Kontos and Hubbell 2012). Changes in net charge might possibly result in longer half-life, but can also cause lower tissue distribution, and are therefore application dependent measures (Boswell et al. 2010). The second central route of protein elimination is the degradation of endocytosed plasma proteins in the lysosome. In contrast to most other serum proteins, immunoglobulins of the γ class and albumin undergo less lysosomal degradation, since they are salvaged by the neonatal Fc receptor. Via nonspecific fluid phase endocytosis serum proteins are internalized into endosomes that get gradually acidified. Due to conformational changes and the formation of salt bridges with protonated histidine residues upon acidification, IgG molecules can bind to the FcRn via the interface of their C_H2 and C_H3 domains (Martin et al. 2001). On the other side, the interaction of the FcRn with albumin at acidic pH is independent from IgG binding and requires the elaboration of hydrophobic pockets and the stabilization of loops (Chaudhury et al. 2003, 2006; Schmidt et al. 2013). From the acidified endosome FcRn and its bound cargo are sorted into recycling endosomes and further back to the cell surface, where the cargo is released at physiological pH (Lencer and Blumberg 2005; Roopenian and Akilesh 2007; Weflen et al. 2013). FcRn is expressed on the surface of endothelial, epithelial and hematopoietic cells including organs such as skin, muscle, kidney, liver, spleen

and placenta. Although expressing FcRn, liver and spleen are the major sites of IgG catabolism in rodents on a tissue mass-normalized basis, whereas the skin and muscle are actually more important since they comprise a greater percentage of body weight (Yip et al. 2014).

1.2 Strategies for half-life extension

In order to overcome the limitation of a short half-life and low bioavailability, many approaches have been successfully established, focusing on the increase of the hydrodynamic radius. Di- or multimerization of recombinant fusion proteins enlarge the hydrodynamic radius and can therefore prevent rapid renal clearance. Apart from half-life extension, in particular antibody fusion proteins can benefit from higher valency, due to an increased avidity effect (Seifert et al. 2014). One of the most approved methods for half-life elongation is the attachment of highly flexible, hydrophilic polymers via chemical conjugation or genetic fusion. Polyethylene glycol is a synthetic polymer consisting of repeating units of ethylene glycol that are attached to proteins for example via a maleimide group that interacts with the free thiol group of a cysteine or via succinimide to form bonds to primary amines (Kang, Deluca, and Lee 2009). Besides the increase in hydrodynamic radius followed by lower renal clearance and longer half-life, PEGylation can also reduce immunogenicity and increase solubility and stability of the biotherapeutic. Several small recombinant proteins conjugated to PEG chains are used as therapeutic, including IFNα2b, human growth hormone and erythropoietin (Ezan 2013). An alternative to the synthetic PEG is the recombinant addition of a hydrophilic polypeptide chain to the biotherapeutic. Issues of cost and intrinsic heterogeneity of the PEG, as well as possible vacuolation in the renal tubules or the formation of PEG hydrates in the kidney can therefore be avoided (Schellenberger et al. 2009; Schlapschy et al. 2013). Furthermore, chemical conjugation of biodegradable hydroxyethyl starch (HES) as well as the coupling of polysialic acid can prolong the terminal half-life, depending on size and structure (Gregoriadis et al. 2005; Liebner et al. 2014). Likewise, posttranslational modifications leading to additional glycosylation can improve the pharmacokinetic performance, either by adding a glycosylated tail (Stork, Müller, and Kontermann 2007) or by mutating different residues within the sequence of the therapeutic protein, which has been successfully employed to human erythropoietin (Powell and Gurk-Turner 2002).

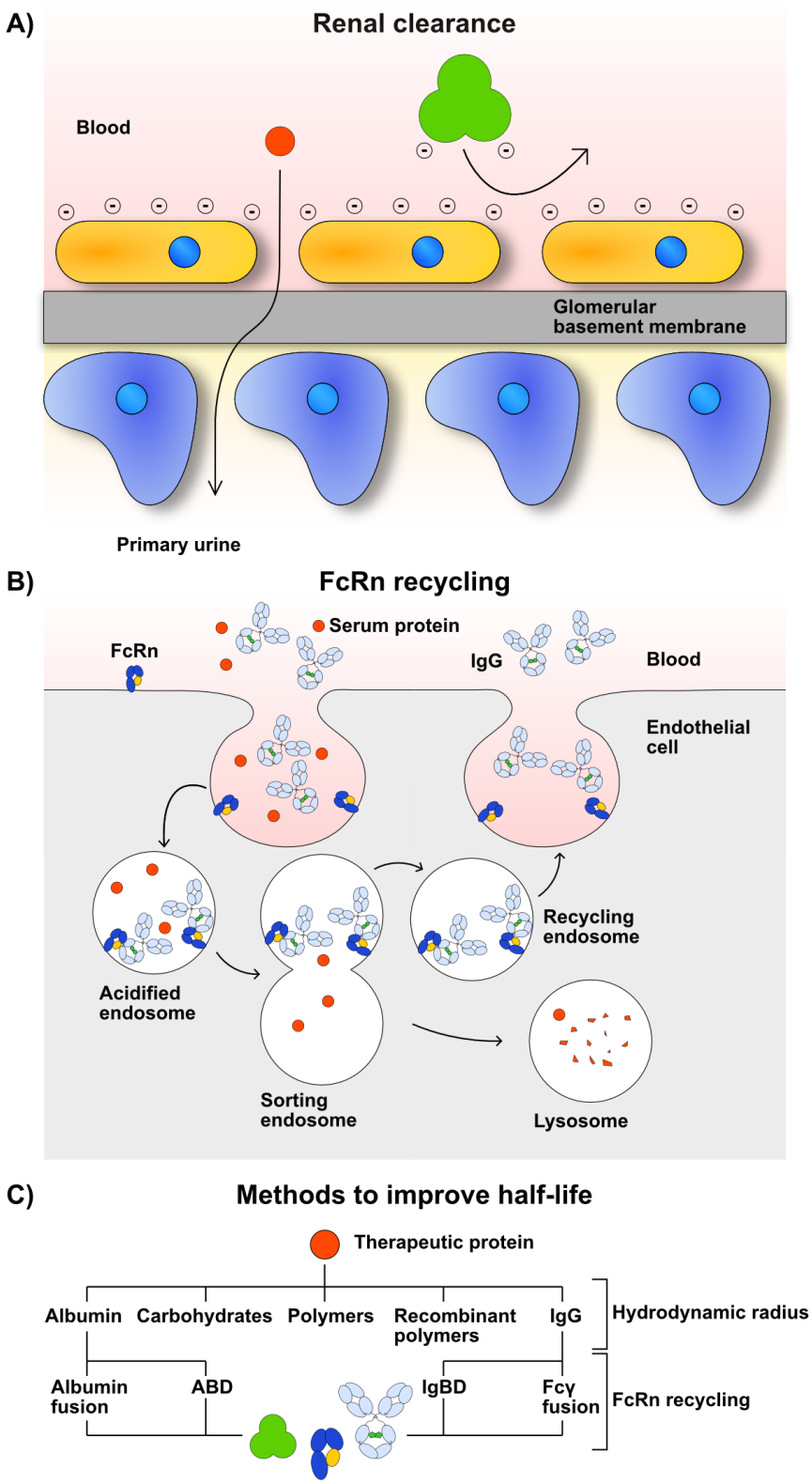

Figure 1-1: Half-life extension

A) Small uncharged serum proteins can float freely across the glomerular filter in the kidney, whereas bigger and negatively charged molecules are retained in the blood. B) FcRn expressing endothelial cells internalize proteins from plasma. Only proteins with affinity towards FcRn at acidic conditions (IgG and albumin) are sorted into a recycling endosome and transferred back to the cell surface, where they are released back to the blood. Other proteins are degraded in the lysosome. C) Half-life extension strategies are based on increased hydrodynamic radius and on FcRn mediated recycling. Various half-life extension modules can be chemically coupled or genetically fused to the therapeutic protein.

A straightforward approach for half-life extension is the fusion of therapeutic proteins with long circulating serum proteins. Since albumin and IgG are the longest lasting serum proteins, much effort has been placed in the understanding of their long half-life as well as the generation of therapeutics (Kontermann 2009). The benefit of the salvage from lysosomal degradation via the FcRn is the key factor for the long half-life and success of recombinant antibodies. However, not only antibodies utilize FcRn-mediated recycling, but also albumin. Thus, fusion of albumin or the Fc part of long-lasting IgGs is a suitable measure to improve pharmacokinetics, since supplementary to the recycling the size of the fusion proteins is augmented above the threshold for renal clearance. Direct fusion to albumin has been applied to a variety of therapeutic proteins, including IFNα2b, insulin, factor VIIa, scFvs and others and strongly increased their pharmacokinetic performance, leading to several biotherapeutics in clinical tests (Sleep, Cameron, and Evans 2013). On the other side, fusion to an Fc part can protect from lysosomal degradation, but also leads to a homodimerization, which can be advantageous in terms of affinity and avidity. However, for distinct applications monomeric interactions are necessary in order to prevent a crosslinked network in plasma or unwanted agonist activity (Berger et al. 2013; Ishino et al. 2013). Many therapeutic fusion proteins comprising an Fc part have been successfully generated, including fusions to TNFR2, CTLA-4, EPO, factor VIII and also recombinant antibody fragments (Kontermann 2009). A further advantage of albumin and IgG molecules is the enhanced permeability and retention effect that occurs in solid tumors and inflamed tissue. These macromolecules accumulate in the modified tissues due to their unique vascular characteristics, resulting in higher concentration and possibly also higher treatment benefit (Matsumura and Maeda 1986).

As an alternative to direct fusion of serum proteins to the therapeutic protein, several strategies have been employed to take advantage of the long half-life of IgG and albumin by transient and reversible binding. Using transient binding instead of fusion or conjugation to increase the hydrodynamic radius of recombinant therapeutics is often advantageous, since dissociation of the molecules facilitates tissue penetration (Stork et al. 2009). The natural function of albumin is that of a carrier protein for various molecules, including long-chain fatty acids. Therefore, the fusion of for example myristic acid to insulin (Insulin detemir) can lead to a substantial increase in

albumin affinity and improvement in pharmacokinetics (Havelund et al. 2004). Likewise, peptides that have been selected to bind to albumin also represent small fusion partners that are able to augment the circulation time of biotherapeutics. Hereby, the affinity of the peptides correlates clearly with the half-life extension properties, meaning that further improvement in affinity should translate into better pharmacokinetics (Nguyen et al. 2006). Besides albumin cargos and peptides, there are naturally occurring albumin binding proteins, namely streptococcal Protein G. Protein G contains three homologous albumin binding domains and in particular the 46 amino acid long domain 3 has been extensively studied for half-life elongation (Andersen et al. 2011; Stork, Müller, and Kontermann 2007). Recycling by the FcRn was investigated in a comparative study with FcRn wild-type and FcRn heavy chain knockout mice demonstrating that the bound ABD does not interfere with FcRn binding of albumin (Stork et al. 2009). Affinity improvement of the ABD towards serum albumin did only result in a moderate augmentation of terminal half-life when fused to an scDb molecule (Hopp et al. 2010). Furthermore, other albumin-binding proteins like nanobodies, single-domain antibodies and alternative scaffolds have been used for half-life extension (Kontermann 2011). Strategies to transiently bind to IgG molecules have also been investigated, revealing an Fc binding peptide that is able to substantially elongate the plasma half-life of a recombinant fusion protein (Sockolosky, Kivimäe, and Szoka 2014). Similar to albumin, there are also other proteins that have been used as a fusion partner in order to target endogenous IgG for a pharmacokinetic purpose. By generation of a bispecific diabody targeting IgG molecules, the terminal half-life experienced a 5-fold increase (Holliger et al. 1997). Analogous to the albumin-binding domain, there are several bacterial proteins that possess affinity towards immunoglobulins. The immunoglobulin-binding domains (IgBD) from Protein A, Protein G and Protein L have demonstrated to enhance the circulation time as fusion partners to an scFv or scDb (Hutt et al. 2012; Unverdorben et al. 2012).

1.3 Immunoglobulin-binding domains

The rationale in using immunoglobulin-binding domains instead of albumin-binding domains is that the terminal half-life of IgG with up to 23 days in humans is even higher than the 19 days of albumin (Kontermann 2009). Even more important is the recycling effect mediated by the neonatal Fc receptor. The efficiency in recycling for IgG is better than for albumin because of a higher FcRn saturation of albumin, owing

to its higher plasma concentration and the 1 to 2 stoichiometry of IgG to the FcRn (Kim et al. 2007). Upon knock-out of the functional FcRn, the terminal half-life of IgG decreases from 95 h to only 19 h, whereas the half-life of albumin is less shortened from 39 h to about 25 h in C57BL/6J mice (Chaudhury et al. 2003). In a recent study the potential of various IgBDs for half-life extension was demonstrated by binding to different parts of IgG molecules (Hutt et al. 2012). These IgBDs are composed of 50 – 60 amino acids and form either 3 α-helix bundles or structures of 4 β-sheets packed against a central α-helix (Tashiro and Montelione 1995). As a fusion partner to an scDb or scFv, the 56 amino acid long domain C3 from *Streptococcus* Protein G (SpG_{C3}) showed the highest potential in enhancing the circulation time (Hutt et al. 2012). SpG_{C3}, comprised of 4 β-sheets and one α-helix, is able to bind to IgG molecules at two distinct binding sites, the interface of C_H2 and C_H3 domain on the Fc part and the C_H1 domain on the Fab arm (Figure 1-2). Its primary binding site is located at the Fc part, overlapping with the interaction site of the FcRn (Burmeister, Huber, and Bjorkman 1994; Sauer-Eriksson et al. 1995). In contrast to other IgBDs, SpG_{C3} was able to maintain binding under physiological and acidic conditions, meaning that stable complexes during circulation in the blood as well as during FcRn recycling can be formed. However, the overlapping binding site of SpG_{C3} and the FcRn might cause interference in an acidified lysosome, possibly hampering the recycling. The terminal half-life of roughly one day that was reached with immunoglobulin-binding domains so far is distant from the pharmacokinetic properties of the endogenous mouse IgG with up to 8 days (Vieira and Rajewsky 1988) indicating the interference with FcRn at the Fc part and leaving space for further improvements.

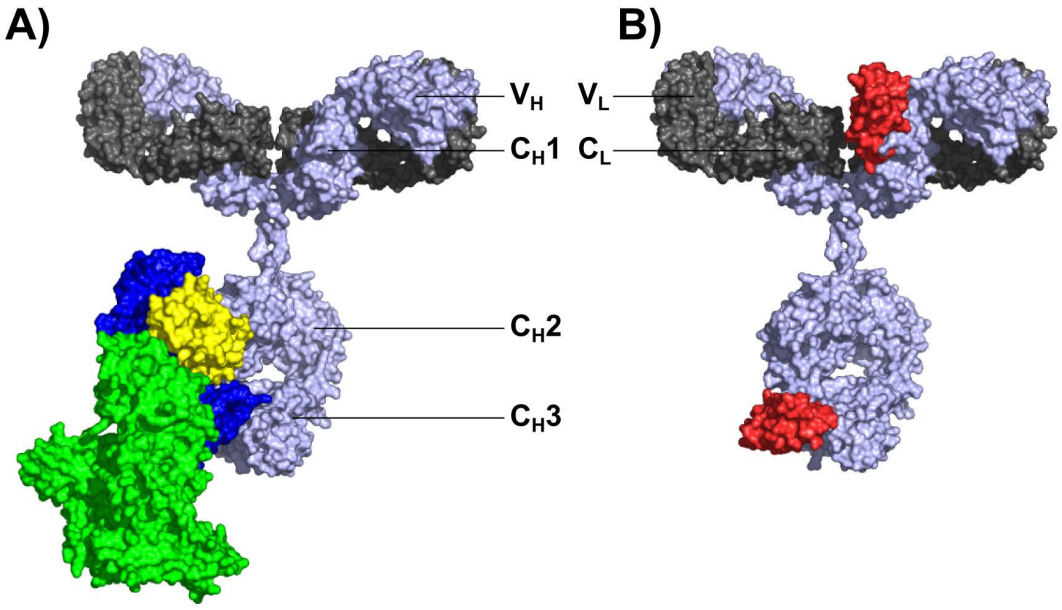

Figure 1-2: Interactions of IgG

A) The binding site of serum albumin towards the neonatal Fc receptor at acidic pH is distinct from the IgG binding site. FcRn binds to an immunoglobulin at the interface of C_H2 and C_H3 on its Fc part. B) SpG_{C3} has two separate binding sites on an IgG molecule, one located on the Fc part at the interface of C_H2 and C_H3, the other on at the C_H1 domain. The binding of FcRn and SpG_{C3} is only depicted on one IgG heavy chain, but since IgGs are symmetrical molecules, similar binding could occur at the second heavy chain. Albumin: green; FcRn heavy chain: blue; β_2-microglobulin: yellow; SpG_{C3}: red; IgG heavy chain: violet; IgG light chain: grey; PDB entries: 4N0U (Oganesyan et al. 2014), 1IGC (Derrick and Wigley 1994), 1FCC (Sauer-Eriksson et al. 1995).

1.4 Deimmunization

Over the last decade the use of biopharmaceuticals has immensely increased, using the high binding specificity of antibodies, the catalytic efficiency and specificity of enzymes or the strong ligand receptor interaction that can lead to proliferation or cell death, depending on the drug. All these macromolecules exhibit a remarkable potential, but even fully human biopharmaceuticals can cause an immune response and the generation of anti-drug antibodies (ADA) (Baker et al. 2010). These ADAs will have severe influence on pharmacokinetic and pharmacodynamic properties of the drug, with effects like increased clearance, neutralization or even allergic responses (Barbosa and Celis 2007; Chirmule, Jawa, and Meibohm 2012). Anti-drug antibodies can form immune complexes triggering rapid elimination of the therapeutic protein. An example for the effect on pharmacokinetic properties was seen during treatment of chronic inflammatory bowel disease with infliximab. In patients developing anti-drug antibodies against infliximab, the clearance was 2.7 times higher and terminal half-life was 34 % lower (Ternant et al. 2008). However, immunogenicity can not only have consequences for the therapeutic, but also to

endogenous proteins, which was seen during an immunologic reaction to a treatment of renal dysfunction with recombinant human erythropoietin. The formation of anti-drug antibodies against the recombinant therapeutic protein resulted in the recognition of endogenous EPO, causing red-cell aplasia in several patients (Casadevall et al. 2002).

The most easily explained mechanism is a ‘vaccine-like’ response to foreign proteins, involving T-cells, B-cells and the innate immune system (De Groot and Scott 2007). In order to induce naïve B-cells to produce antibodies against a therapeutic protein, an activated T-helper cell is necessary. First, the protein is nonspecifically internalized and processed by professional antigen presenting cells (APC), mostly dendritic cells. Upon cleavage of the biotherapeutic, an immunogenic peptide can bind to the antigen-binding groove in the major histocompatibility complex class II molecule (MHCII) and is subsequently transported to the surface of the cell (Figure 1-3). In the lymph nodes, the MHCII with bound peptide is presented to naïve T-cells, together with a costimulatory signal, like CD80 or CD86. When a CD4 positive T-cell is able to recognize the bound peptide and receives the additional costimulatory signal via CD28, it will get fully activated and can activate reactive B-cells to expand, perform immunoglobulin class switch and differentiate (Alberts et al. 2002; Sauerborn et al. 2010). Besides this T-cell dependent mechanism, there are other ways to provoke immunogenicity reaction, like low-level contamination with bacterial DNA, lipids or endotoxins, posttranslational protein modification (alternative glycosylation) or chemical decomposition (e.g. oxidation) that can contribute to immunologic responses (Hermeling et al. 2004). Additionally, aggregation of the therapeutic protein can strongly induce immunogenicity (Prümmer 1997). Therefore, reducing the total number of doses, minimizing aggregates, diminishing T-cell activation and avoiding delivery vehicles that have adjuvant effects are rational strategies for reducing immunogenicity (De Groot and Scott 2007). A subsequent strategy to overcome immunologic reactions is the deimmunization of therapeutic proteins. Varying with the allelic distribution of the human leukocyte antigens (HLA) of class II, only certain peptides will fit into the antigen-binding groove. This is dependent on the amino acids (size, charge, hydrophobicity) of the peptide, whether their side chains fit into the pocket of the HLA molecule and can be presented to the T-cells (Scott and De Groot 2010).

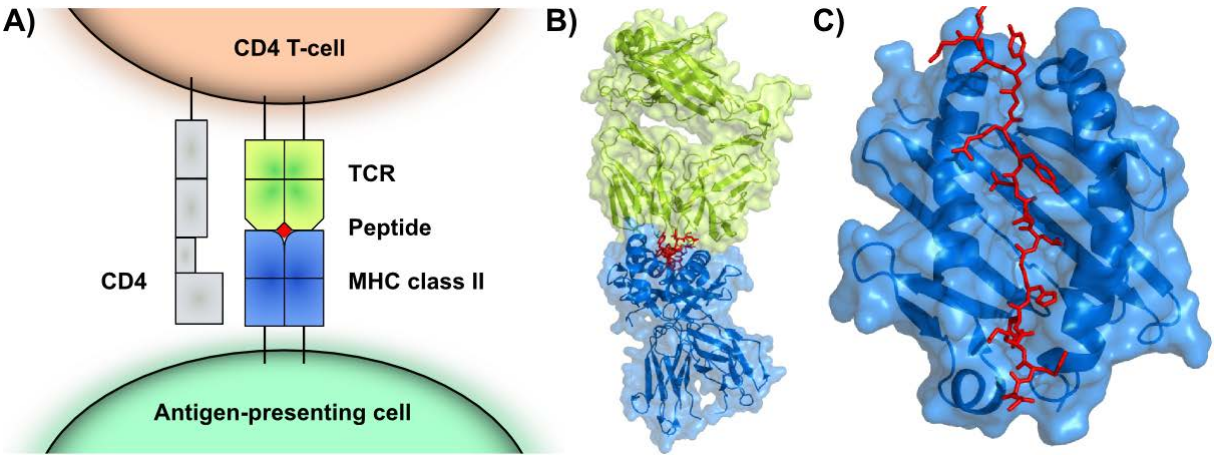

Figure 1-3: First signal in activation of CD4 T-cells by antigen presenting cells

A) CD4 T-cells recognize peptides that are presented via the MHC class II molecules of antigen presenting cells with their T-cell receptor (TCR). B) Model of the TCR (green) recognizing a peptide (red) in the peptide-binding groove of mouse MHC class II molecule (blue). C) Top view to the antigen-binding groove of MHCII molecule with immunodominant hen egg lysozyme 11-27 peptide; PBD entry: 3MBE (Yoshida et al. 2010)

Peptides that bind into the pocket of MHC class II molecules usually range from anywhere between 12 and 25 amino acids. For HLA-DR1 (and probably other HLA-DR molecules), the groove-anchored stretch of peptides is (in most cases) exactly nine amino acids long with anchoring sites specific for the allelic distribution (Rammensee 1995). This nonamer of amino acids that binds specifically to a MHC class II molecule will subsequently be referred to as T-cell epitope. In order to prevent an immunologic reaction to a therapeutic protein, its sequence ought to possess as little T-cell epitopes as achievable. From a protein engineer's point of view, this can be achieved by deimmunization of the sequence. First, possible T-cell epitopes have to be identified, for example by *in silico* analysis involving large artificial neural networks that include data of confirmed MHC binders as well as known non-binders. Additionally, force field analysis based on structural information and prediction of cleavage site and transport can help to recognize potential epitopes (Brinks et al. 2013). Once identified, these epitopes can be deleted using computational approaches that induce point mutations to minimize the occurrence of predicted T-cell epitopes, while maintaining therapeutic activity (Parker et al. 2010). A special focus is placed on the removal of promiscuous epitopes that will fit into a number of different HLA pockets, meaning that they could be immunogenic in the general population (Scott and De Groot 2010). In the end, a complete lack of T-cell epitopes would prevent APCs from presenting peptides from the biotherapeutic to

T-helper cells, resulting in missing activation of reactive B-cells and their subsequent apoptosis (De Groot and Scott 2007).

1.5 Recombinant human erythropoietin

Small recombinant proteins have a very broad field of possible applications, but an obstacle for the creation of an efficient therapeutic is often their rapid elimination from the body (Kontermann 2011). One of those proteins exhibiting such a short circulation time in the blood is erythropoietin with a terminal half-life of just 6 to 8 hours in humans (Macdougall 2008). Much effort has been placed in the prolongation of serum persistence resulting in products like CERA and Aranesp. These products have a strongly improved terminal half-life, but due to their modification also a decreased EPO receptor affinity (Jelkmann 2007). Instead of using posttranslational modifications or chemical coupling mechanisms to increase the hydrodynamic radius, the use of Immunoglobulin-binding domains can also prevent lysosomal degradation via the neonatal Fc receptor. Therefore, a set of human EPO fusion proteins with IgBDs was generated to increase the serum half-life via transient binding to long lasting IgG molecules.

With an increased concentration of erythropoietin, a variety of cells can be stimulated during the maturation process of red blood cells. The first steps during hematopoiesis take place in the bone marrow where pluripotent stem cells can differentiate through the erythrocyte lineage depending on different cytokines, including EPO (Figure 1-4). The earliest cell to express the erythropoietin receptor and to respond to EPO stimulation is the burst forming unit-erythroid. All subsequent cell types are dependent on EPO in their development until the stage of erythroblasts (Jones, Anderson, and Longmore 2005; Sinclair 2013). Colony forming unit-erythroids begin synthesis of hemoglobin and differentiate into erythroblasts. Erythroblasts enucleate forming reticulocytes that migrate to the peripheral blood for the final step of hematopoiesis, where they differentiate into erythrocytes (Elliott and Sinclair 2012).

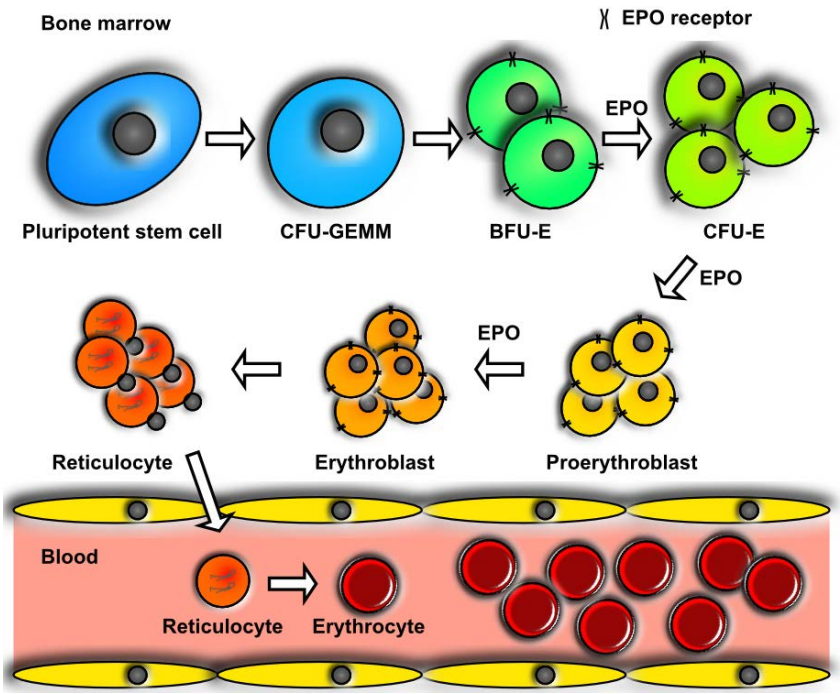

Figure 1-4: Erythropoiesis

This schematic illustration shows the erythropoiesis in the bone marrow and blood. The earliest cell to depend on EPO presence is the BFU-E (burst forming unit-erythroid). The EPO receptor is expressed until the stage of erythroblasts. CFU-GEMM: colony forming unit-granulocyte, erythroid, macrophage, megakaryocyte; CFU-E: colony forming unit-erythroid

Recombinant human erythropoietin has been used as treatment for anemia for over two decades, but due to the low terminal half-life of huEPO two to three intravenous applications per week are required for an effective therapy (Egrie et al. 2003). Therefore, huEPO presents a therapeutically relevant target molecule to half-life extension strategies. Furthermore, functional activity can be assayed rather easily, since EPO retains its activity across most species (Koury 2005). Various strategies to extend the serum half-life were applied to human EPO, like hyperglycosylation to increase the hydrodynamic radius together with the addition of negatively charged sialic acids. This resulted in second and third-generation erythropoietins Darbepoietin alfa (Aranesp) and CERA (pegylated epoietin β), respectively (Kang, Deluca, and Lee 2009). The hyperglycosylated variant Aranesp exhibits a terminal half-life that is roughly 3-fold elongated compared to huEPO (Macdougall et al. 1999), but it also displays a lower *in vitro* activity, determined in an EPO dependent cell line (Sinclair 2013). Increasing the glycosylation lowers the affinity towards the EPO receptor and thus also the *in vitro* activity. Both, slower association and faster dissociation rate contribute to the decreased affinity (Gross and Lodish 2006). More precisely, the sialic acid content of the EPO isotype is responsible for decreased receptor binding and lower proliferation rate, but it also reflects in longer half-life (Egrie and Browne

2001). Despite its reduction in activity, but also because of the lower affinity and degradation of Aranesp, only 1/200 of dosage is needed to achieve the same clinical effect as withunmodified recombinant human EPO (Gross and Lodish 2006; Hörl 2013).

1.6 IgG derivates

With about 350 immunoglobulin-based therapeutics approved for clinical therapy or in the commercial pipeline and development, these recombinant proteins represent the most important class of biotherapeutics (Rath et al. 2013). Their advantage is dependent on the fusion to an Fc part that mediates dimerization and can therefore contribute to higher bioactivity. This dimerization can provoke an avidity effect that is beneficial when targeting cells with an IgG or scFv-Fc, but the effect of a therapeutic fusion partner can also be augmented (Gieffers et al. 2013). More important, the Fc part increases the size of the recombinant fusion protein to prevent rapid renal clearance and it is responsible for the salvage from lysosomal degradation via FcRn recycling (Figure 1-1). Additionally, fusion to an Fc part often results in improved stability and solubility, as well as expression or secretion. The cost-effective purification via Protein A affinity chromatography further favors IgG based therapeutics (Carter 2011). If desired, the Fc part is able to mediate effector functions, such as antibody dependent cellular cytotoxicity or complement dependent cytotoxicity by specifically recognizing Fcγ receptors or complement proteins, dependent on the subclass (Kapur, Einarsdottir, and Vidarsson 2014). The human IgG1 Fc part is glycosylated at the asparagine residue 297. This glycosylation is necessary for proper effector functions, but can be tailored to show better binding to activating or inhibiting Fcγ receptors (Czajkowsky et al. 2012). Besides full length monoclonal antibodies, 9 other Fc fusion proteins are clinically approved, including etanercept (Enbrel), which consists of the extracellular domain of TNF receptor II fused N-terminally to an IgG1 Fc part, abatacept (Orencia) and belatacept (Nulojix) comprising CTLA-4 and romiplostim (Nplate) containing peptide thrombopoietin (TPO) mimetic fused to the C-terminus of aglycosylated human IgG1 Fc (Beck and Reichert 2011; Levin et al. 2014). Other peptides or therapeutic fusion proteins like huEPO, factor VIII or VEGF receptor have been fused to either the C-terminus or the N-terminus of the Fc part (Kontermann 2012; Way et al. 2005) (Figure 1-5). Also the combination of a targeting moiety, like an scFv directed against CD30 or targeting

EpCAM, combined with a therapeutic molecule, like IL-2 or IL-12, is under close investigation (Gillies et al. 2002; Hombach, Heuser, and Abken 2005).

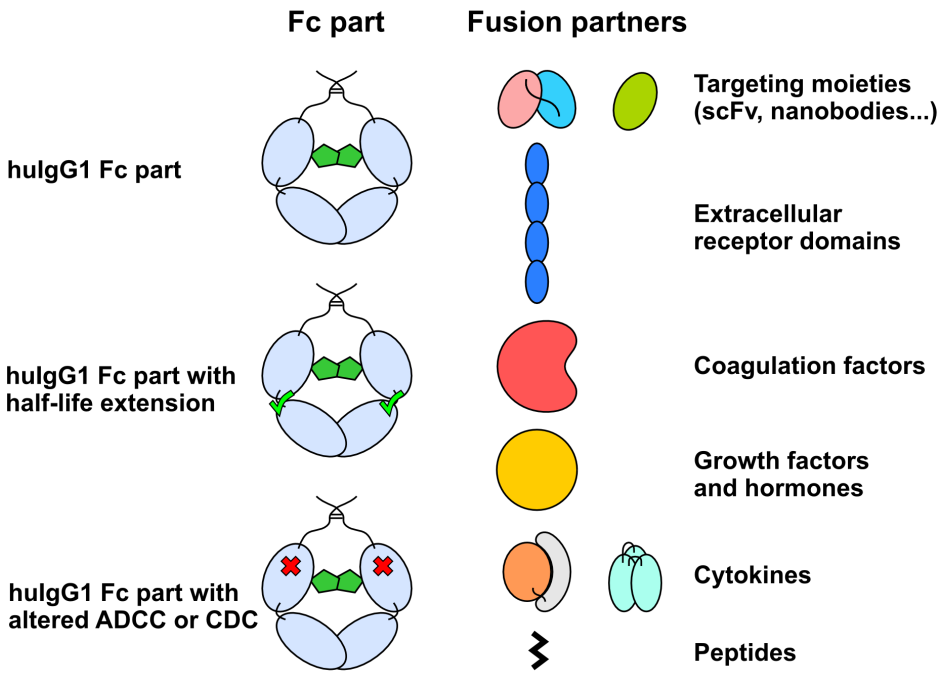

Figure 1-5: Fc fusion proteins

Various therapeutic proteins, targeting moieties or peptides can be genetically fused to a human Fc part in order to generate dimeric, long-lasting fusion proteins. The fusion partners can be added to the N- and/or C-terminus of an Fc part with the possibility of additional bispecificity. Modifications in protein sequence or the glycosylation of the Fc part can mediate half-life extension and enhancement or deactivation of Fc effector functions.

Fusion of an scFv to a human IgG1 Fc part increases its molecular weight and hydrodynamic radius above the renal threshold and the Fc part enables FcRn-mediated salvage from lysosomal degradation. These measures result in a considerably extended terminal half-life in a mouse model (Kenanova et al. 2005). However, it has been demonstrated that full-length immunoglobulins with the same specificity and identical Fc part still exhibited a longer circulation time than an scFv-Fc (Hopp et al. 2010). Differences in binding affinity to the FcRn have previously been identified as plausible reason for shorter retention time of Fc fusion proteins, possibly caused by altered conformation of the C_H2-C_H3 domain interface or steric hindrance (Suzuki et al. 2010). The affinity relation between pH6 and pH7.4 has also been investigated, claiming that low affinity under physiological conditions is crucial for low clearance and long serum persistence (Borrok et al. 2014). A recent study revealed a contribution of the Fab fragment to FcRn recycling, showing unknown FcRn interaction sites in the Fab region or possible conformational links between IgG Fc and Fab regions upon FcRn binding (Jensen et al. 2015). However,

other studies could not detect an association between FcRn affinity and the plasma circulation time of antibodies in mouse models (Gurbaxani et al. 2006).

1.7 Goal of this study

The aim of this study was to advance the half-life extension strategy of the immunoglobulin-binding domains. Hitherto, domain C3 from *Streptococcus* Protein G (SpG_{C3}) exhibited the most favorable properties in improving the pharmacokinetics of small recombinant antibody fusion proteins (Hutt et al. 2012). In order to generate long-lasting fusion proteins with IgBDs, some criteria have to be fulfilled. Stable formation of complexes with IgG under physiological conditions, but also at acidic pH, is necessary to guarantee reduced renal clearance as well as salvage from lysosomal degradation via FcRn-mediated recycling. Furthermore, an interference or competition with the FcRn during endosomal recycling has to be avoided. Deletion of the Fc binding site of SpG_{C3} and simultaneous improvement of the C_H1 binding properties are possibilities to enhance the performance of the IgBDs. After having determined affinities to immunoglobulins and fragments, the most promising candidates are subject for pharmacokinetic analysis as scDb-IgBD fusion protein. Decreasing the impact on functionality of the fusion proteins is also a key requirement for new IgBDs, since previous domains demonstrated reduced activity or altered binding in the presence of IgG (Hutt et al. 2012; Unverdorben et al. 2012).

Since the immunoglobulin-binding domains are derived from bacterial proteins, there might be possible concerns with immunogenicity and the generation of anti-drug antibodies as answer to a treatment with IgBD fusion proteins. In order to solve this issue, a deimmunization strategy can be applied to the sequence of the previously improved IgBDs. First, possible T-cell epitopes have to be identified by sequence- and structure-based analysis. Knowing the number and location of these epitopes, a combination of amino acid substitutions is needed that is able to eliminate as many epitopes as possible without impeding the functionality of the IgBD. These properties have to be determined by *in vitro* characterization, especially the affinity towards IgG, as well as the *in vivo* half-life extension of selected deimmunized IgBDs.

Having determined the *in vitro* bioactivity and pharmacokinetic parameters of IgBDs as scDb fusion proteins, their benefit for another therapeutic molecule has to be verified. For this purpose, recombinant human erythropoietin was selected. The IgBD

fusion proteins have to prove their *in vitro* proliferative effect on an EPO-dependent cell line prior to determining the pharmacokinetic parameters. Finally, the ability to act as therapeutic drug and increase the hemoglobin level in a mouse model has to confirm the potential of the IgBDs to improve the efficacy of biotherapeutics as half-life extension modules.

Furthermore, the pharmacokinetics and the biochemical properties of various IgG-based fusion proteins are compared. These fusion proteins all contain the same human IgG1 Fc part, but they differ in the N-terminal fusion moiety. This study includes a full-length IgG, as well as an scFv-Fc, an scDb-Fc and a single chain version of IgG, where an scFv is fused to a single-chain version of the constant domains of the Fab fragment (scFv-scCLCH1-Fc). Combination of thermal and serum stability as well as FcRn binding affinities, size and isoelectric point are investigated to explain possible differences in half-life. An scDb-C_H2 fusion protein is incorporated, since the C_H2 domain is jointly responsible for FcRn recycling.

2 Materials and methods

2.1 Materials

2.1.1 Instruments

Balances	Feinwaage Basic (Sartorius AG, Göttingen, Germany) 440-39N and 443-33N (Kern, Balingen, Germany)
Cell counting chamber	Counting chamber Neubauer improved (Plan Optik, Elsoff, Germany)
Centrifuges	Avanti J-30I and J2-MC with rotors JA10, JA14, JA20, JA30.5 Optima TL with rotor TLA 100.3 (all: Beckman Coulter, Krefeld, Germany) Eppendorf 5804R (Eppendorf, Hamburg, Germany)
Electrophoresis system	Mini-Protean 3 Cell Electrophoresis System Ready Agarose Precast Gel Electrophoresis Power Pac Basic and HC (all: Bio-Rad, Munich, Germany)
Electroporation	Gene Pulser Xcell Electroporation System (BioRad, Munich, Germany)
ELISA reader	Infinite M200 (Tecan, Crailsheim, Germany)
Flow cytometer	MACSquant Analyzer 10 (Milteny, Bergisch Gladbach, Germany)
Gel documentation	Transilluminator, Gel documentation system Felix (Biostep, Jahnsdorf, Germany)
HPLC system	Waters HPLC-System (Millipore, Billerica, USA) Yarra SEC-2000 column (Phenomenex, Aschaffenburg, Germany)
Incubator for bacteria	Infors HT Multitron 2 (Infors Ag, Basel, Switzerland)
Incubator for cell culture	CO_2 Incubator 2424-2 (Zapf, Sarstedt, Germany)
Laminar flow cabinet	Variolab Mobilien W90, (Waldner-Laboreinrichtungen, Wangen, Germany)
PCR cycler	Robocycler 96 (Stratagene, La Jolla, USA)
Quartz crystal microbalance	Attana Cell A200 with C-fast system (Attana AB, Stockholm, Sweden)
Spectrophotometer	NanoDrop ND-1000 (Thermo Fisher Scientific, Darmstadt, Germany)
ZetaSizer	ZetaSizer Nano ZS 12 mm square glass cell for 90 sizing (Malvern Instruments, Herrenberg, Germany)

2.1.2 Implements

All cell culture and other plastic material was derived from Greiner Bio-One (Frickenhausen, Germany), if not stated otherwise.

Attana sensor chips	Low nonspecific binding-carboxyl chips Biotin sensor chip (Attana AB, Stockholm, Sweden)
Dialysis membranes	ZelluTrans MWCO 6000 (Roth, Karlsruhe, Germany)

Dynabeads	Dynabeads M-280 Streptavidin Dynabeads MPC-S (Magnetic Particle Concentrator) (Thermo Fisher Scientific, Darmstadt, Germany)
Electroporation cuvettes	Gene Pulser electroporation cuvettes 1 mm (BioRad, Munich, Germany)
IMAC beads	Protino Ni-NTA agarose (Macherey-Nagel, Düren, Germany)
Immunotubes	5 ml immunotubes Nunc MaxiSorp (Thermo Fisher Scientific, Darmstadt, Germany)
Microhematocrit tubes	Heparinized (Thermo Fisher Scientific, Darmstadt, Germany)
Protein A beads	TOYOPEARL AF rProtein A-650F (Tosoh Bioscience, Stuttgart, Germany)

2.1.3 Chemicals

All chemicals were purchased from Roth (Karlsruhe, Germany), Merck (Darmstadt, Germany), Roche (Basel, Switzerland) and Sigma-Aldrich (Taufkirchen, Germany), if not stated otherwise.

2.1.4 Bacterial culture and phage display

All media are prepared as aqueous solution.

Ampicillin	100 mg/ml as 1000 x stock solution
IPTG	1 M isopropyl β-D-1-thiogalactopyranoside as 1000 x stock
Kanamycin	30 mg/ml as 1000 x stock solution
$LB_{Amp,Glc}$ agar plates	LB-medium, 2.0 % (w/v) agar, after autoclaving adding of ampicillin to 100 µg/ml and 1 % (w/v) glucose
LB medium	1 % (w/v) peptone, 0.5 % (w/v) yeast extract, 0.5 % (w/v) NaCl
Minimal plates	1.5 % (w/v) agar, 0.2 % (w/v) glucose, 1 mM $MgSO_4$, 2 µg/ml vitamine B1, 1 x M9 stock solution
10 x M9 stock solution	0.5 M Na_2HPO_4, 0.22 M KH_2PO_4, 5 % (w/v) NaCl, 10 % (w/v) NH_4Cl, pH7.2
SOB medium	0.5 % (w/v) yeast extract, 2 % (w/v) peptone, 10 mM NaCl, 2.5 mM KCl, 10 mM $MgSO_4$, 10 mM $MgCl_2$
SOC medium	SOB medium, 20 mM glucose
TY medium	1.6 % (w/v) peptone, 1 % (w/v) yeast extract, 0.5 % (w/v) NaCl

2.1.5 Cell culture

All media and supplements were purchased from Thermo Fisher Scientific (Darmstadt, Germany), if not stated otherwise.

Eosin solution	0.4 % (w/v) eosin G, 0.02 % (w/v) NaN_3 in sterile PBS pH7.4
EPO	Recombinant human EPO (Sigma-Aldrich, St. Louis, USA)

2.1.6 Solutions

All solutions prepared contained water as solvent, if not stated otherwise.

Bradford reagent	BioRad protein assay (BioRad, Munich, Germany)
Coomassie staining solution	0.008 % (w/v) Coomassie Brilliant Blue G-250, 35 mM HCl
DNA loading buffer (5 x)	25 % (v/v) glycerol, 0.02 % (w/v) bromphenol blue in 5 x TAE buffer
ELISA blocking/MPBS	2 % (w/v) non-fat dry milk powder in 1 x PBS
ELISA developing	100 mM Na-acetate (NaOAc) pH6, 0.1 mg/ml 3,3',5,5'-tetramethylbenzidine, 0.006 % (v/v) H_2O_2
ELISA stopping	1 M H_2SO_4
ELISA washing	0.05 % (v/v) Tween 20 in 1 x PBS
Ficoll	LSM 1077 Lymphocyte Separation Medium (PAA Laboratories, Pasching, Austria)
Freezing solution	10 % (v/v) dimethyl sulfoxide in FCS
Glycogen	20 mg/ml (Thermo Fisher Scientific, Darmstadt, Germany)
IMAC elution buffer	250 mM imidazole in 1x sodium phosphate buffer
IMAC wash buffer	30 mM imidazole in 1x sodium phosphate buffer
Laemmli buffer (5 x)	Non-reducing: 10 % (w/v) SDS, 25 % (v/v) glycerin, 0.05 % (w/v) bromphenol blue in 312.5 mM Tris-HCl pH6.8 Reducing: non-reducing buffer, 25 % (v/v) β-mercatoethanol
MTT	0.5 % (w/v) thiazol blue tetrazolium bromide
MTT lysis buffer	15 % (w/v) SDS in Dimethylformamide/H_2O (1:1) with 80 % acetic acid pH4-5
PBA	2 % (v/v) FCS, 0.02 % (w/v) NaN_3 in 1 x PBS
Periplasmic preparation buffer	30 mM Tris-HCl pH8, 1 mM ethylenediaminetetraacetic acid (EDTA), 20 % (w/v) sucrose
Phage precipitation buffer	20 % (w/v) PEG6000, 2.5 M NaCl (autoclaving essential)
PBS (10 x)	80.6 mM Na_2HPO_4, 14.7 mM KH_2PO_4, 1.37 M NaCl, 26.7 mM KCl; used as 1x PBS diluted in dH_2O
PBST (0.1 %)	PBS with 0.1 % (v/v) Tween 20
Protein A elution	100 mM glycine-HCl pH3
Protein A neutralization	1 M Tris-HCl pH7
SDS running (10 x)	1.92 M glycine, 0.25 M Tris, 1 % (w/v) SDS, pH8.3
Sodium phosphate (5 x)	210 mM Na_2HPO_4, 40 mM NaH_2PO_4, 1.25 M NaCl, pH7.5
TAE (50 x)	2 M Tris, 1 M glacial acetic acid, 50 mM EDTA, pH8

2.1.7 Enzymes

Lysozyme	Roche Diagnostics (Mannheim, Germany)
N-Glycosidase F	Roche Diagnostics (Mannheim, Germany)
O-Glycosidase	Roche Diagnostics (Mannheim, Germany)
Neuraminidase	Roche Diagnostics (Mannheim, Germany)

The following enzymes for cloning were all purchased from Thermo Fisher Scientific (Darmstadt, Germany): AgeI, BamHI, BstWI, EcoRI, Fast alkaline phosphatase, NcoI, NotI, SalI, SfiI, T4 DNA ligase, Taq polymerase (recombinant), XbaI

2.1.8 Antibodies and immobilized proteins

Table 2-1: Antibodies and immobilized proteins

Protein	Source	Concentration
Anti-His-tag antibody-HRP	Santa Cruz Biotech (Santa Cruz, USA)	1:2000 (ELISA)
Anti-His-tag antibody-PE	Miltenyi Biotec (Bergisch Gladbach, Germany)	1:150 (FACS)
Anti-human IgG-HRP (Fc specific)	Sigma-Aldrich (St.Louis, USA)	1:5000 (ELISA)
CEA	Antikörper-online.de (Aachen, Germany)	3 µg/ml (ELISA)
Human serum IgG	Sigma-Aldrich (St.Louis, USA)	100 µg/ml (ELISA, FACS, IL-2 release)
Human serum IgG Fab fragment	EMELCA (Breda, Netherlands)	QCM
Human serum IgG Fc fragment	EMELCA (Breda, Netherlands)	QCM
Mouse FcRn (biotinylated)	Novimmune (Geneva, Switzerland)	QCM
Mouse serum IgG	Sigma-Aldrich (St.Louis, USA)	QCM
Mouse serum IgG Fab fragment	EMELCA (Breda, Netherlands)	QCM
Mouse serum IgG Fc fragment	EMELCA (Breda, Netherlands)	QCM
Protein L-HRP	Genscript (Piscataway, USA)	1:5000 (ELISA)

2.1.9 Kits and markers

Amine coupling kit (EDC + sNHS)	(Attana AB, Stockholm, Sweden)
Biotin-Streptavidin coupling kit	(Attana AB, Stockholm, Sweden)
EZ-Link Sulfo-NHS-Biotin	(Thermo Fisher Scientific, Darmstadt, Germany)
GeneMorph II Random Mutagenesis kit	(Agilent, Waldbronn, Germany)
Hemoglobin assay kit	(Sigma-Aldrich, St. Louis, USA)
Interleukin-2 Sandwich ELISA	(R&D Systems, Abingdon, UK)
NucleoBond Xtra Midi	(Macherey-Nagel, Düren, Germany)
NucleoBond Gel and PCR Clean-up	(Macherey-Nagel, Düren, Germany)
NucleoBond Plasmid	(Macherey-Nagel, Düren, Germany)
GeneRuler DNA ladder mix	(Thermo Fisher Scientific, Darmstadt, Germany)
PageRuler prestained protein ladder	(Thermo Fisher Scientific, Darmstadt, Germany)

2.1.10 Bacteria and phages

Escherichia coli TG1	Genotype: *supE thi-1* Δ(*lac-proAB*) Δ(*mcrB-hsdSM*)*5* (rK– mK–) [F´ *traD36 proAB lacI*q*Z*Δ*M15*] (Stratagene,La Jolla, USA)
Phage VCS M13	Interference-resistant helper phage (Stratagene, La Jolla, USA)

2.1.11 Cell lines

Eucaryotic cells were cultivated at 37 °C in a humidified incubator in 5 % CO_2 atmosphere.

Table 2-2: Cell lines

Cell line	Origin	Culture medium
CHO-K1	Chinese hamster ovary	RPMI 1640 + 5 % FCS
HEK293	Human embryonic kidney	RPMI 1640 + 5 % FCS
LS174T	Colon carcinoma	RPMI 1640 + 5 % FCS
PBMCs	Buffy coat from healthy donors	RPMI 1640 + 10 % FCS
UT-7/EPO	Human leukemic EPO dependent	IMDM + 10 % FCS + 1 U/ml EPO

2.1.12 Plasmids

pAB1	Vector for prokaryotic expression in periplasm of *E.coli* TG1 (Müller et al. 2007)
pEE14.4	Glutamine sythetase encoding eukaryotic expression vector (Lonza Biologics, Berkshire, UK)
pHEN3	Phagemid vector (based on pHENIX, with additional His-tag (Finnern et al. 1997)
pSecTagA	Eukaryotic expression vector (Thermo Fisher Scientific, Darmstadt, Germany)
pSecTagAL1	Modified pSecTagA with additional AgeI restriction site (K. Zettlitz)

2.1.13 Primers

All primers were synthesized by Sigma-Aldrich (St. Louis, USA) and dissolved in water to a final concentration of 50 µM.

Table 2-3: Primer for sequencing

Name	Target	Sequence (5' – 3')
pET-Seq1	pSecTagA (forward)	TAA TAC GAC TCA CTA TAG GG
pSec-Seq2	pSecTagA (reverse)	TAG AAG GCA CAG TCG AGG
LMB4	pAB1 (reverse)	GCA AGG CGA TTA AGT TGG
LMB3	pHEN3 (forward)	CAG GAA ACA GCT ATG ACC
fd-SEQ1	pHEN3 (reverse)	GAA TTT TCT GTA TGA GG
V_LCEA-back	V_L scFvCEA (forward)	GAG GCT GAA GAT GCT GCC
Fc fusions	C_H2 domain (reverse)	TGG GGG GAA GAG GAA GAC

Table 2-4: Primer for cloning of IgBD fusion proteins

Name	Sequence (5' – 3')
NotI-Linker-SpG$_{C3Fab}$-back	A TTT GCG GCC GCA GGC GGA TCT GGC GGA ACA ACA TAC AAG CTC GTG
EcoRI-Stop-His-SpG$_{C3}$-for	G ATC GAA TTC TCA TCA GTG GTG ATG GTG GTG GTG GGA TCC GCC CTC GGT CAC GGT GAA GGT
SpG$_{C3Fab}$T1A,E15Q-back	G ATC GCG GCC GCA GGC GGA TCT GGC GGA GCA ACA TAC AAG CTC GTG ATC AAC GGC AAG ACC CTG AAG GGC CAG ACA ACC ACC AAA GCC G
SpG$_{C3Fab}$K50Q-for	GAT CGA ATT CTC ATC AGT GGT GAT GGT GGT GGT GGG ATC CGC CCT CGG TCA CGG TGA AGG TCT GGG TGG CGT CGT CGT AGG
SpG$_{C3Fab}$K4E-back	G ATC GCG GCC GCA GGC GGA TCT GGC GGA ACA ACA TAC GAG CTC GTG ATC AAC GGC AAG
SpG$_{C3Fab}$L5A-back	G ATC GCG GCC GCA GGC GGA TCT GGC GGA ACA ACA TAC AAG GCC GTG ATC AAC GGC AAG ACC
SpG$_{C3Fab}$V6A-back	G ATC GCG GCC GCA GGC GGA TCT GGC GGA ACA ACA TAC AAG CTC GCG ATC AAC GGC AAG ACC CTG
SpG$_{C3Fab}$I7E-back	G ATC GCG GCC GCA GGC GGA TCT GGC GGA ACA ACA TAC AAG CTC GTG GAA AAC GGC AAG ACC CTG AAG
SpG$_{C3Fab}$I7L-back	G ATC GCG GCC GCA GGC GGA TCT GGC GGA ACA ACA TAC AAG CTC GTG CTC AAC GGC AAG ACC CTG AAG
SpG$_{C3Fab}$N8D-back	G ATC GCG GCC GCA GGC GGA TCT GGC GGA ACA ACA TAC AAG CTC GTG ATC GAC GGC AAG ACC CTG AAG GGC
SpG$_{C3Fab}$K10E-back	G ATC GCG GCC GCA GGC GGA TCT GGC GGA ACA ACA TAC AAG CTC GTG ATC AAC GGC GAG ACC CTG AAG GGC GAG ACA
SpG$_{C3Fab}$L12A-back	A TTT GCG GCC GCA GGC GGA TCT GGC GGA ACA ACA TAC AAG CTC GTG ATC AAC GGC AAG ACC GCG TCT GGC GAG ACA ACC ACC
SpG$_{C3Fab}$T44S-for	G ATC GGA TCC GCC TTC GGT CAC GGT GAA GGT CTT GGT GGC GTC GTC GTA GGA CCA CAC GCC GTC CAC GCC
SpG$_{C3Fab}$A48G-for	G ATC GGA TCC GCC TTC GGT CAC GGT GAA GGT CTT GGT GCC GTC GTC GTA GGT CCA CAC
SpG$_{C3Fab}$DI1-back	G ATC GCG GCC GCA GGC GGA TCT GGC GGA ACA ACA TAC GAG CTC GCG ATC AAC GGC CAG ACC CTG AAG GGC GAG ACA
SpG$_{C3Fab}$DI2-back	G ATC GCG GCC GCA GGC GGA TCT GGC GGA ACA ACA TAC AAG GTC GCG ATC AAC GGC CAG ACC CTG AAG GGC GAG ACA
SpG$_{C3Fab}$DI3-back	G ATC GCG GCC GCA GGC GGA TCT GGC GGA ACA ACA TAC AAG CTC ACG ATC GAC GGC AAG ACC CTG AAG GGC
SpG$_{C3Fab}$DI4-back	G ATC GCG GCC GCA GGC GGA TCT GGC GGA ACA ACA TAC AAG CTC ACG ATC AAC GGC GAG ACC CTG AAG GGC GAG ACA
SpG$_{C3Fab}$Y33A-back	G ATC GTC GAC GCC GAA ACA GCC GCC GCT GCC TTT GCC CAG GCT GCC AGG AGG AAT GGC GTG
SpG$_{C3Fab}$Y33T-back	G ATC GTC GAC GCC GAA ACA GCC GCC GCT GCC TTT GCC CAG ACT GCC AGG AGG AAT GGC GTG

Table 2-5: Primer for phage display

Name	Sequence (5' – 3')
NcoI-SpG$_{C3Fab}$-back	C ATG CCA TGG CCA CAA CAT ACA AGC TCG TGA TCA ACG
NotI-SpG$_{C3Fab}$-for	ATT TGC GGC CGC CTC GGT CAC GGT GAA GGT
NcoI-SpG$_{C3Fab}$ΔN-back	CAT GCC ATG GCC TGA CCA AAG CCG TCG ACG
SalI-SpG$_{C3Fab}$ΔN-back	T CGA GTC GAC AGT ACG CCA ACG ATA ATG GCG
SpG$_{C3Fab}$ Library1-back	CCG GCC ATG GCC ACA ACA TAC NNK CTC GTG ATC AAC GGC AAG ACC CTG AAG GGC NNK NNK NNK ACC AAA GCC GTC GAC GCC GAA ACA
SpG$_{C3Fab}$ Library2-back	CCG GCC ATG GCC ACA ACA TAC AAG CTC GTG ATC AAC GGC AAG NNK NNK NNK NNK GAG ACA ACC ACC AAA GCC GTC GAC
SpG$_{C3Fab}$ Library3-back	T CGA GTC GAC GCC GAA ACA GCC GCC GCT GCC TTT GCC CAG NNK GCC NNK NNK NNK GGC GTG GAC GGC GTG TGG ACC

NNK triplets were used at the sites that encode for amino acids binding to the C_H1 domain.

Table 2-6: Primer for Fc fusion proteins

Name	Sequence (5' – 3')
BsiWI-scFv-for	G ATC CGT ACG TTT CAG CTC CAG CTT GGT GCC
BsiWI-CLkappa-back	G ATC CGT ACG GTG GCA GCG CCA TCT GTC TTC ATC
BamHI-CLkappa-for	G ATC GGA TCC ACC GCC CCC TGA CCC ACC GCC TCC ACA CTC TCC CCT GTT GAA
BamHI-CH1-back	G ATC GGA TCC GGG GGA GGC GGT TCA GGA GGC GGT GGG AGT GCC TCC ACC AAG GGC CCA
NotI-CH1-for	GAT CGC GGC CGC ACA AGA TTT GGG CTC AAC
NotI-CH2-back	G ATC GCG GCC GCA GGC GGA TCT GGC GGC GCA CCT GAA CTC CTG GGG
BamHI-CH2-for	G ATC GGA TCC TCC TTT GGC TTT GGA GAT GGT

2.1.14 Programs and online tools

Attana evaluation software 3.3.4	Attana AB (Stockholm, Sweden)
C-Fast Software	Attana AB (Stockholm, Sweden)
ExPASY Prot Param	http://web.expasy.org/protparam/
FlowJo 8.8.6	http://www.flowjo.com/
GraphPad Prism 5.01	GraphPad software (La Jolla, USA)
Microsoft Excel and Add-Ins	Microsoft Corporation
MacPYMOLEdu	http://pymol.org/educational/
RCSB protein databank	http://www.rcsb.org/pdb/home/home.do
Serial Cloner 2.6.1	http://serialbasics.free.fr/Serial_Cloner.html
TraceDrawer 1.6	Attana AB (Stockholm, Sweden)

2.2 Cloning

2.2.1 Cloning of antibody fragment-IgBD fusion proteins

The DNA sequences encoding for SpG_{C3Fab}, SpG_{C3Fc} and SpG_{C2} were synthesized from Geneart (Regensburg, Germany) including the linker between the antibody fragment and the IgBD as well as the C-terminal His-tag followed by a Stop codon. These sequences were ligated into the eukaryotic expression vector pSecTagA, either containing an scDb or scFv (Hutt et al. 2012). The identical modular system with NotI and EcoRI as restriction sites was used for the generation of the prokaryotic expression vector pAB1 scFv-IgBDs (Hopp et al. 2010). Analogously, all affinity-maturated variants have been introduced into the expression vectors by PCR using the primers NotI-Linker-SpG_{C3Fab}-back and EcoRI-Stop-His-SpG_{C3}-for and the pHEN3 vector of the selected clone as template (Table 2-4). Only SpG_{C3Fab}T1A,E15Q and SpG_{C3Fab}K50Q needed other primers (SpG_{C3Fab}T1A,E15Q-for, SpG_{C3Fab}K50Q-back), since their mutations were at the

beginning or the end of the transferred sequence, respectively. In order to introduce the deimmunized variants into the expression vectors, the same strategy was applied, using the primers with the corresponding mutations and pSecTagA-SpG_{C3Fab} as template for PCR.

2.2.2 Cloning of huEPO-IgBD fusion proteins

The DNA for the huEPO-IgBD fusion proteins was synthesized by Geneart (Regensburg, Germany), including a hexahistidyl tag, with flanking AgeI and XbaI restriction sites for cloning into pSecTagAL1. Additionally, a NotI site was included prior to the His-tag in order to insert the IgBD sequences via NotI and XbaI from the pSecTagA vectors used above.

2.2.3 Cloning strategy for phage display

For the generation of the phage display libraries 1, 2 and 4, an acceptor vector had to be created, comprising a 5' terminally truncated version of SpG_{C3Fab} in the phagemid vector pHEN3 (pHEN3 SpG_{C3Fab}ΔN) that was cloned using NcoI-SpG_{C3Fab}ΔN-back (forward) and NotI-SpG_{C3Fab}-for (reverse) as primers for the SpG_{C3Fab} sequence from pSecTagA. For library 3, the SalI and NotI restriction sites were necessary. Therefore, another acceptor vector was created via the alternative forward primer SalI-SpG_{C3Fab}ΔN-back. The PCR product from the degenerate primers (Table 2-5) as forward primers and NotI-SpG_{C3Fab}-for as reverse primer was digested with NcoI (Libraries 1, 2 and 4) or SalI (Library 4) and NotI for subsequent ligation to the corresponding acceptor vector.

2.2.4 Cloning of Fc fusion proteins

In order to generate tag free Fc fusion proteins, the scFv and the scDb were transferred to an already existing pSecTagA-Fc vector via the restriction site SfiI and NotI from the vectors mentioned above. The scFv-scCLCH1-Fc had to be cloned in several steps, adding one immunoglobulin domain at a time. First, the PCR product of the primers BamHI-CH1-back and NotI-CH1-for (Table 2-6) with the vector pEE14.4 IgG1CEA as template was integrated via BamHI and NotI. Next, a PCR was performed in order to generate the C_L domain with restriction sites for BsiWI and BamHI using the primers BsiWI-CLkappa-back and BamHI-CLkappa-for for the IgG template. Since the scFv could not be transferred via the NotI site as previously described, the BsiWI restriction site had to be added using the primers pET-Seq1 (Table 2-3) and BsiWI-scFv-for for amplification of the scFv out of the vector

pSecTag scFv-Fc. The scDb-C_H2 was cloned via PCR with the primers NotI-C_H2-back and BamHI-CH2-for and the IgG template. The resulting PCR product was digested with NotI and BamHI and ligated into the cut pSecTagA scDb-SpG_{C3Fab}.

2.2.5 Polymerase chain reaction

The polymerase chain reaction (PCR) was used in order to amplify desired sequences with the necessary restriction sites or to introduce single amino acid substitutions. The PCR protocol for the generation of the libraries 1 – 3 was identical to other PCR reaction, only using degenerate primers to create diversity.

PCR Taq buffer with $(NH_4)_2SO_4$ (10 x)	5 µl
$MgCl_2$ (25 mM)	4 µl
dNTP mix (5 mM each nucleotide)	2.5 µl
Forward primer (50 µM)	1 µl
Reverse primer (50 µM)	1 µl
Template (100 ng/µl)	1 µl
H_2O	34.25 µl
Taq polymerase (1 U/µl)	1.25 µl

The amplification was performed as described in Table 2-7, with an elongation time that was dependent on the resulting PCR product. A synthesis rate of 1000 nucleotides per minute was assumed for the Taq polymerase, with a minimal elongation time of 0.5 min. For the generation of the libraries, only 25 cycles were applied.

Table 2-7: PCR program

PCR step	Temperature	Time [min]	Number of cycles
Initial denaturation	94 °C	5	1 x
Denaturation	94 °C	0.5	30 x
Annealing	50 °C	0.5	
Elongation	72 °C	dependent	
Final elongation	72 °C	5	1 x

2.2.6 Error prone PCR

In order to generate a library with amino acid substitutions distributed across the whole sequence, an error prone PCR approach was pursued. The PCR program was similar to the previously programs, using 0.5 min of elongation and 40 cycles.

H_2O	40 µl
Mutazyme II reaction buffer (10 x)	5 µl
dNTP mix (10 mM each nucleotide)	1 µl
Primer LMB3 (50 µM)	1 µl
Primer LMB4 (50 µM)	1 µl
Template pHEN3-SpG_{C3Fab} (0.11 ng/µl)	1 µl
Mutazyme II DNA polymerase (2.5 U/µl)	1 µl

2.2.7 DNA electrophoresis and gel extraction

After amplification or digestion of DNA, the resulting fragments were analyzed and purified via horizontal agarose gel electrophoresis. Depending on the size of the fragments, 1 – 2 % (w/v) agarose was boiled in TAE buffer until it was completely dissolved. Subsequently, ethidium bromide was added to a final concentration of 1 µg/ml. DNA was mixed 5 x DNA loading buffer and applied to the precast gel at 80 V for 30 minutes. After analysis under ultra violet light, relevant bands were excised and purified with a NucleoSpin Gel and PCR Clean-up kit according to manufacturer's protocol.

2.2.8 Restriction digestion

10 µg of vector DNA or alternatively the whole elution from previous DNA purification was digested in a total volume of 50 µl. When temperatures and buffer conditions were identical for both enzymes, the DNA was incubated with both enzymes (1 µl each) in the corresponding buffer for 2 h. If temperature or buffer conditions were unsuitable, the digestions were performed consecutively, with additional purification step. The buffer exchange was again performed with the NucleoSpin Gel and PCR Clean-up kit. The vector DNA was dephosphorylated using Fast alkaline phosphatase (1 µl) after the last digestion step for 1 h at 37 °C. Next, fragments were analyzed via agarose gel electrophoresis.

2.2.9 Ligation and heat shock transformation

A molar ratio of 1 : 3 was chosen for the ligation of vector and insert DNA with a total DNA amount of 250 ng. The ligation reaction was carried out at room temperature for 1 h with 1 U of T4 DNA ligase in a total volume of 20 µl. Chemically competent *E.coli* TG1 were thawed on ice, the ligation was added to 100 µl of bacteria and incubated on ice for 5 minutes. Heat shock was subsequently applied for 45 seconds at 42 °C and cells were placed back on ice together with 1 ml of LB medium for

recovery for 2 minutes. Cells were harvested by centrifugation (10,000 g, 30 sec) and plated on $LB_{Amp,Glc}$ agar plates for over night incubation at 37 °C.

2.2.10 Plasmid DNA isolation and sequence analysis

One single clone was inoculated into an 5 ml/100 ml LB medium (Mini/Midi-preparation) containing 1 % (w/v) glucose and ampicillin, shaken at 37 °C. Cells were harvested the next day and DNA was purified according to manufacturers protocol with the NucleoSpin Plasmid kit for Mini-preparation and the NuceloBond Xtra Midi kit for Midi-preparation. The DNA was sequenced by GATC Biotech AG (Konstanz, Germany) using the corresponding primers from Table 2-3.

2.3 Phage display

2.3.1 Preparation of electrocompetent cells

A single colony of *E.coli* TG1 from a minimal plate was inoculated for a 10 ml over night culture. The next day, 5 ml thereof were inoculated into 450 ml SOB medium and vigorously shaken at 37 °C for about 3 h to reach an OD_{600} of about 0.75. The cells were chilled on ice for 1 h and harvested by centrifugation (2000 g, 10 min). All of the following steps were performed on ice and with chilled liquids, centrifuges and tubes. The bacteria pellet was resuspended in 200 ml H_2O and again centrifuged at 2000 g for 15 minutes. The resulting pellet was again resuspended in 200 ml H_2O and incubated on ice for 30 min. Cells were harvested (2000 g, 15 min) and resuspended in 25 ml 10 % (v/v) glycerol. The solution was incubated for 30 minutes and again harvested by centrifugation (1500 g, 15 min). The ensuing cell pellet was resuspended in a final volume of 1 ml 10 % glycerol and immediately used for electroporation.

2.3.2 Ethanol precipitation of DNA

In order to guarantee a better quality and yield of DNA for the generation of libraries, the DNA was precipitated after the ligation. For a 50 µl sample, 5 µl of 3 M sodium acetate pH5.2 and 2.5 µl of glycogen (20 mg/ml stock concentration) were added. 125 µl of 100 % ethanol were applied and after mixing, the solution was incubated at -80 °C for 1 h. After centrifugation (13,000 g, 15 min, 4 °C) the DNA pellet was washed twice with 70 % ethanol, air-dried and resuspended in 22 µl of water for a total of 10 electroporation runs.

2.3.3 Electroporation

All tubes and cuvettes were previously chilled and always handled on ice. 40 µl of electrocompetent *E.coli* TG1 were mixed with 2 µl of ligated DNA and set on ice for 1 minute. The electroporator was set to a voltage of 1700 V, a resistance of 200 Ω and a capacity of 25 µF. After a single pulse, the sample was immediately resuspended in 1 ml warm SOC medium and incubated for 1 h at 37 °C shaking. Afterwards, the cells were harvested and plated onto $LB_{Amp,Glc}$ agar plates over night at 37 °C. The next day, colonies were collected for phage rescue and for the generation of a library stock at -80 °C in 30 % glycerol.

2.3.4 Phage rescue

50 ml TY medium with ampicillin and 2 % (w/v) glucose were inoculated from the phagemid library or from previous selection rounds to an optical density of 0.05. Cells were incubated at 37 °C with vigorous shaking for about 2 h until reaching an OD_{600} of 0.5, then VCS M13 helper phages were added and further incubated without shaking for 30 min, followed by 30 min with shaking. After harvesting the cells (3000 g, 10 min), the pellet was resuspended in 50 ml TY medium containing ampicillin and kanamycin and shook over night at 30 °C. The bacteria were removed by centrifugation (4700 g, 20 min, 4 °C) and phages were precipitated from 40 ml supernatant with 10 ml phage precipitation buffer for 1.5 h while rotating at 4 °C. The phages were pelleted by centrifugation (4700 g, 30 min) and the pellet was resuspended in 1 ml cold PBS. To remove residual bacteria, the phage solution was centrifuged for 1 minute at 13,000 g and phage-containing supernatant was collected.

2.3.5 Immunotube selection

Immunotubes were coated over night with 1 ml PBS containing 10 µg/ml human or mouse Fab fragment. A single *E.coli* TG1 colony from a minimal plate was inoculated in 10 ml TY medium for an over night culture. The next day, immunotubes were blocked with MPBS and 10 µl of phages were preincubated with MPBS. Subsequently the phages were incubated in the immunotube for 2 h, followed by 20 washing steps with PBST (0.1 %) and PBS. In the mean time, 50 ml of TY medium were inoculated from the over night culture to an OD_{600} of 0.05 and grown until reaching 0.4 – 0.5. 1 ml of 100 mM triethylamine for 8 min eluted the phages and was neutralized with 0.5 ml 1 M Tris-HCl pH7.5. The phages were added to the log-phase bacteria and incubated 30 min standing and 30 min shaking at 37 °C, prior

to harvesting and plating the transduced cells on $LB_{Amp,Glc}$ agar plates over night. For subsequent rounds, the binding and washing conditions were more stringent by reducing the coated antigen and washing more harshly (more steps, additional incubation for dissociation, pH6 washing).

2.3.6 Selection with biotinylated antigen

Biotinylation of human Fab fragment was performed with the EZ-Link Sulfo-NHS-Biotin kit according to manufacturer's protocol. *E.coli* TG1 were prepared as described for the immunotube selection. 10 µl of phages and 10 µl magnetic streptavidin coated dynabeads were blocked with 1 % BSA separately. Biotinylated antigen (100 nM) was added to the phages and incubated for 1 h. In order to remove unbound phages, the phage/biotinylated Fab solution was added to the magnetic dynabeads for 15 min and subsequently removed using a magnetic particle concentrator. The beads were washed 4 times with PBST (0.1 %) and twice with PBS. For elution of the phages, the beads were incubated with 200 µl 10 mM dithiothreitol for 5 min. Eluted phages were subsequently treated as described for the immunotube selection. Stringency was increased over the rounds by decreasing the concentration of biotinylated Fab fragment by factor 10 each round and performing the binding and washing steps at pH6.

2.4 Cell culture and transfection

All eukaryotic cell lines were cultivated at 37 °C in a humidified 5 % CO_2 atmosphere in the corresponding medium (Table 2-2). Cell lines were passaged every third day, by detaching adherent cells with Trypsin/EDTA, centrifugation (500 g, 5 min) and splitting 1:20. For long-term storage, harvested cells were resuspended in FCS containing 10 % (v/v) DMSO and slowly frozen in isopropanol filled cryoboxes to -80 °C. For thawing, cells were incubated at 37 °C, centrifuged (500 g, 5 min) to remove the residual DMSO and resuspended in the corresponding medium.

For selection of HEK293 cells to express recombinant protein, pSecTagA plasmids were transfected by lipofection. 10^6 cells were seeded in a 6-well tissue culture plate over night in 2 ml culture medium. The next day, 330 µl of serum free Opti-MEM medium were incubated with 7 µl Lipofectamine 2000 for 5 min and subsequently mixed with 3 µg plasmid DNA. The culture medium was withdrawn from the cells and replaced by 1.5 ml Opti-MEM. After 20 min incubation, the lipofectamine-DNA

solution was carefully applied to the cells and incubated over night at 37 °C. Supernatant was then removed and cells were detached and transferred to 10 cm tissue culture plates with culture medium. For selection, zeocin was added after 4 h to a final concentration of 300 µg/ml. Upon successful selection, zeocin concentration was reduced to 50 µg/ml.

2.5 Expression and purification of recombinant proteins

2.5.1 Periplasmic protein expression in *E.coli* TG1

2 l of TY medium containing ampicillin and 0.1 % (w/v) glucose were inoculated 1:100 from an over night culture of pAB1 transformed *E.coli* TG1 and shook at 37 °C until reaching OD_{600} 0.8. The protein expression was induced by the addition of IPTG, followed by 3 h shaking at room temperature. Cells were harvested (6000 g, 10 min, 4 °C) and cell pellet was resuspended in 100 ml resuspension buffer. From now, all steps were performed on ice and with chilled liquids and centrifuges. Cell wall lysis was accomplished by addition of 10 mg lysozyme and 30 min incubation, followed by the addition of $MgSO_4$ to a final concentration of 10 mM to stabilize spheroblasts. The supernatant was collected by centrifugation (10,000 g, 30 min) and dialyzed over night against 5 l PBS. This solution was subject to purification via IMAC.

2.5.2 Protein expression in mammalian cells

After selection, stably transfected cells were expanded to triple flasks (Thermo Fisher Scientific, Darmstadt, Germany) in their selection medium. HEK293 cells were incubated in RPMI 1640 with 5 % FCS and 50 µg/ml zeocin, pEE14.4 transfected CHO-K1 cells with glutamine free RPMI 1640 with 10 % dialyzed FCS and 25 µM methionine sulfoximine. Upon reaching 80 % confluence, the medium was changed to serum free Opti-MEM, which was collected every other day for up to two weeks. All further steps were carried out at 4 °C. Proteins from cell free supernatant (centrifugation at 500 g for 5 min) were precipitated by addition of 390 g/l $(NH_4)_2SO_4$ addition and stirring for 1 h. Consequently, the protein was harvested by centrifugation (11,250 g, 30 min) and the resulting pellet was resuspended in cold PBS. Recombinant proteins with His-tag were purified via IMAC, Fc fusion proteins with Protein A chromatography.

2.5.3 Immobilized metal affinity chromatography

All proteins containing a His-tag were purified via IMAC, using a batch method, where the protein solution is incubated with 0.5 ml of beads for at least 1 h. All steps were carried out on ice and with chilled liquids. The beads were subsequently collected in a column and unspecifically bound proteins were washed away with at least 40 column volumes of IMAC wash buffer, containing 30 mM imidazole. Protein content of wash fractions as well as following elution fractions was determined using qualitative Bradford assay, where 90 µl of assay solution was mixed with 10 µl of fraction. Blue color identified eluted protein. After washing, the specifically bound protein was eluted with IMAC elution buffer, containing 250 mM imidazole, in 500 µl fractions and main elution fractions (determined by Bradford assay) were pooled for dialysis against 5 l PBS over night.

2.5.4 Protein A chromatography

All Fc fusion proteins and IgG molecules were purified via Protein A chromatography after ammonium sulfate precipitation. All steps were performed on ice and with chilled liquids. The resuspended protein was incubated with 250 µl Protein A beads over night and loaded onto a purification column. The beads were washed with 40 column volumes of PBS and protein content of the wash was determined with Bradford reagent as described above. Specifically bound proteins were eluted in 250 µl fractions with Protein A elution buffer (10 mM glycine-HCl pH3) and neutralized with 25 µl Protein A neutralization buffer (1 M Tris-HCl pH8). Main elution fractions were pooled and dialyzed against 5 l PBS over night.

2.6 Biochemical characterization

2.6.1 Protein concentration

The concentration of all proteins was determined with a spectrophotometer (NanoDrop), based on the absorbance of tryptophan and tyrosine residues at a wavelength of 280 nm. The molar extinction coefficient ε [l/(mol x cm)] and molecular weight (MW [g/mol]) were calculated by the online tool ‘ProtParam’ and the concentration was computed as follows, where b [cm] represents the path length:

$$c\ [\mu g/ml] = OD_{280} \times MW / (\varepsilon \times b)$$

2.6.2 SDS-PAGE

In order to determine integrity and purity of the recombinant proteins, SDS-PAGE analysis was performed. Samples were mixed with 5 x reducing or non-reducing Laemmli buffer and boiled at 94 °C for 5 min. Depending on the molecular mass of the protein, different acrylamide concentrations were used when preparing the gels (Table 2-8). Samples and molecular mass standard were applied to the precast polyacrylamide gel, which was then run for 1 h at 40 mA. After boiling in deionized water to remove residual salt and detergent, the gel was incubated with Coomassie staining solution for more than 1 h and destained over night in water.

Table 2-8: Polyacrylamide gels for SDS-PAGE

Substance	Stacking gel	Separating gel	
	5 %	10 %	12 %
dH_2O	2.1 ml	2.95 ml	2.45 ml
30 % Acrylamide mix	500 µl	2.5 ml	3 ml
1.5 M Tris-HCl pH8.8	-	1.9 ml	1.9 ml
1 M Tris-HCl pH6.8	380 µl	-	-
10 % (w/v) SDS	30 µl	75 µl	75 µl
10 % APS	30 µl	75 µl	75 µl
TEMED	5 µl	5 µl	5 µl

2.6.3 Deglycosylation of proteins

10 µg of glycosylated protein were diluted in 50 µl PBS and denatured for 5 min at 94 °C. After reaching room temperature, 2 U of N-glycosidase F, O-glycosidase and neuraminidase were added and incubated over night at 37 °C. The next day, samples were diluted with 5 x Laemmli buffer and boiled, followed by SDS-PAGE analysis together with untreated samples.

2.6.4 Size exclusion chromatography

High performance liquid chromatography was performed using size exclusion columns for the determination of purity and integrity of the purified proteins. 20 µl of protein sample with a concentration ranging from 0.3 to 0.5 mg/ml were injected at a PBS mobile phase flow rate of 0.5 ml/min. The following standard proteins were used for calculation of molecular mass and hydrodynamic radius: thyroglobulin (669 kDa, 8.5 nm), apoferritin (443 kDa, 6.1 nm), bovine γ globulin (158 kDa, 5.3 nm), β-amylase (200 kDa, 5.4 nm), bovine serum albumin (67 kDa, 3.55 nm), ovalbumin

(44 kDa, 3.2 nm), carbonic anhydrase (29 kDa, 2.35 nm) and cytochrome c (12.5 kDa, 1.77 nm).

2.6.5 Thermal stability

The melting point of proteins was determined by thermal denaturation via the ZetaSizer Nano ZS. 100 µg of recombinant protein in 1 ml PBS were sterile-filtered into a quartz cuvette. The temperature at which the protein starts to aggregate was determined by the increase of the mean count rate of dynamic laser light scattering and defined as the melting point. Hereby, the temperature was raised in 1 °C intervals from 35 to 92 °C with 2 minutes equilibration time.

2.7 Quartz crystal microbalance

Affinities of the IgBD fusion proteins towards immunoglobulins and fragments were determined via quartz crystal microbalance, using the Attana Cell A200 instrument. Human and mouse full-length immunoglobulins, Fab fragments or Fc fragments were immobilized via the amine coupling kit (EDC + sNHS, Attana AB, Stockholm, Sweden) on the surface of low nonspecific-binding carboxyl chips in a density that resulted in a frequency change of 70 – 90 Hz. All measurements were performed at 25 °C with a flow-rate of 25 µl/min of PBST (0.1 %) pH7.4 or pH6. Regeneration of the binding was performed twice with 10 mM glycine-HCl pH3 for 30 sec. After every second measurement a buffer injection was performed to determine the baseline, which was subsequently subtracted from the neighboring measurements. Proteins were injected in random order and a two-fold dilution series, with the highest concentration of 1 µM for the scDb-IgBD fusion proteins and 2 µM for the scFv-IgBD fusion proteins. Data were analyzed with the Attana evaluation software (Version 3.3.4) and TraceDrawer 1.6, using a one-to-two binding model to determine the binding parameters.

The interaction of the Fc fusion proteins with the mouse FcRn were also determined via QCM, using PBST (0.1 %) pH6 or pH7.4 as running buffer (25 µl/min) at 37 °C. The FcRn was immobilized via the streptavidin coupling kit on biotinylated sensor chip (Attana AB, Stockholm, Sweden) resulting in a frequency shift of 50 Hz. The highest analyte concentration was 100 nM for the Fc fusion proteins and 1 µM for the scDb-C_H2 and two-fold dilution were prepared. PBST (0.1 %) pH7.4 was used for the

regeneration of the Fc fusion proteins, 20 mM glycine-HCl pH1.95 for the scDb-C_H2. All other conditions were identical to the previously described method.

2.8 Enzyme-linked immunosorbent assay

In order to determine the half-maximal binding or the concentration of recombinant protein in a sample, CEA-binding ELISA was performed for all scDb, scFv or Fc fusion proteins. CEA was coated over night with a concentration of 3 µg/ml in 100 µl PBS per well of a 96-well plate. The next day, remaining binding sites were blocked with MPBS, which was also used for adjacent dilutions of samples and detection antibodies. Binding was also determined in the presence of excess amounts of human IgG (100 µg/ml), which was preincubated with the samples in MPBS. After 2 h of blocking, 100 µl of diluted samples in duplicates were added to the plate and incubated for 1 h. For the removal of unbound protein, the plates were washed twice with PBST (0.1 %) and once with PBS. Detection of His-tagged proteins was performed with 100 µl HRP coupled anti-His-tag antibody (1:2000) and anti-huIgG-HRP was used 1:5000 for the detection of Fc fusion proteins (Table 2-1). Another washing step was performed after 1 h incubation of the detection antibody. Finally, the ELISA was developed using 100 µl ELISA developing solution (100 mM NaOAc buffer pH6, 0.1 mg/ml TMB, 0.006 % H_2O_2). The enzymatic reaction was stopped upon addition of 50 µl ELISA stop solution (2 N H_2SO_4). The absorbance was measured at 450 nm in an ELISA reader. Data were fitted with GraphPad Prism software (La Jolla, USA) from three independent binding curves.

The capability of phages to bind to immunoglobulins and fragments thereof was also determined via ELISA. The procedure was similar to the previously described protocol with following modifications: 1 µg/ml of immunoglobulins was coated over night and detection was performed with anti-M13-HRP antibody.

2.9 Flow cytometry

2.9.1 Flow cytometry

The binding of the scDb-IgBD fusion proteins towards CEA and CD3 on the cell surface was investigated in a flow cytometric approach using CEA bearing LS174T cells and CD3 positive peripheral blood mononuclear cells purified from the buffy coat of healthy donors. Cells were detached from tissue culture flasks as described previously, centrifuged and resuspended in PBA to achieve a concentration of

2 x 10^6 cells/ml. All steps were subsequently performed on ice and with chilled liquids and centrifuges. All centrifugation steps were performed with 500 g for 5 minutes. The scDb-IgBD fusion proteins were diluted in PBA to a concentration of 1 µM, either in the absence or presence of 100 µg/ml huIgG. PBMCs were preincubated with 100 µg/ml huIgG for 15 min to block Fcγ receptors in order to prevent unspecific binding of the detection antibody. 100 µl of cell suspension per well were transferred to a U-shaped 96-well plate and supernatant was removed after centrifugation. The cell pellets were resuspended in the samples and incubated for 2 h. Supernatant was again removed after centrifugation and cells were washed twice with 150 µl PBA. The cells were incubated with 1:150 diluted anti-His-tag antibody conjugated with phycoerythrin for 2 h in the dark and subsequently washed twice with 150 µl PBA. Finally, cells were analyzed via the MACSquant Analyzer 10 (Milteny, Bergisch Gladbach, Germany) using channel B2. Data were fitted with GraphPad Prism software (La Jolla, USA) from three independent binding curves.

2.9.2 Purification of peripheral blood mononuclear cells

PBMCs were isolated from the buffy coat of healthy donors provided by the Katharinenhospital (Stuttgart, Germany). The buffy coat was diluted in RPMI 1640 to a total volume of 240 ml. 30 ml thereof were carefully added to 10 ml Ficoll per tube, followed by centrifugation (800 g, 20 min, without brake). The resulting interphase was collected and diluted in RPMI 1640 to 40 ml and centrifuged (645 g, 15 min). The cell pellet was resuspended in RPMI 1640 and washed twice by centrifugation (200 g, 10 min) to remove residual platelets. For storage, cells were frozen in FCS containing 10 % DMSO in an isopropanol containing cryobox at -80 °C until usage.

2.10 Serum stability

Serum stability was determined for the Fc fusion proteins. The recombinant proteins were diluted to a final concentration of 200 nM in 50 % mouse serum and incubated at 37 °C for 0, 1 or 7 days and immediately frozen at -20 °C. The content of intact protein was determined by CEA-binding ELISA as described above. The samples were diluted to their previously determined EC_{50} value and concentrations were determined by interpolation from a standard curve.

2.11 Interleukin release

Carcinoembryonic antigen positive LS174T cells were seeded in a 96-well cell culture plate (10^5 cells per well in 100 µl culture medium). Additionally, purified PBMCs were

thawed and placed on tissue culture plates over night. The next day, supernatant was removed and the LS174T cells were incubated with serial dilutions of scDb-IgBD fusion proteins starting at a final concentration of 31.6 nM in RPMI 1640 and 10 % FCS. The fusion proteins were incubated with or without 100 µg/ml huIgG (final concentration) prior to the addition to the LS174T cells. After 1 h binding at 37 °C, 2 x 10^5 PBMCs that were not attached to the plastic surface were added in each well and incubated at 37 °C. 24 h later, the tissue culture plate was centrifuged (500 g, 5 min) and the cell-free supernatant was collected and frozen for further analysis via the IL-2 sandwich ELISA kit according to manufacturer's protocol.

2.12 EPO dependent proliferation

UT-7/EPO cells were starved over night in IMDM with 10 % FCS, but without EPO. On day 0, 5000 cells per well were seeded into a flat bottom tissue culture 96-well plate. Dilutions of huEPO-IgBD proteins were incubated with or without an excess of huIgG (100 µg/ml) prior to addition to the cells. The tissue culture plate with a total volume of 100 µl per well was then incubated for 4 days at 37 °C. In order to determine the proliferative potential of the huEPO-IgBD fusion proteins, an MTT assay was performed. 10 µl of MTT were added to the cells and enzymatic reduction reaction of the thiazol blue tetrazolium bromide was carried out for 2 h at 37 °C. The reaction was stopped by adding 90 µl of MTT lysis buffer and shaking for 3 h at 37 °C, to dissolve the converted formazan. By measuring absorption at 570 and 660 nm in the ELISA reader, the relative amount of proliferating cells could be determined. Data were fitted with GraphPad Prism software (La Jolla, USA) from three independent binding curves.

2.13 Pharmacokinetics

Animal care and all experiments performed were in accordance with federal guidelines and have been approved by university and state authorities. Female CD1 mice of 6-12 weeks (25-35 g) received one intravenous injection of 25 µg recombinant protein in a total volume of 150 µl. Blood samples (50 µl) were collected from the tail vein at 3 min, 30 min, 1 h, 2 h, 6 h, 1 day, 3 days and 7 days and immediately incubated on ice. Serum was separated by centrifugation (13,000 g, 20 min, 4 °C) and stored at -20 °C. Serum concentration of CEA-binding scDb-IgBD, scFv-IgBD and Fc fusion proteins was determined by ELISA (as explained above) and normalized to the first time point (3 min). Concentration of huEPO-IgBD fusion

proteins was obtained by EPO dependent proliferation of UT-7/EPO cells as described above. Pharmacokinetic parameters (initial and terminal half-life and area under the curve) were calculated using Excel.

2.14 Pharmacodynamics

Animal care and all experiments performed were in accordance with federal guidelines and have been approved by university and state authorities. 20 µg of huEPO and 26.7 µg of huEPO-IgBD fusion proteins (due to the increased size of the IgBD fusion proteins) and the corresponding amount of Aranesp (3.3 µg, calculated from the bioactivity in UT-7/EPO proliferation) in a total volume of 100 µl were injected intravenously into female CD1 mice (6 weeks, 25 g, groups of 7 animals). Blood samples were collected at day 0, 3, 7, 10, 14, 17 and 21 from the tail vein with heparinized microhematocrit tubes (20 µl) to prevent clotting. Samples were diluted 1:500 in water and hemoglobin concentration was determined via hemoglobin assay kit, according to manufacturer's protocol, based on colorimetric conversion and measurement in the ELISA reader at 400 nm.

2.15 Statistical analysis

All *in vitro* values are shown as mean and the corresponding standard deviation. Likewise the pharmacokinetic experiments are displayed with mean and standard deviation, only the hemoglobin concentration was depicted as mean and standard error. Significances were always calculated with GraphPad prism one-way Anova with Tukey's post-test. * represents a p-value below 0.05, ** below 0.01 and *** below 0.001.

3 Results

3.1 New domains from *Streptococcus* Protein G

The *Streptococcus* Protein G encloses three domains that are capable of high affinity binding to Immunoglobulin G, namely C1, C2 and C3 (Akerström and Björck 1986). These domains possess two different binding sites on an IgG molecule, one located at the C_H1 domain of the Fab arm and the other at the interface of C_H2 and C_H3 overlapping with the binding site of the neonatal Fc receptor (Figure 3-1) (DeLano et al. 2000). In an acidified endosome, an immunoglobulin-binding domain (IgBD) bound to the Fc part could possibly interfere with the FcRn and prevent the recycling. For that reason, we identified amino acids that are responsible for binding to the Fc and Fab part from the crystal structures of the homologous domain SpG_{C2} bound to the Fc part (Sauer-Eriksson et al. 1995) and the domain SpG_{C3} together with the Fab fragment (Derrick and Wigley 1994). Thus, we endeavored to generate mutants of SpG_{C3} that selectively bind to the Fc or Fab arm of an IgG molecule.

3.1.1 Generation of a Fab and Fc fragment specific IgBD

In order to create an IgBD that specifically binds to the Fab fragment of an IgG molecule, the binding to the Fc part had to be disrupted by converting three amino acids located in the α-helix of SpG_{C3} into alanines (SpG_{C3Fab}: Glu27, Lys28, Lys31).

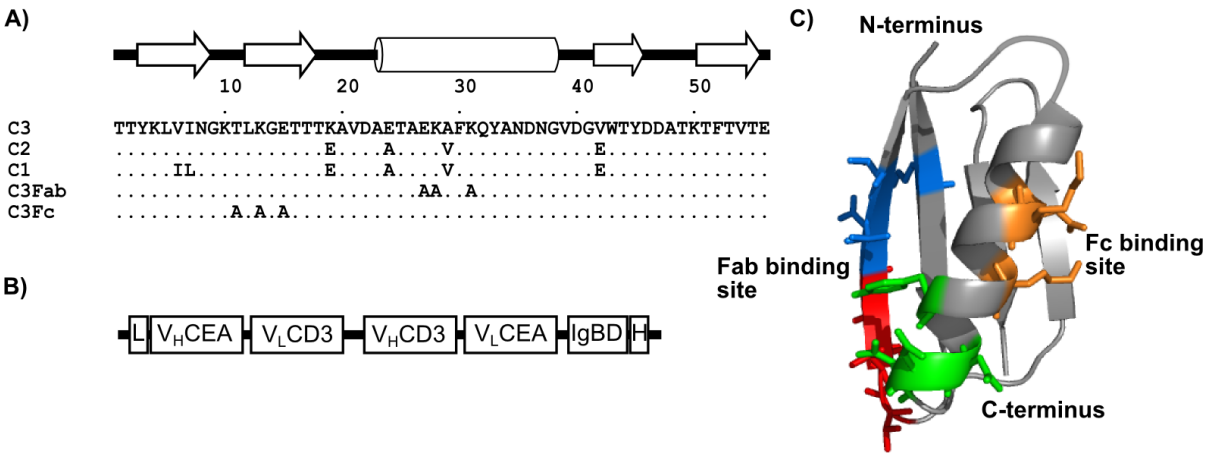

Figure 3-1: Fab and Fc binding sites in SpG_{C3}

A) Alignment of the different Protein G derived IgBDs as well as the mutated variants for specific binding. Arrows indicate the position of β-strands, the cylinder represents the α-helix. (Derrick and Wigley 1994; Sauer-Eriksson et al. 1995) B) Schematic model of the genetic composition of an scDb-IgBD. The Ig kappa leader is represented by "L", the hexahistidyl-tag by "H". C) Crystallized structure of SpG_{C3} domain with the Fab binding site highlighted in blue, red and green and the Fc binding amino acids in orange.

The major binding site for the C_H1 domain lies on the opposite site of the helix and is predominantly composed of β-strands. Analogously, three amino acids of that binding site were substituted by alanines (SpG_{C3Fc}: Thr11, Lys13, Glu15). Furthermore, the homologue domain SpG_{C2}, differing in 4 amino acids from SpG_{C3}, was included in the study. The IgBDs were fused C-terminally to a bispecific single-chain diabody (scDb) directed against the carcinoembryonic antigen (CEA) and CD3. For detection and purification, a hexahistidyl-tag was endowed at the very C-terminus. The fusion proteins were stably transfected into HEK293 cells and purified from serum-free cell culture supernatant by immobilized metal affinity chromatography after protein precipitation with ammonium sulfate. The protein integrity was verified via SDS-PAGE analysis as well as size exclusion chromatography (Figure 3-2). All fusion proteins showed clear bands corresponding to their molecular mass of roughly 60 kDa and single peaks with hydrodynamic radii between 2.9 and 3.3 nm (Table 3-2).

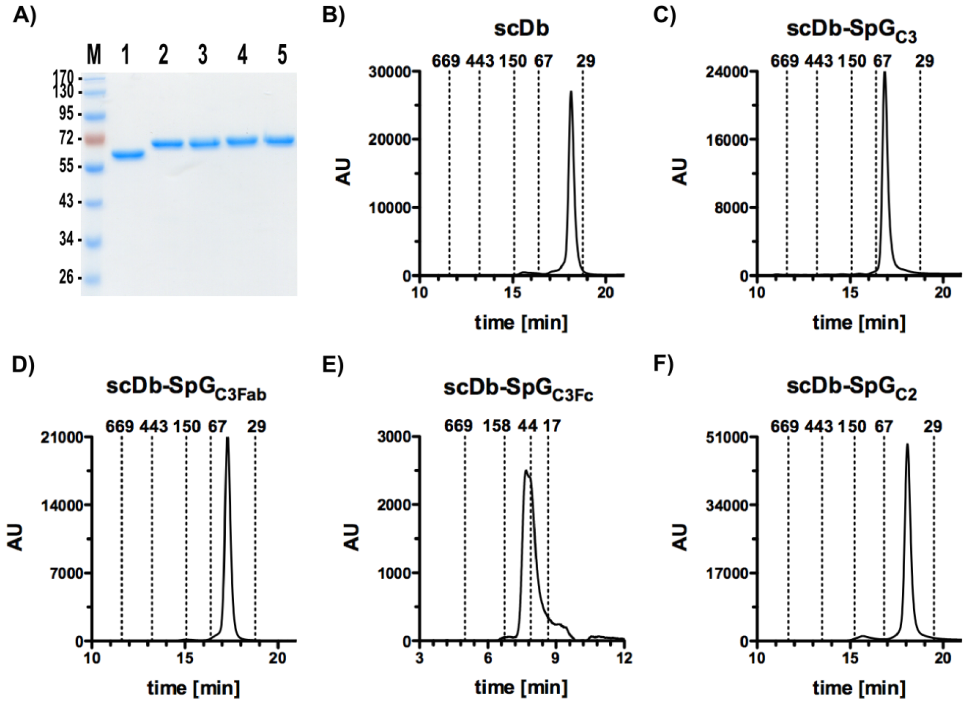

Figure 3-2: Size determination of purified scDb-fusion proteins

A) 3 µg of purified scDb or scDb-IgBD fusion protein per lane were applied to a 12 % PAA-gel under reducing conditions. Lane 1: scDb, 2: scDb-SpG_{C3}, 3: scDb-SpG_{C3Fab}, 4:scDb-SpG_{C3Fc}, 5: scDb-SpG_{C2}. B-F) 20 µl of 0.5 mg/ml scDb-IgBD fusion proteins were analyzed for their purity and integrity via size exclusion chromatography on a Yarra SEC-2000 column, with PBS as liquid phase. Dashed lines represent the retention time of standard proteins with their molecular masses indicated above the lines.

3.1.2 *In vitro* characterization of new IgBDs

The binding properties of the IgBDs towards immunoglobulins and fragments thereof were investigated by quartz crystal microbalance (QCM) measurements via the Attana Cell A200 system. For this purpose, human and mouse serum IgG as well as Fab or Fc fragments were chemically immobilized on the surface of sensor chips and binding was determined by a frequency shift upon applying the soluble scDb-IgBD fusion proteins. As seen in a previous study (Hutt et al. 2012), the unmodified SpG_{C3} domain bound strongly to human and mouse IgG and in accordance to the literature both the Fab and the Fc part (Derrick and Wigley 1994; Sauer-Eriksson et al. 1995) (Figure 3-3 and Table 3-1). This could be confirmed for neutral conditions as well as at pH6. By identifying the amino acids that are responsible for binding to the Fc part and converting them to alanines, we were able to generate the mutant SpG_{C3Fab}, which still showed strong binding to human and mouse IgG and Fab, but no or only minor binding was detected towards the Fc fragments at neutral pH. Of note, the affinity towards the Fab fragments was maintained or even slightly enhanced at acidic and physiological settings with below 100 nM for all conditions (Table 3-1). On the other side, the affinity to the full-length IgG could not be completely conserved, still showing an affinity of 120 nM and 61 nM to human and mouse IgG, respectively. Interestingly, the SpG_{C3Fab} domain was able to bind to as well the human as the mouse Fc part to some extent under acidic conditions. All binding profiles revealed biphasic interaction curves, presumably due to the heterogeneity of the immunoglobulin preparations. Therefore, all dissociation constants were determined with a biphasic fit. The domains SpG_{C3Fc} and SpG_{C2} displayed binding kinetics that were comparable with the ones determined for the SpG_{C3} domain and with dissociation constants in a similar range. Taken together, the amino acid substitutions of SpG_{C3Fab} (E27A, K28A, K31A) specifically eliminated the binding of the domain to the Fc part, at least under neutral conditions. More importantly, the binding to the Fab fragment was sustained.

All scDb-IgBD variants showed dose-dependent binding to CEA in ELISA with comparable EC_{50} values in the low or even sub-nanomolar range (Figure 3-4 and Table 3-2). Without IgG being present during the binding reaction, all fusion proteins displayed similar binding curves. Excess amounts of IgG in the surrounding medium did not alter the behavior of the scDb or the scDb-SpG_{C3Fab}, but the fusion to either

the wild-type domains SpG_{C3} and SpG_{C2} or SpG_{C3Fc} resulted in a lower binding to CEA. The EC_{50} values of these constructs that are able to bind to the Fc part are shifted significantly by a factor of 5 to 10, compared to the unmodified scDb as well as to the scDb-SpG_{C3Fab}.

Table 3-1: Affinities of IgBDs towards immunoglobulins and fragments

	pH	human						mouse					
		IgG		Fab		Fc		IgG		Fab		Fc	
		K_{D1}	K_{D2}	K_{D1}	K_{D2}	K_{D1}	K_{D2}	K_{D1}	K_{D2}	K_{D1}	K_{D2}	K_{D1}	K_{D2}
SpG_{C3}	7.4	3	38	159	663	6	17	33	593	118	1100	79	926
	6	2	33	95	667	1	28	27	406	130	874	53	858
SpG_{C3Fab}	7.4	120	983	88	969	-	-	61	1030	96	1620	-	-
	6	169	1520	83	753	767	896	54	822	93	826	38	414
SpG_{C3Fc}	7.4	2	31	74	688	3	52	28	405	112	1860	1710	1870
	6	19	151	76	58	94	526	50	850	61	1050	48	474
SpG_{C2}	7.4	1	26	42	1030	4	12	146	794	54	959	33	648
	6	55	525	42	426	125	803	671	857	75	398	34	389

- no binding detected K_Ds in [nM]

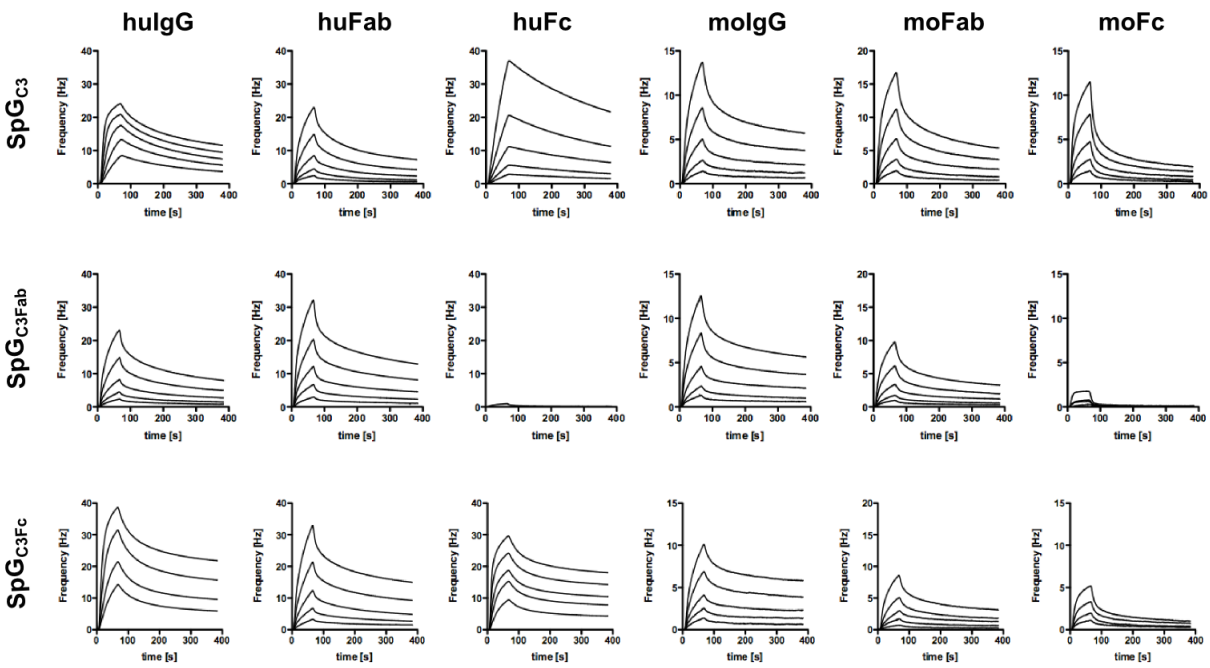

Figure 3-3: Specificity in immunoglobulin binding

Two-fold serial dilutions of scDb-IgBDs in random order were injected into the Attana QCM system. All measurements were performed at pH7.4. The starting concentration was 1000 nM, except for the following conditions: scDb-SpG_{C3} was injected with 250 nM for huIgG, 40 nM for huFc, 500 nM for moIgG, 1500 nM for moFab, 1280 nM for moFc. scDb-SpG_{C3Fc} was injected with 250 nM for huIgG.

The binding properties of the scDb-moiety were also examined in a flow cytometric approach, using CEA bearing LS174T cells and CD3 positive PBMCs to determine

whether the IgBD impacts the cellular binding of the scDb (Figure 3-5 and Table 3-2). The CEA binding on cells was comparable to the binding in the ELISA study with similar EC_{50} values around 1 nM in the absence of IgG for all constructs. Interestingly, unlike in the ELISA, the EC_{50} values of scDb-SpG_{C3} and scDb-SpG_{C3Fc} hardly changed with excess IgG, similar to the unmodified scDb and scDb-SpG_{C3Fab}. Next, the binding to the CD3 was investigated, which is located on the surface of T-cells, a subpopulation of purified PBMCs. The binding profile of scDb-SpG_{C3} and scDb-SpG_{C3Fc} already differed from the unmodified scDb and scDb-SpG_{C3Fab} without the excess of IgG, causing a 4 to 5-fold weaker binding (3.4 and 2.2 nM, compared to 0.6 nM). Again, no negative impact of IgG was observed for the scDb and scDb-SpG_{C3Fab}, but especially the scDb-SpG_{C3} was strongly influenced resulting in an EC_{50} value of about 26 nM indicating a more than 40-fold decreased binding towards CD3 in the presence of IgG than the scDb alone.

Table 3-2: Characterization of scDb-IgBD fusion proteins

	M [kDa]	S_r [nm]	ELISA EC_{50} CEA [nM]		FACS EC_{50} CEA [nM]		FACS EC_{50} CD3 [nM]	
			- IgG	+ IgG	- IgG	+ IgG	- IgG	+ IgG
scDb	52.9	2.6	0.7	0.7	1.0	1.1	0.5	0.6
scDb-SpG_{C3}	59.6	3.2	0.4	3.4	1.2	2.1	3.4	26.3
scDb-SpG_{C3Fab}	59.5	3.0	0.3	0.4	0.7	1.0	0.6	0.6
scDb-SpG_{C3Fc}	59.5	3.3	0.3	3.2	0.8	1.5	2.2	7.6
scDb-SpG_{C2}	59.6	2.9	0.4	1.7	n.d.	n.d.	n.d.	n.d.

n.d. not determined

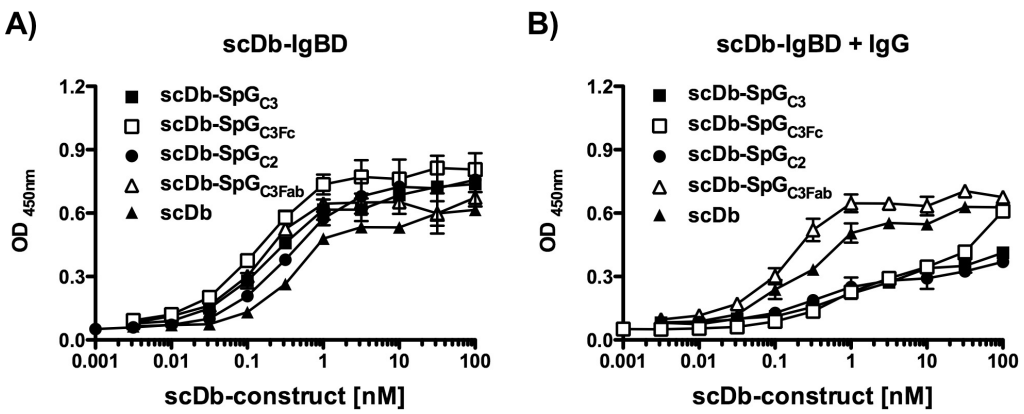

Figure 3-4: CEA-binding ELISA

Binding of scDb-IgBD fusion proteins to CEA was investigated by ELISA in the absence (A) or presence (B) of 100 µg/ml huIgG during the binding reaction. Serial dilutions of scDb-IgBD fusion proteins were applied to immobilized CEA on ELISA plates. The fusion proteins were detected via HRP coupled anti-His-tag antibody.

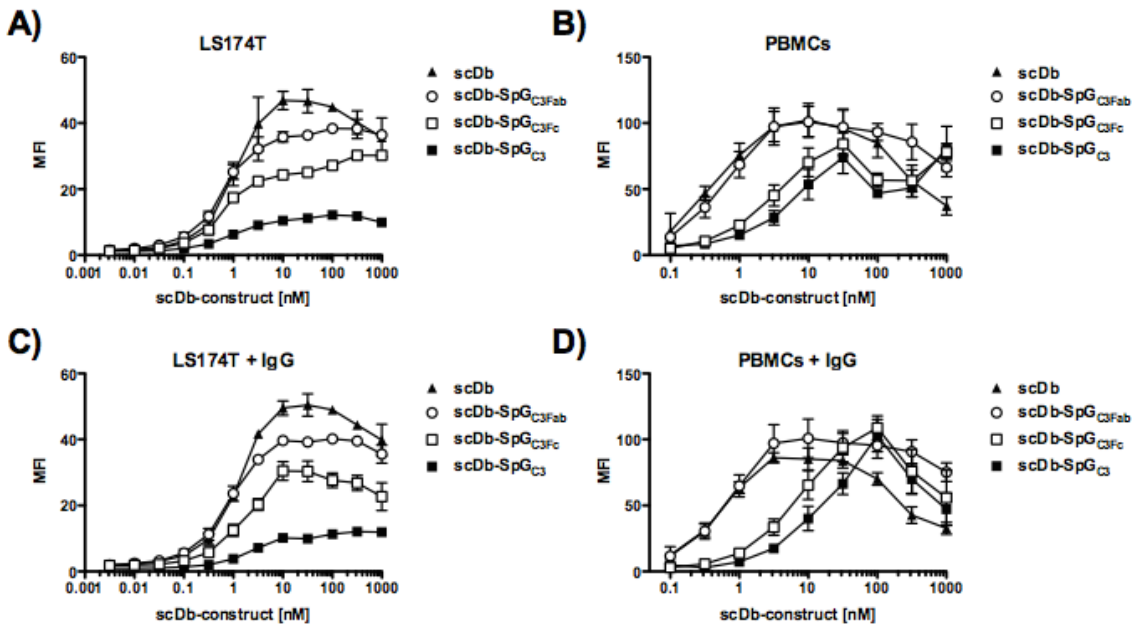

Figure 3-5: Flow cytometry

Binding of CEA and CD3 by scDb-IgBD fusion proteins on the surface of cells was determined with CEA bearing LS174T cells (A and C) and CD3 positive PBMCs (B and D) in the absence (A and B) or presence (C and D) of 100 µg/ml huIgG during the binding reaction. In order to avoid unspecific binding of the PE-labeled anti-His-tag detection antibody, the Fc receptors on the surface of purified PBMCs were blocked with 100 µg/ml huIgG prior to the addition of the scDb fusion proteins.

After the binding studies, the functionality of the scDb moiety to crosslink T-cells to antigen bearing cells and subsequently activate them was examined in an interleukin-2 release assay. The colon carcinoma cell line LS174T that is positive for the tumor-associated antigen CEA (Mayer et al. 1999) was incubated with PBMCs as effector cells with different concentrations of the scDb-IgBD fusion proteins. All of the scDb fusion proteins were able to stimulate effector T-cells to produce IL-2 in a dose dependent manner, resulting in a maximal secretion between 3 and 10 nM of scDb-IgBD (Figure 3-6). In the absence of excess amounts of human IgG, all scDb fusion proteins exhibited the same activation level as the unmodified scDb. Conversely, performing the assay in the presence of huIgG leads to a reduction in the secretion of IL-2 for the scDb-SpG$_{C3}$ and scDb-SpG$_{C3Fc}$. The scDb-SpG$_{C3Fab}$ is the only IgBD-fusion protein that was able to stimulate the T-cell response in the same manner as the unmodified scDb in the presence of human IgG.

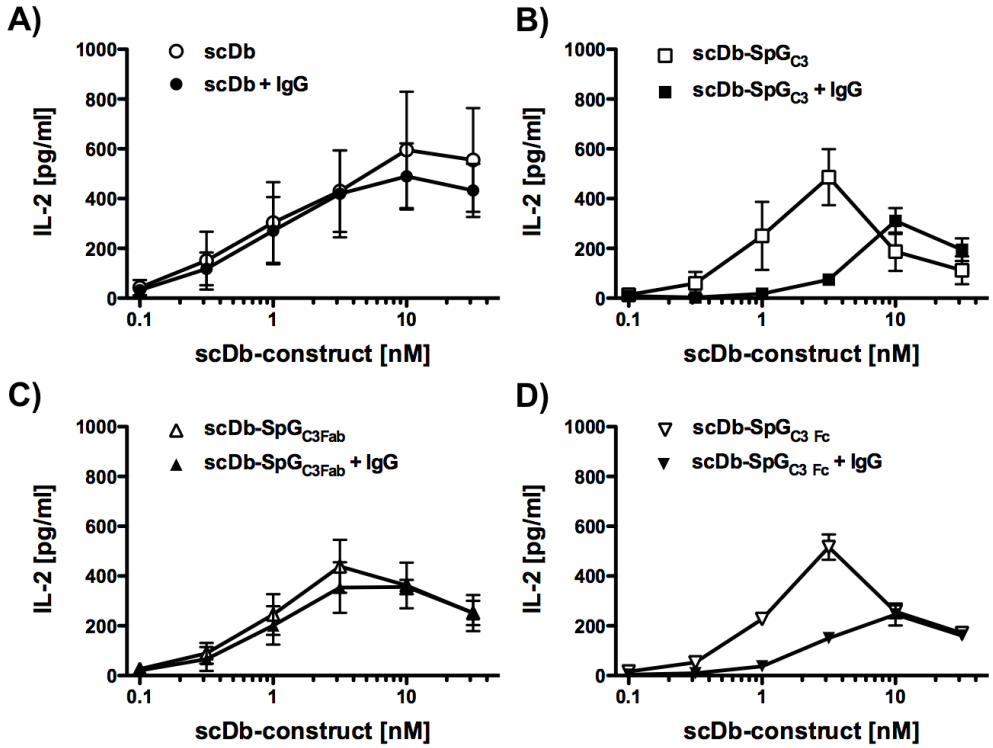

Figure 3-6: scDb mediated IL-2 release through crosslinking of target and effector cell

LS174T colon carcinoma cells were preincubated with serial dilutions of scDb-IgBD fusion proteins. Purified PBMCs were added and enclosed T-cells subsequently crosslinked to the target cell. Activation was determined via IL-2 ELISA from cell free supernatant. The assay was performed in the absence (open symbols) or presence of 100 µg/ml huIgG (filled symbols).

3.1.3 *In vivo* characterization of new scDb-IgBDs

The pharmacokinetic properties were investigated after a single injection of 25 µg of fusion protein intravenously into female CD1 mice. The serum concentration was determined in a CEA-binding ELISA. The unmodified scDb molecule was rapidly cleared from the bloodstream, reaching the limit for detection after only 6 h. This resulted in a terminal half-life of 1.3 h (Figure 3-7 and Table 3-3). By the fusion of the SpG$_{C3Fab}$ domain, we could elongate the half-life to 15.1 h, going along with a more than 18-fold enhancement in the area under the curve. Nonetheless, the pharmacokinetic properties of scDb-SpG$_{C3}$ with a terminal half-life of 24.3 h could not be reached. The scDb-SpG$_{C2}$ obtained a terminal retention time of 17.3 h and is only marginally better than the scDb-SpG$_{C3Fab}$ although it is able to bind to the Fc part. On the other side, the scDb-SpG$_{C3Fc}$ mutant exhibited a terminal half-life of 32.5 h and is even better than the unmodified SpG$_{C3}$ fusion protein. These finding are all reflected in the bioavailability of the molecules determined as area under the curve. The elongation in half-life strongly correlated with an increase in the AUC, with the scDb-SpG$_{C3}$ augmenting the AUC by a factor of more than 33 and the SpG$_{C3Fc}$ fused

scDb even 38-fold. However, the fusion of the SpG_{C3Fab} domain also resulted in a more than 18-fold amelioration of the bioavailability of the scDb moiety.

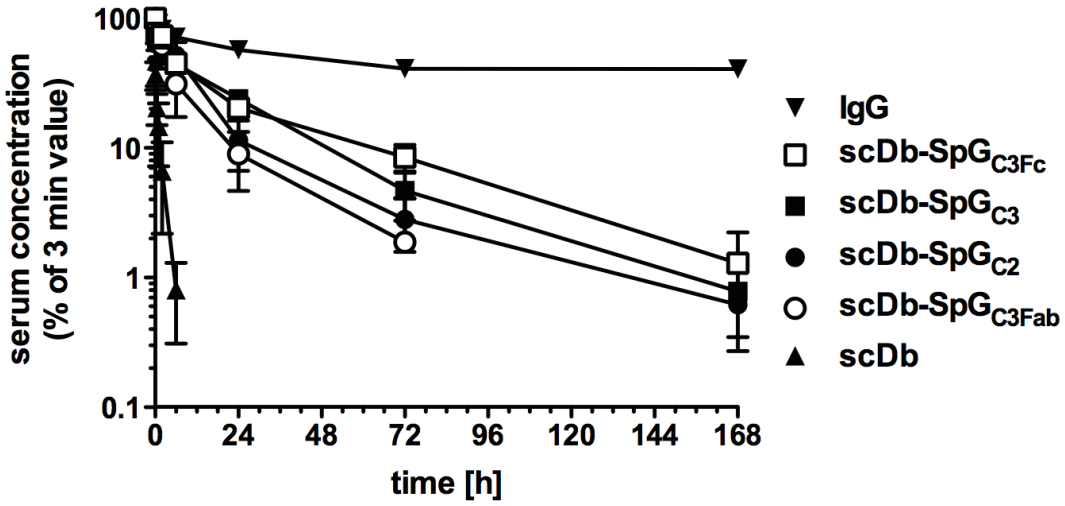

Figure 3-7: Pharmacokinetic properties of scDb-IgBD fusion proteins

25 µg of purified scDb-IgBD fusion protein were injected intravenously in to female CD1 mice. Blood samples were collected at indicated time points and serum concentration was determined using a CEA-binding ELISA. Concentrations were normalized to the value determined at 3 minutes.

Table 3-3: Pharmacokinetic properties of the scDb-IgBD fusion proteins

	Initial half-life [h]	Terminal half-life [h]	AUC [%h]
scDb	0.4 ± 0.1	1.3 ± 0.2	56 ± 15
scDb-SpG_{C3}	3.8 ± 1.4	24.3 ± 6.8	1879 ± 279
scDb-SpG_{C3Fab}	3.7 ± 2.7	15.1 ± 4.8	1027 ± 506
scDb-SpG_{C3Fc}	5.3 ± 1.0	32.5 ± 7.2	2146 ± 243
scDb-SpG_{C2}	4.3 ± 0.9	17.3 ± 4.1	1364 ± 332

3.2 Affinity maturation of SpG_{C3Fab}

A plausible reason for the shortened half-life of the scDb-SpG_{C3Fab} might be the loss of affinity towards the whole IgG molecule and thus an increased clearance. Therefore, we attempted to increase the affinity towards the C_H1 domain in order to get the same protection from renal filtration and to avoid the possible interference with the FcRn during the recycling process. A phage display approach was chosen to fulfill this requirement and the amino acids that were identified to contribute to the C_H1 binding were randomized.

3.2.1 Phage display selection of affinity maturated SpG_{C3Fab} variants

Four different libraries were generated, three of them with site-directed mutagenesis via degenerate primers comprising a set of 4 amino acid substitutions each, the

fourth via error prone PCR over the whole SpG_{C3Fab} domain (Figure 3-8). For the libraries with site-directed mutagenesis, 4 amino acids were substituted with all 20 possible amino acids, meaning a diversity of 20^4 = 160,000 mutants. To cover the full diversity of the library, at least a ten-fold excess of different mutants in the generation of the library is needed. Having a size of 2 to 8 x 10^6 clones, all libraries met this criterion and were subsequently rescued for phage display. Library 4 was generated using a random mutagenesis approach for the whole sequence of the SpG_{C3Fab} domain. This resulted in a library comprising of 25 x 10^6 clones, with a rate of about 2.4 nucleotide exchanges per 168 nucleotide long sequence and an average of 1.5 amino acid substitutions per domain.

All libraries were selected over three to four rounds, either by immunotube selection against mouse Fab fragment or by incubation with biotinylated mouse Fab fragment and subsequent pull-down with streptavidin-coated beads with increasing stringency. In order to reveal the progress of the selection, polyclonal phage ELISA was conducted to see the enrichment of high affinity phages (Figure 3-9). After selection, single clones were picked and a small-scale rescue in a 96-well plate was performed to screen for the best binders. Top candidates were sequenced and subject to further investigation and subcloning as scDb-fusion proteins.

```
                        10        20        30        40        50        Size
                         .         .         .         .         .        [10^6]
SpG_C3Fab       TTYKLVINGKTLKGETTTKAVDAETAAAAFAQYANDNGVDGVWTYDDATKTFTVTE
Library 1       ...X..........XXX.......................................    8
Library 2       ..........XXXX.........................................    2
Library 3       ...............................X.XXX...................    2
Library 4       1.5 mutations equally distributed throughout sequence      25
```

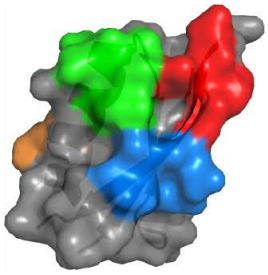

Figure 3-8: Libraries for phage display

Three different libraries were generated with 4 amino acid substitutions into all 20 possible amino acids (Library 1: blue, library 2: red, library 3: green). Library 4 was derived from a random mutagenesis approach via error prone PCR, including the whole SpG_{C3Fab} domain.

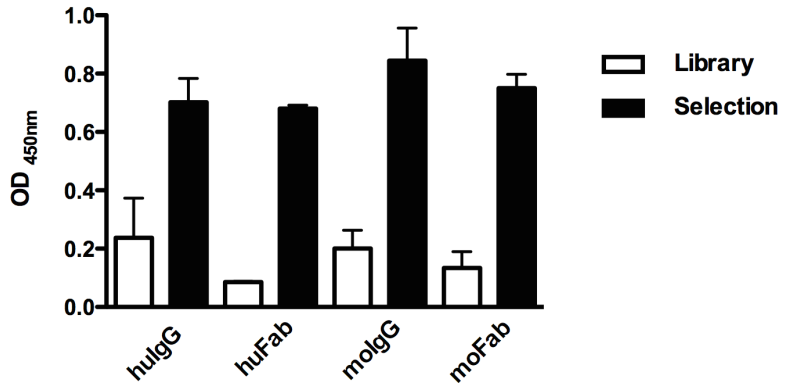

Figure 3-9: Polyclonal phage ELISA

The binding of the phages from the rescued library 3 was compared to the third selection round against biotinylated mouse Fab fragment. Similar amounts of precipitated phages were incubated with immobilized immunoglobulins and Fab fragments from mouse and human and detection was carried out with an anti-M13 HRP-conjugated antibody.

The binding of the resulting SpG_{C3Fab} mutants towards IgGs and fragments thereof was examined by quartz crystal microbalance measurements of the scDb fusion proteins to immobilized IgGs and fragments (Table 3-4). Most of the new mutants showed similar binding affinities as the wild-type. The two selected clones that exhibited the best binding properties, especially to mouse Fab fragment, were SpG_{C3Fab}RR and SpG_{C3Fab}K10Q,HNS, originating from library 3 and 4, respectively. In particular, their affinity under acidic conditions was augmented, for the murine Fab (19 and 25 nM, compared to 93 nM of SpG_{C3Fab}) and the whole IgG molecule (34 and 1 nM, compared to 54 nM of SpG_{C3Fab}), but their binding to the Fc part was not altered. They both displayed a marginally enhanced affinity at neutral pH towards the whole mouse IgG and Fab fragment, but as the SpG_{C3Fab} wild-type no binding to the mouse Fc part. Concerning the binding towards the human equivalents, SpG_{C3Fab}RR revealed the highest affinities towards the Fab fragment and full-length IgG molecule at acidic conditions with 40-50 nM. The binding to human IgG at pH7.4 was also more than 4-fold improved compared to the SpG_{C3Fab} domain and no affinity towards the human Fc part at physiological pH could be detected. Since the mutation E15V was discovered frequently in the selected clones from library 4, this mutant was combined with the SpG_{C3Fab}RR for SpG_{C3Fab}RR,E15V. This arrangement resulted in the lowest dissociation constant for mouse Fab at neutral pH (28 nM) and is also amongst the top candidates for binding to mouse IgG with a minor loss of affinity under acidic conditions. Interestingly, the binding to mouse Fc was restored to some extent at pH7.4, still showing a similar affinity as the wild-type at pH6. The affinity of the SpG_{C3Fab}RR,E15V domain towards human immunoglobulin and Fab fragment

was decreased under neutral and acidic conditions compared to SpG_{C3Fab}RR, with a complete loss of binding to the Fc part.

Table 3-4: Affinities of phage display derived SpG_{C3Fab} mutants

scDb-SpG_{C3Fab}	pH	human						mouse						Lib
		IgG		Fab		Fc		IgG		Fab		Fc		
		K_{D1}	K_{D2}	K_{D1}	K_{D2}	K_{D1}	K_{D2}	K_{D1}	K_{D2}	K_{D1}	K_{D2}	K_{D1}	K_{D2}	
wt	7.4	120	983	88	969	-	-	61	1030	96	1620	-	-	-
	6	169	1520	83	753	767	896	54	822	93	826	38	414	
TTR	7.4	1460	2500	n.d.	n.d.	n.d.	n.d.	207	1660	369	1220	n.d.	n.d.	1
	6	66	1560	n.d.	n.d.	n.d.	n.d.	81	1080	95	1550	n.d.	n.d.	
HTM	7.4	579	2060	n.d.	n.d.	n.d.	n.d.	237	1570	n.d.	n.d.	n.d.	n.d.	1
	6	328	1080	n.d.	n.d.	n.d.	n.d.	92	1150	n.d.	n.d.	n.d.	n.d.	
K13S	7.4	127	1730	n.d.	n.d.	n.d.	n.d.	72	889	95	1220	n.d.	n.d.	2
	6	179	1570	n.d.	n.d.	n.d.	n.d.	44	729	147	771	n.d.	n.d.	
FRQ	7.4	94	800	n.d.	n.d.	n.d.	n.d.	87	857	129	775	n.d.	n.d.	3
	6	n.d.	n.d.	n.d.	n.d.	n.d.	n.d.	48	688	n.d.	n.d.	n.d.	n.d.	
RR	7.4	29	385	167	1040	-	-	55	388	62	413	-	-	3
	6	49	191	43	461	39	227	34	296	19	255	40	289	
T1A,E15Q	7.4	84	1120	251	1080	-	-	61	1440	91	1210	-	-	4
	6	341	727	n.d.	n.d.	416	634	60	567	93	618	n.d.	n.d.	
E15V	7.4	89	1000	157	1700	-	-	69	838	73	876	-	-	4
	6	610	2060	47	648	517	1540	43	584	66	677	41	371	
E15V,YY	7.4	123	854	150	1030	-	-	40	247	50	342	-	-	4
	6	184	805	147	1270	91	424	14	177	45	241	78	460	
K10Q,HNS	7.4	159	1330	277	1280	-	-	36	380	58	525	-	-	4
	6	122	1070	83	795	19	427	1	233	25	315	75	560	
N35Y	7.4	92	1120	n.d.	n.d.	n.d.	n.d.	56	880	64	840	n.d.	n.d.	4
	6	n.d.	n.d.	n.d.	n.d.	n.d.	n.d.	25	579	41	414	n.d.	n.d.	
K50Q	7.4	112	1320	173	1210	-	-	65	1160	80	996	-	-	4
	6	695	1280	50	610	596	2050	53	516	90	530	45	462	
RR,E15V	7.4	326	1570	243	1730	-	-	38	177	28	161	106	617	3+4
	6	118	1080	242	1550	-	-	68	205	71	172	38	750	

n.d. not determined - no binding detected wt wild-type Lib Library K_Ds in [nM]

3.2.2 *In vitro* characterization of affinity maturated SpG_{C3Fab} mutants

The antigen binding of all scDb fusion proteins was subsequently examined in an ELISA to determine whether the modification of the SpG_{C3Fab} sequence had an impact on the functionality of the fusion partner. As seen before, all scDb-IgBDs that were derived from the SpG_{C3Fab} domain revealed full binding potential towards CEA in the subnanomolar range, independent from the presence of excess amounts of human IgG (Figure 3-10, data not shown). Analogous results were seen for the flow

cytometry with CEA bearing LS174T cells. Without IgG, the EC_{50} values were in the low nanomolar range and were not changed upon addition of IgG. Only the binding curves of scDb-SpG_{C3} and SpG_{C3Fc} were slightly, but significantly, shifted towards lower binding. The binding towards CD3 on cells was also only impacted for scDb-IgBDs that can bind strongly to the Fc part. All IgBDs originating from the SpG_{C3Fab} domain had similar EC_{50} values under both conditions.

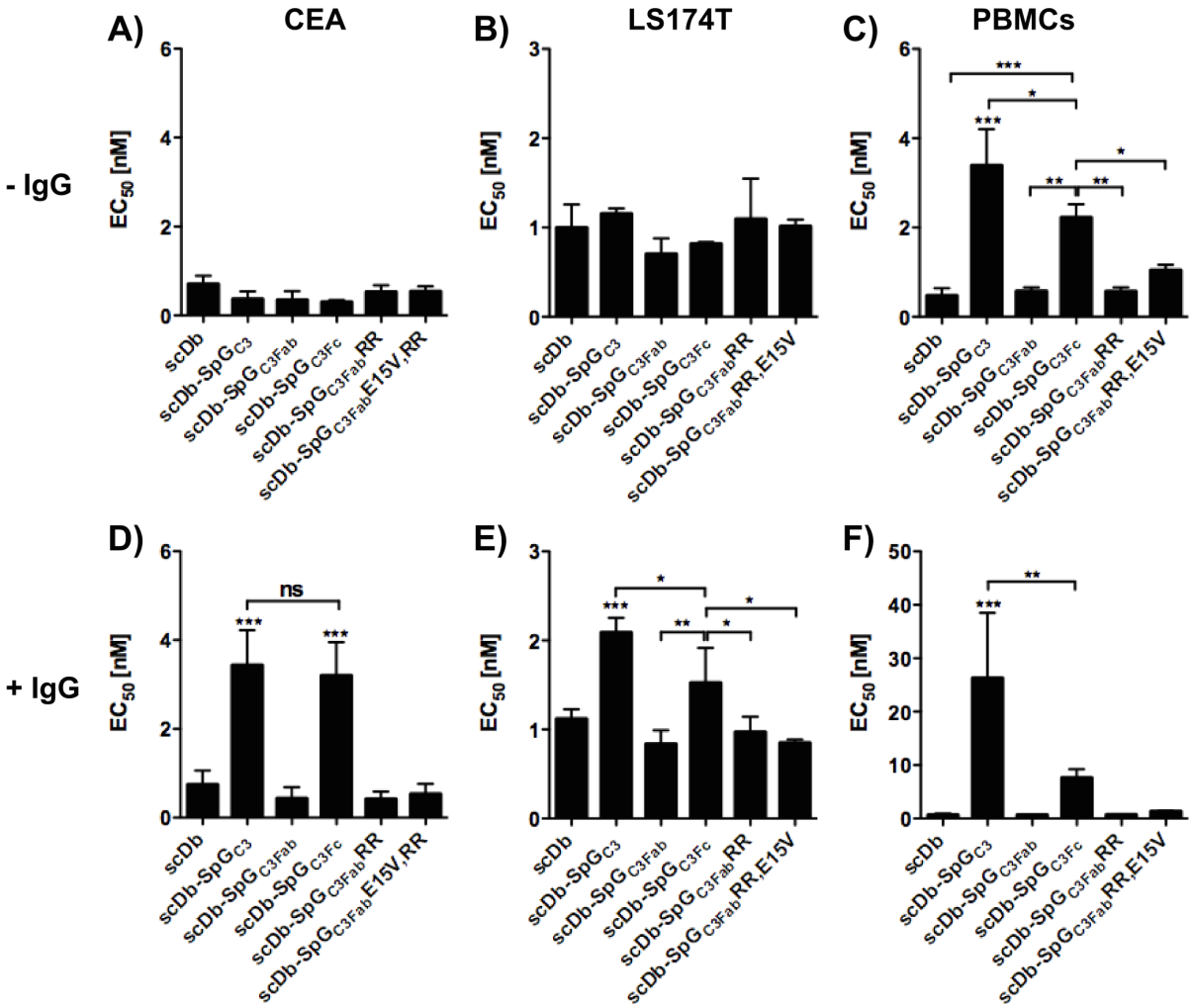

Figure 3-10: CEA-binding ELISA of affinity maturated SpG_{C3Fab} mutants

All scDb-IgBD constructs were titrated without (A, B, C) or with (D, E, F) 100 µg/ml huIgG to detect the binding of the scDb moiety. Binding to CEA was detected in an ELISA (A, D) and on LS174T colon carcinoma cells (B, E) via flow cytometry. Binding to CD3 was examined by flow cytometry on PBMCs (C, F). The EC_{50} values were calculated from the resulting binding curves with GraphPad Prism and were compared using one-way Anova together with Tukey's post-test.

The functionality of the new scDb-IgBDs was investigated by an IL-2 release assay (Figure 3-11). For each protein a different batch of PBMCs had to be used, but the unmodified scDb was always included as a positive control. Therefore, the maxima in activation were similar for all scDb-IgBD fusion proteins, only varying due to the

activity of the corresponding PBMC batch. The activation went along with the already obtained results that the scDb-IgBD variants derived from SpG_{C3Fab} were not hindered in their functionality in the presence of excess IgG. Hence, both new fusion proteins scDb-SpG_{C3Fab}RR and scDb-SpG_{C3Fab}RR,E15V stimulated the PBMCs to secrete IL-2 in an equivalent manner as the unmodified scDb.

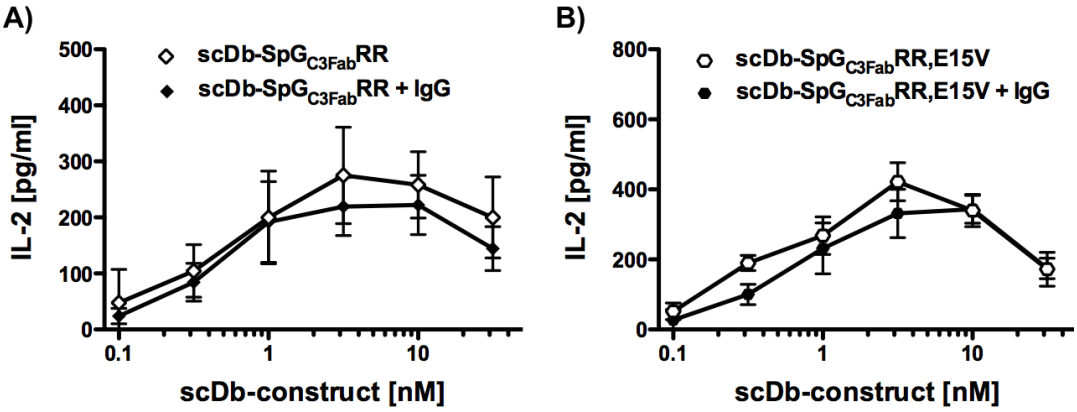

Figure 3-11: IL-2 release of affinity maturated SpG_{C3Fab} mutants

The IL-2 release assay was performed as described above with different batches of PBMCs for different proteins. Open symbols represent the scDb-IgBD in the absence of excess IgG, solid symbols represent the presence of 100 µg/ml huIgG.

3.2.3 *In vitro* characterization of scFv-IgBD fusion proteins

In order to demonstrate the power of the immunoglobulin-binding domains to improve the pharmacokinetics for different proteins than the scDb, a set of scFv-IgBD fusion proteins was generated and investigated to see the half-life extension effect also on molecules that possess half the size of an scDb. The proteins were expressed in HEK293 cells and purified via IMAC after ammonium sulfate precipitation. All scFv fusion proteins showed single bands at the calculated molecular mass of about 33 kDa in an SDS-PAGE analysis, both under reducing and non-reducing conditions (Figure 3-12). Additionally, the protein integrity and tendency to aggregate was determined via size exclusion chromatography. Again, all scFv-fusion proteins eluted in one single peak with similar hydrodynamic radii that were smaller than those of the corresponding scDb-IgBD fusion proteins (Table 3-6).

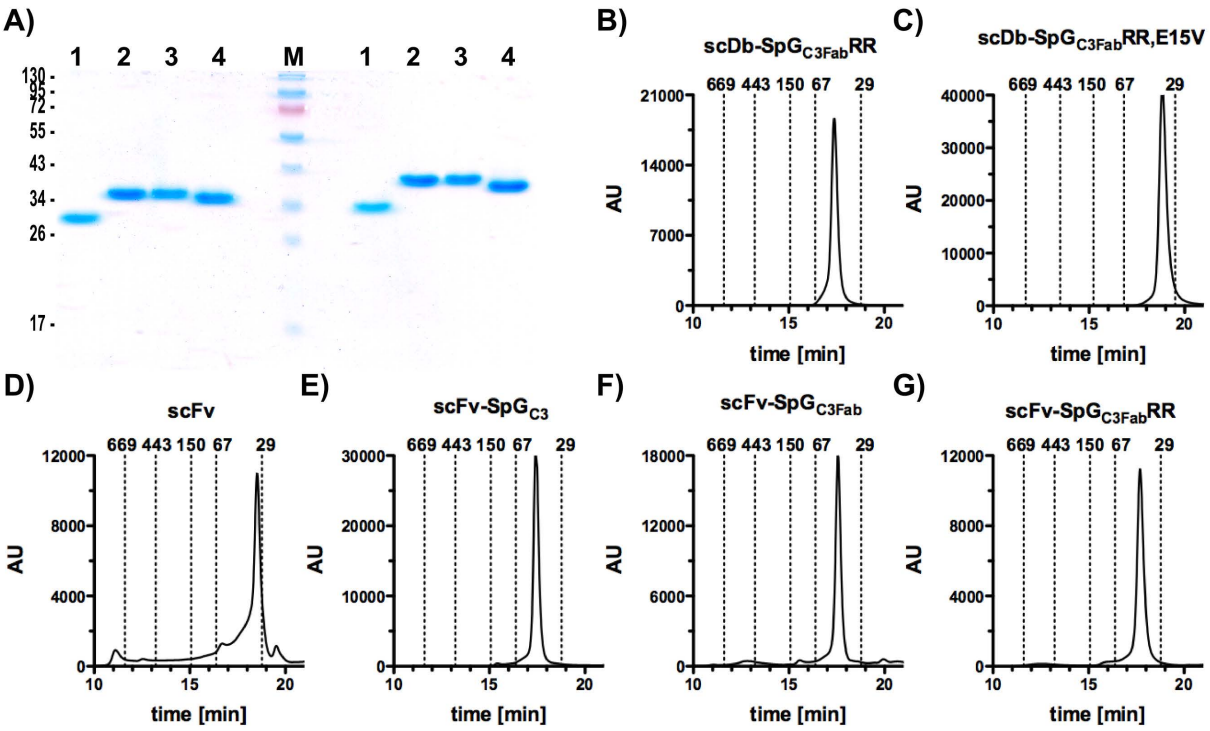

Figure 3-12: Purification of scFv and scDb-IgBDs

A) SDS-PAGE analysis was performed under reducing (left) and non-reducing (right) conditions on a 12 % PAA-gel. Lane 1: scFv; 2: scFv-SpG_{C3}; 3: scFv-SpG_{C3Fab}; 4: scFv-SpG_{C3Fab}RR; M: protein ladder with molecular masses in kDa. B-G) Size exclusion chromatography was performed to determine the integrity of scDb and scFv fusion proteins. Dashed lines represent the retention time of standard proteins with their molecular masses indicated above the lines.

3.2.4 *In vivo* characterization of affinity maturated scFv and scDb-IgBDs

Ultimately, the pharmacokinetic properties of the affinity maturated SpG_{C3Fab} mutants were determined by injection of scDb and scFv fusion proteins into CD1 mice (Figure 3-13). The variants of SpG_{C3Fab} that arose from library 1 displayed a pharmacokinetic profile below that of the scDb-SpG_{C3Fab}, going along with lower terminal half-lives and areas under the curve (Table 3-5). The only variant from library 2, SpG_{C3Fab}K13S, had equal properties in increasing the serum concentration as the wild-type SpG_{C3Fab} domain. The domain SpG_{C3Fab}RR that already exhibited superior binding properties extended the terminal half-life to 47.8 h, which is a more than 36-fold enhancement compared to the unmodified scDb and more than 3-fold the half-life of scDb-SpG_{C3Fab}. This elongation even exceeded the performance of the scDb-SpG_{C3} by almost a factor of 2 (24.3 h). Moreover, this gain in half-life was also reflected in an augmented area under the curve, where the scDb-SpG_{C3Fab}RR also had the best effect with about twice the area of the scDb-SpG_{C3Fab} and an almost 40-fold raised AUC compared to the scDb alone. Besides the scDb, we also used scFvs as model molecules and together with the SpG_{C3Fab}RR variant the fusion protein experienced

the strongest increase in half-life extension (Figure 3-14, Table 3-6). The half-life as well as the AUC are both more than 26-fold improved compared to the unmodified scFv and slightly better than for the scFv-SpG$_{C3}$. The remaining domain from library 3 (SpG$_{C3Fab}$FRQ) and the variants from library 4 were also examined in pharmacokinetic studies.

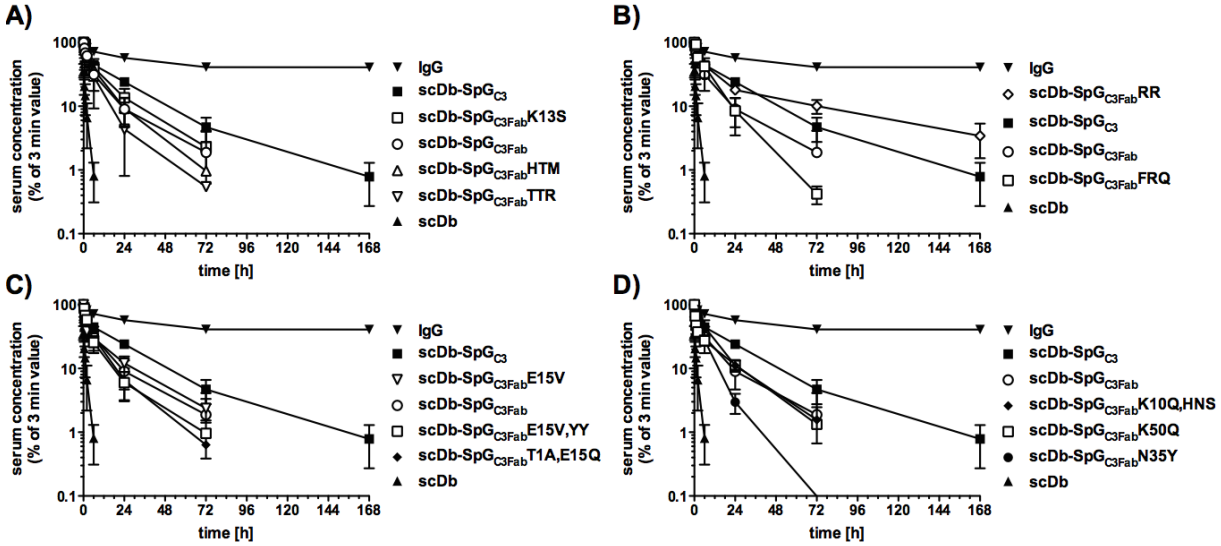

Figure 3-13: Pharmacokinetics of affinity maturated SpG$_{C3Fab}$ mutants as scDb fusion proteins

25 µg of scDb-fusion protein were injected intravenously into female CD1 mice. Blood samples were taken at indicated time points and serum concentration was determined via CEA-binding ELISA. Concentrations were normalized to the 3 minute value. The affinity maturated mutants from library 1 and 2 are shown in A), library 3 in B) and library 4 in C) and D).

Table 3-5: Pharmacokinetic properties of affinity maturated SpG$_{C3Fab}$ variants

	Initial half-life [h]	Terminal half-life [h]	AUC [%h]
scDb	0.4 ± 0.1	1.3 ± 0.2	56 ± 15
scDb-SpG$_{C3}$	3.8 ± 1.4	24.3 ± 6.8	1879 ± 279
scDb-SpG$_{C3Fab}$	3.7 ± 2.7	15.1 ± 4.8	1027 ± 506
scDb-SpG$_{C3Fab}$TTR	2.1 ± 0.7	6.2 ± 1.1	582 ± 322
scDb-SpG$_{C3Fab}$HTM	3.8 ± 1.5	8.0 ± 1.8	784 ± 123
scDb-SpG$_{C3Fab}$K13S	1.7 ± 0.3	15.4 ± 4.1	1187 ± 421
scDb-SpG$_{C3Fab}$FRQ	3.2 ± 2.2	8.7 ± 2.0	994 ± 435
scDb-SpG$_{C3Fab}$RR	2.1 ± 0.3	47.8 ± 10.3	2228 ± 380
scDb-SpG$_{C3Fab}$T1A,E15Q	1.6 ± 0.6	8.5 ± 2.4	719 ± 244
scDb-SpG$_{C3Fab}$E15V	1.5 ± 0.4	19.0 ± 5.0	981 ± 233
scDb-SpG$_{C3Fab}$E15V,YY	2.5 ± 0.5	14.2 ± 1.8	761 ± 202
scDb-SpG$_{C3Fab}$K10Q,HNS	4.7 ± 9.8	13.9 ± 2.1	1310 ± 325
scDb-SpG$_{C3Fab}$N35Y	1.3 ± 0.1	8.4 ± 0.7	614 ± 44
scDb-SpG$_{C3Fab}$K50Q	1.4 ± 0.1	14.4 ± 1.6	1004 ± 256
scDb-SpG$_{C3Fab}$RR,E15V	2.7 ± 1.8	67.0 ± 24.4	2843 ± 831

Only scDb-SpG$_{C3Fab}$E15V exhibited a slightly longer terminal half-life than scDb-SpG$_{C3Fab}$, all the other mutations did not improve the performance of the fusion protein. Combining these results, the new mutant SpG$_{C3Fab}$RR,E15V was generated and investigated as fusion partner for the scDb. This domain was able to further promote the terminal half-life to 67 h, a more than 50-fold amelioration of the original scDb. This strong benefit in half-life was also mirrored in a strongly amplified AUC (2843 %h) that is significantly better than the AUC of scDb-SpG$_{C3}$.

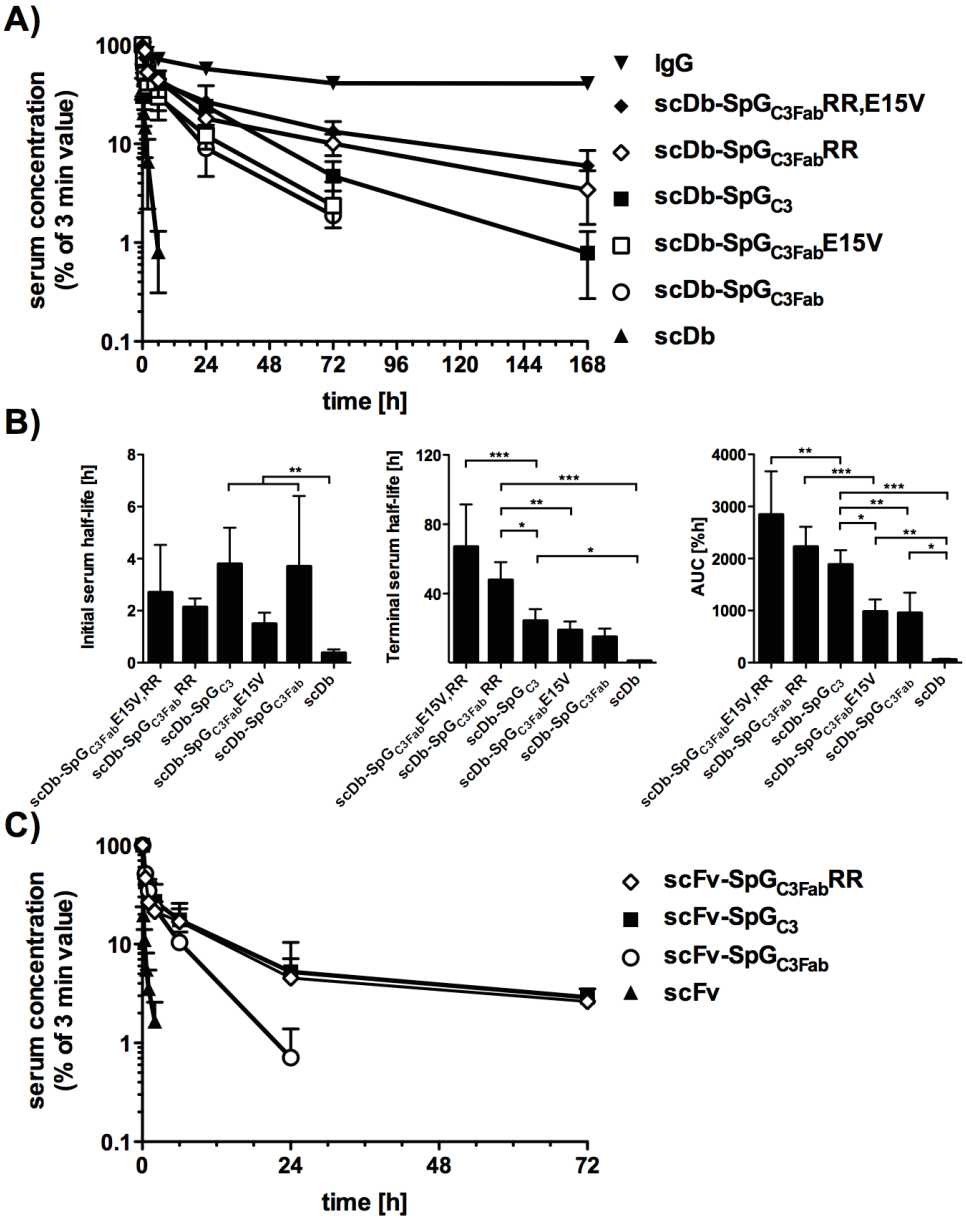

Figure 3-14: Pharmacokinetic studies of most improved IgBDs

25 µg of scDb-IgBDs (A) or scFv-IgBDs (C) were injected intravenously into CD1 mice to determine the pharmacokinetic properties. Half-lives and AUC were calculated with Excel and statistical analysis was performed with GraphPad Prism as one-way Anova with Tukey's post-test (B).

Table 3-6: Characterization and pharmacokinetics of scFv-IgBDs

	MW [kDa]	S_r [nm]	Initial half-life [h]	Terminal half-life [h]	AUC [%h]
scFv	26.7	2.5	0.2 ± 0.1	0.6 ± 0.2	16 ± 4
scFv-SpG_{C3}	33.3	2.9	1.2 ± 0.5	13.1 ± 6.1	426 ± 175
scFv-SpG_{C3Fab}	33.2	2.8	1.0 ± 0.1	4.4 ± 1.6	252 ± 43
scFv-SpG_{C3Fab}RR	33.2	2.8	0.9 ± 0.1	15.7 ± 9.4	458 ± 229

3.3 Deimmunization of SpG_{C3Fab}

Since the immunoglobulin-binding domains are derived from bacterial proteins, it is likely that the immune system will recognize IgBD fusion proteins as foreign and direct an immunological reaction. However, the bacterial origin itself is not a reason for immunogenicity, since even fully human proteins can cause an immunologic response and the generation of anti drug antibodies (Bertolotto et al. 2004; Radstake et al. 2009). The crucial factor for immunogenicity is the recognition and binding of the processed peptides to major histocompatibility complex class II molecules on the surface of antigen presenting cells. If the therapeutic protein contains such a recognition sequence, which is always dependent on the HLA set of the patient, it can cause the production of anti-drug antibodies.

3.3.1 Identification and elimination of possible T-cell epitopes

Therefore, the sequence of SpG_{C3Fab} was analyzed for possible T-cell epitopes. Not only sequence, but also structure based prediction methods were used for the evaluation of the recognition sites. The methods used have their origin in the TEPTIOPE method (Sturniolo et al. 1999), which describes the binding potential of 9-mer peptides to a rather large set of HLA-DRB1 alleles (MHC class II). This scanning was performed for a set of the 8 most frequent HLA class II alleles that represent a majority of the complete human population (Gragert et al. 2013; Maiers, Gragert, and Klitz 2007). With this computational approach, 9 possible T-cell epitopes within the sequence of SpG_{C3Fab} were detected that fulfill the sequential and structural requirements to bind to human MHC class II molecules on the surface of APCs (Figure 3-15). Additionally, the affinity maturated variant SpG_{C3Fab}RR was added to the panel for deimmunization as it revealed strongly beneficial pharmacokinetic properties. The scanning of the SpG_{C3Fab}RR mutant revealed three additional possible T-cell epitopes compared to the wild-type SpG_{C3Fab} fragment, two of them overlapping in DRB1_0801 and one in DRB1_1301.

```
SpG_C3Fab                10        20        30        40        50
                         .         .         .         .         .
DRB1_0101   TTYKLVINGKTLKGETTTKAVDAETAAAAFAQYANDNGVDGVWTYDDATKTFTVTE
DRB1_0301   TTYKLVINGKTLKGETTTKAVDAETAAAAFAQYANDNGVDGVWTYDDATKTFTVTE
DRB1_0401   TTYKLVINGKTLKGETTTKAVDAETAAAAFAQYANDNGVDGVWTYDDATKTFTVTE
DRB1_0701   TTYKLVINGKTLKGETTTKAVDAETAAAAFAQYANDNGVDGVWTYDDATKTFTVTE
DRB1_0801   TTYKLVINGKTLKGETTTKAVDAETAAAAFAQYANDNGVDGVWTYDDATKTFTVTE
DRB1_1101   TTYKLVINGKTLKGETTTKAVDAETAAAAFAQYANDNGVDGVWTYDDATKTFTVTE
DRB1_1301   TTYKLVINGKTLKGETTTKAVDAETAAAAFAQYANDNGVDGVWTYDDATKTFTVTE
DRB1_1501   TTYKLVINGKTLKGETTTKAVDAETAAAAFAQYANDNGVDGVWTYDDATKTFTVTE

SpG_C3FabRR              10        20        30        40        50
                         .         .         .         .         .
DRB1_0101   TTYKLVINGKTLKGETTTKAVDAETAAAAFAQYARRNGVDGVWTYDDATKTFTVTE
DRB1_0301   TTYKLVINGKTLKGETTTKAVDAETAAAAFAQYARRNGVDGVWTYDDATKTFTVTE
DRB1_0401   TTYKLVINGKTLKGETTTKAVDAETAAAAFAQYARRNGVDGVWTYDDATKTFTVTE
DRB1_0701   TTYKLVINGKTLKGETTTKAVDAETAAAAFAQYARRNGVDGVWTYDDATKTFTVTE
DRB1_0801   TTYKLVINGKTLKGETTTKAVDAETAAAAFAQYARRNGVDGVWTYDDATKTFTVTE
DRB1_1101   TTYKLVINGKTLKGETTTKAVDAETAAAAFAQYARRNGVDGVWTYDDATKTFTVTE
DRB1_1301   TTYKLVINGKTLKGETTTKAVDAETAAAAFAQYARRNGVDGVWTYDDATKTFTVTE
DRB1_1501   TTYKLVINGKTLKGETTTKAVDAETAAAAFAQYARRNGVDGVWTYDDATKTFTVTE
```

Figure 3-15: Predicted HLA-DRB1 epitopes in SpG_{C3Fab} and SpG_{C3Fab}RR for the 8 most frequent HLA class II alleles in the western population.

Sequential and structure based prediction algorithms were used to determine possible sites for immunogenicity of SpG_{C3Fab} and SpG_{C3Fab}RR. Possible anchor sequences of T-cell epitopes are 9 amino acids long and underlined in red. Blue denotes the corresponding starting position of new or overlapping T-cell epitopes.

After identification of the T-cell epitopes, a calculation of which and how many amino acid exchanges was necessary to eliminate these epitopes, using amongst others the DPDP approach (Parker et al. 2010). One of the main challenges is to abolish as many epitopes as possible with a minimal amount of amino acid changes to guarantee the functionality of the domain without generating new epitopes. Since 8 of the 9 epitopes are located in close proximity, a single amino acid exchange can possibly eliminate multiple epitopes. The variants SpG_{C3Fab}V6A and SpG_{C3Fab}RR Y33T,DI1 were selected as example for such a process (Figure 3-16). Starting with 9 epitopes for SpG_{C3Fab}, the introduction of alanine at position 6 eliminates 4 possible epitopes in DRB1_0301, *1101, *1301 and *1501, but also generates one new epitope in DRB1_0401, resulting in a final reduction of 3 T-cell epitopes. Combining

selected mutations can further reduce the number of epitopes, as presented for SpG_{C3Fab}RR Y33T,DI1 that has only one possible epitope in DRB1_0401 left. Several single amino acid mutations as well as combinations with the highest impact on immunogenicity were produced as scFv or scDb fusion protein (Table 3-7).

```
SpGC3FabV6A              10         20         30         40         50
                          .          .          .          .          .
DRB1_0101  TTYKLAINGKTLKGETTTKAVDAETAAAAFAQYANDNGVDGVWTYDDATKTFTVTE
DRB1_0301  TTYKLAINGKTLKGETTTKAVDAETAAAAFAQYANDNGVDGVWTYDDATKTFTVTE
DRB1_0401  TTYKLAINGKTLKGETTTKAVDAETAAAAFAQYANDNGVDGVWTYDDATKTFTVTE
DRB1_0701  TTYKLAINGKTLKGETTTKAVDAETAAAAFAQYANDNGVDGVWTYDDATKTFTVTE
DRB1_0801  TTYKLAINGKTLKGETTTKAVDAETAAAAFAQYANDNGVDGVWTYDDATKTFTVTE
DRB1_1101  TTYKLAINGKTLKGETTTKAVDAETAAAAFAQYANDNGVDGVWTYDDATKTFTVTE
DRB1_1301  TTYKLAINGKTLKGETTTKAVDAETAAAAFAQYANDNGVDGVWTYDDATKTFTVTE
DRB1_1501  TTYKLAINGKTLKGETTTKAVDAETAAAAFAQYANDNGVDGVWTYDDATKTFTVTE

SpGC3FabRR Y33T,DI1      10         20         30         40         50
                          .          .          .          .          .
DRB1_0101  TTYELAINGQTLKGETTTKAVDAETAAAAFAQTARRNGVDGVWSYDDATKTFTVTE
DRB1_0301  TTYELAINGQTLKGETTTKAVDAETAAAAFAQTARRNGVDGVWSYDDATKTFTVTE
DRB1_0401  TTYELAINGQTLKGETTTKAVDAETAAAAFAQTARRNGVDGVWSYDDATKTFTVTE
DRB1_0701  TTYELAINGQTLKGETTTKAVDAETAAAAFAQTARRNGVDGVWSYDDATKTFTVTE
DRB1_0801  TTYELAINGQTLKGETTTKAVDAETAAAAFAQTARRNGVDGVWSYDDATKTFTVTE
DRB1_1101  TTYELAINGQTLKGETTTKAVDAETAAAAFAQTARRNGVDGVWSYDDATKTFTVTE
DRB1_1301  TTYELAINGQTLKGETTTKAVDAETAAAAFAQTARRNGVDGVWSYDDATKTFTVTE
DRB1_1501  TTYELAINGQTLKGETTTKAVDAETAAAAFAQTARRNGVDGVWSYDDATKTFTVTE
```

Figure 3-16: Deimmunization of SpG_{C3Fab}

After the identification of possible T-cell epitopes, single or multiple amino acid exchanges were applied to the sequence to disrupt a multitude of epitopes without the generation of new epitopes and the maintaining of binding activity. Possible anchor sequences of T-cell epitopes are 9 amino acids long and underlined in red. Blue denotes the corresponding starting position of new or overlapping T-cell epitopes. Substituted amino acids for deimmunization are highlighted.

3.3.2 Characterization of deimmunized IgBD variants *in vitro*

All of the newly generated fusion proteins were tested for their binding capability towards immobilized mouse IgG in quartz crystal microbalance measurements at physiological pH as scFv-IgBD fusion proteins (Table 3-7). Most modified IgBDs with single amino acid mutations showed binding to mouse IgG with similar or slightly decreased affinity, but two variants, namely SpG_{C3Fab}T44S and A48G could even

improve the binding to some extent. The combinations of several amino acid exchanges all resulted in variants that show less affinity at neutral pH.

For a more detailed analysis, selected mutants were subcloned as scDb-IgBD fusion proteins and produced in stably transfected HEK293 cells. An SDS-PAGE analysis was performed subsequent to IMAC purification after ammonium sulfate precipitation (Figure 3-17). The scDb-SpG$_{C3Fab}$ as well as the single mutants N8D, K10Q and T44S displayed one clear band at the expected molecular weight. The deimmunized variants with more mutations appeared to have a slightly higher molecular weight, but mostly formed also single bands. Due to this change, the functionality of all scDb-IgBD fusion proteins was assayed via CEA-binding ELISA with all fusion proteins showing a dose dependent binding comparable to the wild-type scDb-SpG$_{C3Fab}$ (Data not shown).

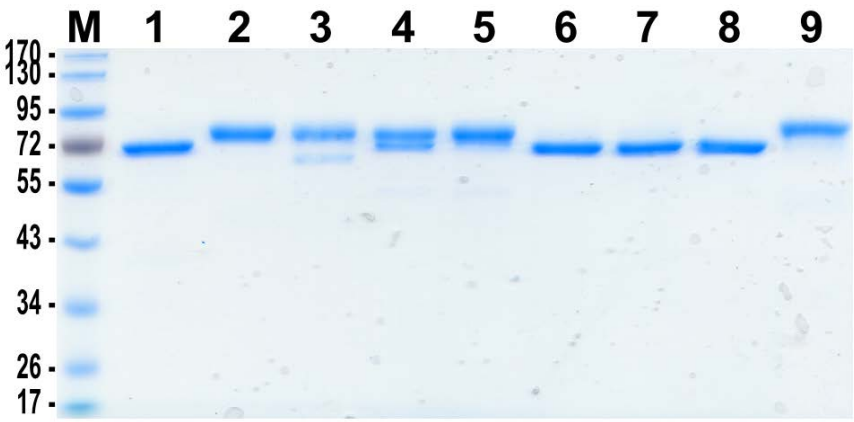

Figure 3-17: SDS-PAGE analysis of deimmunized scDb-IgBD fusion proteins

3 µg of purified scDb-IgBD fusion protein per lane were applied to a 12 % polyacrylamide gel. M denotes the protein ladder with indicated molecular masses in kDa on the left. Lane 1: scDb-SpG$_{C3Fab}$; 2: scDb-SpG$_{C3Fab}$DI1; 3: scDb-SpG$_{C3Fab}$DI2; 4: scDb-SpG$_{C3Fab}$DI3; 5: scDb-SpG$_{C3Fab}$DI4; 6: scDb-SpG$_{C3Fab}$N8D; 7: scDb-SpG$_{C3Fab}$K10Q; 8: scDb-SpG$_{C3Fab}$T44S; 9: scDb-SpG$_{C3Fab}$T44S; 10: scDb-SpG$_{C3Fab}$RR Y33T,DI1

Table 3-7: Elimination of T-cell epitopes and affinities towards mouse IgG

	Sequence	K_{D1} [nM]	K_{D2} [nM]	Epitopes
scFv-SpG$_{C3Fab}$	TTYKLVINGKTLKGETTTKAVDAETAAAAFAQYANDNGVDGVWTYDDATKTFTVTE	67	555	9
scDb-SpG$_{C3Fab}$DI1	...E.A...Q.....G.....	-	-	1
scDb-SpG$_{C3Fab}$DI2	....VA...Q.....G.....	-	-	1
scFv-SpG$_{C3Fab}$DI3	.....T.D.....S.....	301	1670	2
scFv-SpG$_{C3Fab}$DI4	.....T...E.....S.....	134	1340	3
scFv-SpG$_{C3Fab}$DI5	.....D.E.....S.....	162	1300	3
scFv-SpG$_{C3Fab}$K4E	...E.....	1310	6100	8
scFv-SpG$_{C3Fab}$L5A	....A.....	221	2050	5
scFv-SpG$_{C3Fab}$V6A	.....A.....	171	1500	6
scFv-SpG$_{C3Fab}$I7E	.....E.....	447	1100	4
scFv-SpG$_{C3Fab}$I7L	.....L.....	285	1630	9
scFv-SpG$_{C3Fab}$N8D	.....D.....	245	1410	5
scFv-SpG$_{C3Fab}$K10E	.....E.....	184	838	5
scFv-SpG$_{C3Fab}$L12A	.....A.....	-	-	
scFv-SpG$_{C3Fab}$T44S	.....S.....	38	836	8
scFv-SpG$_{C3Fab}$A48G	.....G.....	38	814	8
scFv-SpG$_{C3Fab}$RR	.....RR.....	13	250	12
scFv-SpG$_{C3Fab}$RR Y33A	.....A.RR.....	265	3290	9
scDb-SpG$_{C3Fab}$RR Y33T,DI1	...E.A...Q.....T.RR.....S.....	n.d.	n.d.	1

In order to get a more detailed idea about the binding properties of the deimmunized variants, quartz crystal microbalance measurements comprising different immobilized immunoglobulins and fragments thereof at physiological and acidic conditions were performed. The single mutants N8D, K10Q and T44S exhibited a similar binding towards human and mouse IgG and also their fragments. All K_D values were in a range that was previously measured for the wild-type SpG_{C3Fab} domain, with a marginal tendency towards improved affinity for N8D and T44S. No binding to Fc part was detectable at neutral pH for any of the fusion proteins, but again the shift towards acidic conditions lead to the establishment of a low affinity towards human and mouse Fc part as seen before. The variants with multiple mutations (SpG_{C3Fab}DI1 and DI2) also showed affinity towards mouse IgG at neutral pH, but less binding compared to the wild-type domain could be detected (Figure 3-18). Here, no affinity could be computed due to the low maximal binding that strongly influenced the quality of the fit. The combination of deimmunized and affinity maturated mutant, SpG_{C3Fab}RR Y33T,DI1, resulted in a somewhat lower affinity towards mouse IgG at neutral pH compared to the SpG_{C3Fab} domain (199 nM compared to 61 nM of SpG_{C3Fab}), but similar affinity at physiological pH.

Table 3-8: Affinity of deimmunized SpG_{C3Fab} variants to IgG and fragments

scDb-SpG_{C3Fab}	pH	human						mouse					
		IgG		Fab		Fc		IgG		Fab		Fc	
		K_{D1}	K_{D2}	K_{D1}	K_{D2}	K_{D1}	K_{D2}	K_{D1}	K_{D2}	K_{D1}	K_{D2}	K_{D1}	K_{D2}
wt	7.4	120	983	88	969	-	-	61	1030	96	1620	-	-
	6	169	1520	83	753	767	896	54	822	93	826	38	414
N8D	7.4	67	6270	79	696	-	-	42	1320	75	1290	-	-
	6	71	745	93	661	94	843	48	1260	58	624	46	910
K10Q	7.4	83	1030	155	1430	-	-	71	1550	93	1230	-	-
	6	94	1040	137	760	130	1540	36	670	86	591	55	713
T44S	7.4	69	1260	293	1180	-	-	76	1190	92	1240	-	-
	6	88	909	83	595	63	543	37	863	60	426	80	439
RR Y33T,DI1	7.4	n.d.						199	2970	n.d.			
	6							79	995				
RR	7.4	29	385	167	1040	-	-	55	388	62	413	-	-
	6	49	191	43	461	39	227	34	296	19	255	40	289

-: no binding detected n.d.: not determined K_Ds in [nM]

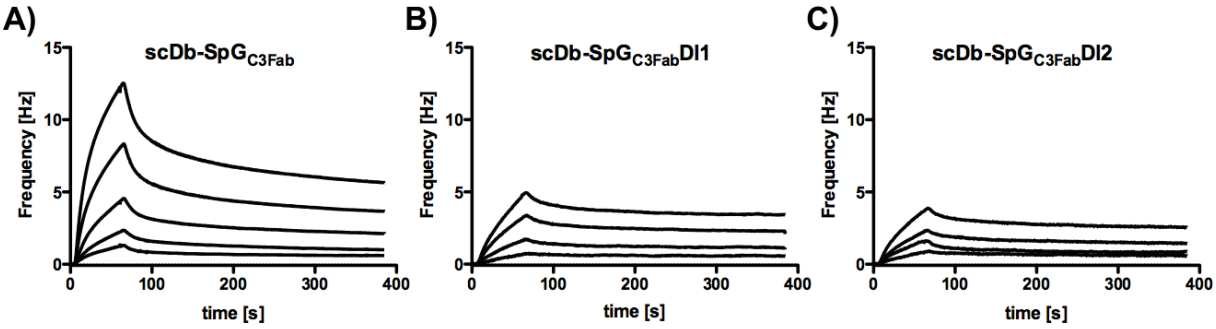

Figure 3-18: Affinity of deimmunized scDb-SpG$_{C3Fab}$ variants towards mouse IgG

The binding kinetics of scDb-SpG$_{C3Fab}$ (A), scDb-SpG$_{C3Fab}$DI1 (B) and scDb-SpG$_{C3Fab}$DI2 (C) towards immobilized full-length mouse IgG were determined in a QCM approach at pH7.4. Two-fold serial dilutions in random order were applied with a starting concentration of 1000 nM for all fusion proteins. 3 to 4 binding curves were measured for each concentration.

3.3.3 Pharmacokinetic behavior of deimmunized scDb-IgBD fusion proteins

Having determined the affinity of the deimmunized fusion proteins towards immunoglobulins, their pharmacokinetic behavior in CD1 mice was determined. All IgBD fusion proteins were able to improve the pharmacokinetics compared to the unmodified scDb molecule alone, meaning that even with numerous amino acid exchanges the binding was not completely abolished (Figure 3-19). However, none of the tested variants exhibited a terminal half-life that was better than the wild-type SpG$_{C3Fab}$. Although the single mutations exhibited an improved affinity towards the whole IgG molecule as well as the Fab fragment, their serum concentration decreased more rapidly than the one of scDb-SpG$_{C3Fab}$. The combination of several mutations to decrease the immunogenicity of the immunoglobulin-binding domain also improved the performance of the scDb, but the terminal half-life of scDb-SpG$_{C3Fab}$DI1 that contained the lowest amounts of T-cell epitopes resulted in only 60 % of the wild-type half-life. When combining the SpG$_{C3Fab}$DI1 with the deimmunized version of the SpG$_{C3Fab}$RR mutant to SpG$_{C3Fab}$RR Y33T,DI1, a terminal half-life of 11.8 h could be achieved, which is about 9-fold as high as for the unmodified scDb. The serum concentration at later time points almost reaches the concentrations of the SpG$_{C3Fab}$ molecule. This also reflected in the area under the curve, which is roughly 10-fold improved compared to the scDb.

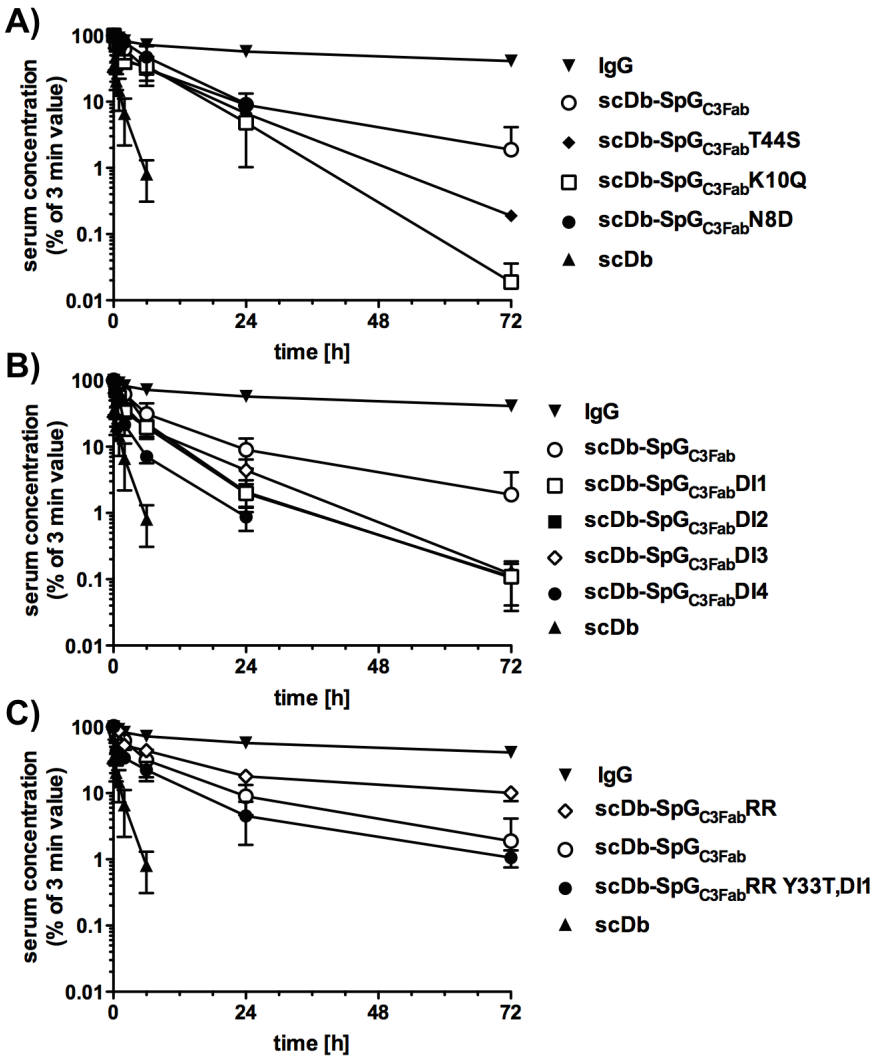

Figure 3-19: Pharmacokinetics of deimmunized SpG$_{C3Fab}$ variants

25 µg of purified fusion protein were injected intravenously into CD1 mice. The serum concentration for scDb-IgBD fusion proteins with a single mutation (A), multiple mutations (B) and the combination with the affinity maturated SpG$_{C3Fab}$RR mutant (C) was determined in a CEA-binding ELISA and normalized to the 3 minute value.

Table 3-9: Pharmacokinetic properties of deimmunized SpG$_{C3Fab}$ variants

	Terminal half-life [h]	AUC [%h]
scDb-SpG$_{C3Fab}$	15.1 ± 4.8	954 ± 389
scDb-SpG$_{C3Fab}$N8D	8.4 ± 2.0	925 ± 351
scDb-SpG$_{C3Fab}$K10Q	5.8 ± 2.2	754 ± 310
scDb-SpG$_{C3Fab}$T44S	7.8 ± 1.0	703 ± 157
scDb-SpG$_{C3Fab}$DI1	9.1 ± 1.0	464 ± 96
scDb-SpG$_{C3Fab}$DI2	8.8 ± 0.5	584 ± 193
scDb-SpG$_{C3Fab}$DI3	7.8 ± 1.1	525 ± 141
scDb-SpG$_{C3Fab}$DI4	5.9 ± 0.6	235 ± 45
scDb-SpG$_{C3Fab}$RR	47.8 ± 10.3	2228 ± 380
scDb-SpG$_{C3Fab}$RR Y33T,DI1	11.8 ± 5.8	559 ± 195
scDb	1.3 ± 0.2	56 ± 15

3.4 Half-life extension of recombinant human erythropoietin

Already since the 1980s, recombinant human erythropoietin became clinically available and was used for numerous purposes. More than 1 million of patients have responded effectively to treatment with recombinant huEPO or a derivate (Bunn 2013). However, a major limitation for therapy with huEPO is the frequency of administration that is necessary in order to maintain a therapeutically effective concentration (Kontermann 2012). For this reason, half-life extension strategies have been applied to huEPO, focusing on the increase of the hydrodynamic radius to reduce renal filtration. Exceeding this strategy, the fusion of the immunoglobulin-binding domains is to reduce lysosomal degradation via binding to IgG and subsequent recycling via the FcRn.

3.4.1 Characterization of huEPO-IgBD fusion proteins

Unmodified human erythropoietin as well as EPO fusion proteins with C-terminal SpG_{C3}, SpG_{C3Fab} or SpG_{C3Fab}RR domain were produced in stably transfected HEK293 cells and purified via immobilized metal affinity chromatography (Figure 3-20). Since human EPO has 3 possible N-glycosylation and one O-glycosylation site in its sequence, the proteins appear as multiple bands without treatment of glycosidases in an SDS-PAGE. Upon treatment with N- and O-glycosidase, all huEPO fusion proteins appear as single bands with the calculated molecular mass of the peptide sequence of 19.5 and about 26 kDa, respectively (Table 3-10).

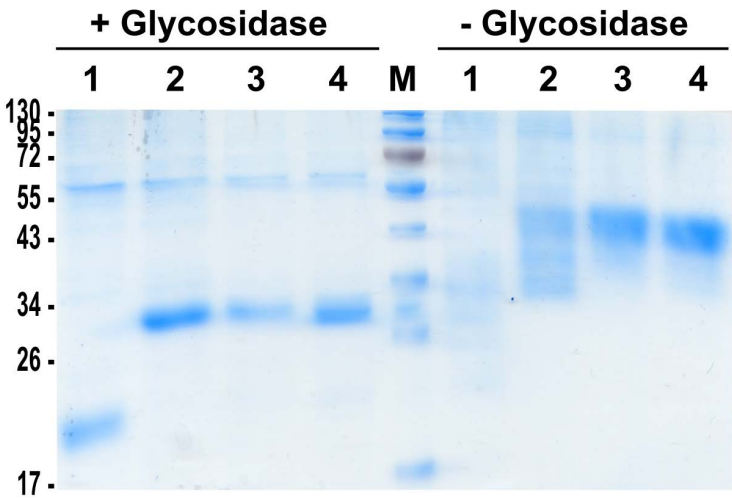

Figure 3-20: Deglycosylation of recombinant human EPO-IgBD fusion proteins

10 µg of purified huEPO-IgBD fusion protein were analyzed by SDS-PAGE (12 % acrylamide) after over night treatment with (left) or without (right) N- and O-glycosidase. Lane 1: huEPO; 2: huEPO-SpG_{C3}; 3: huEPO-SpG_{C3Fab}; 4: huEPO-SpG_{C3Fab}RR; M: protein ladder with indicated molecular mass on the left in kDa.

The functionality of the purified huEPO fusion proteins was determined via a proliferation assay of erythropoietin dependent UT-7/EPO cells. Aranesp was included to determine the quality of an industrially produced biopharmaceutical and to compare its proliferative effect for subsequent *in vivo* studies. All huEPO-IgBD fusion proteins as well as Aranesp were able to stimulate UT-7/EPO cells in a dose dependent manner (Figure 3-21). In the absence of excess amounts of human IgG, no differences in maximal stimulation could be determined. The concentration of half-maximal stimulation for all small scale produced huEPO fusion proteins was in a comparable range of 45 - 87 pM (Table 3-10). Aranesp exhibited a slightly better activation of the UT-7/EPO cells with an EC_{50} value of 11 pM. While the presence of human IgG during the whole 4 day incubation time did not influence the bioactivity of huEPO, huEPO-SpG_{C3Fab} and huEPO-SpG_{C3Fab}RR, the proliferative effect of huEPO-SpG_{C3} was significantly lowered almost 4-fold. This finding corresponds with the CEA binding and the IL-2 stimulatory potential of the scDb-IgBD fusion proteins mentioned above.

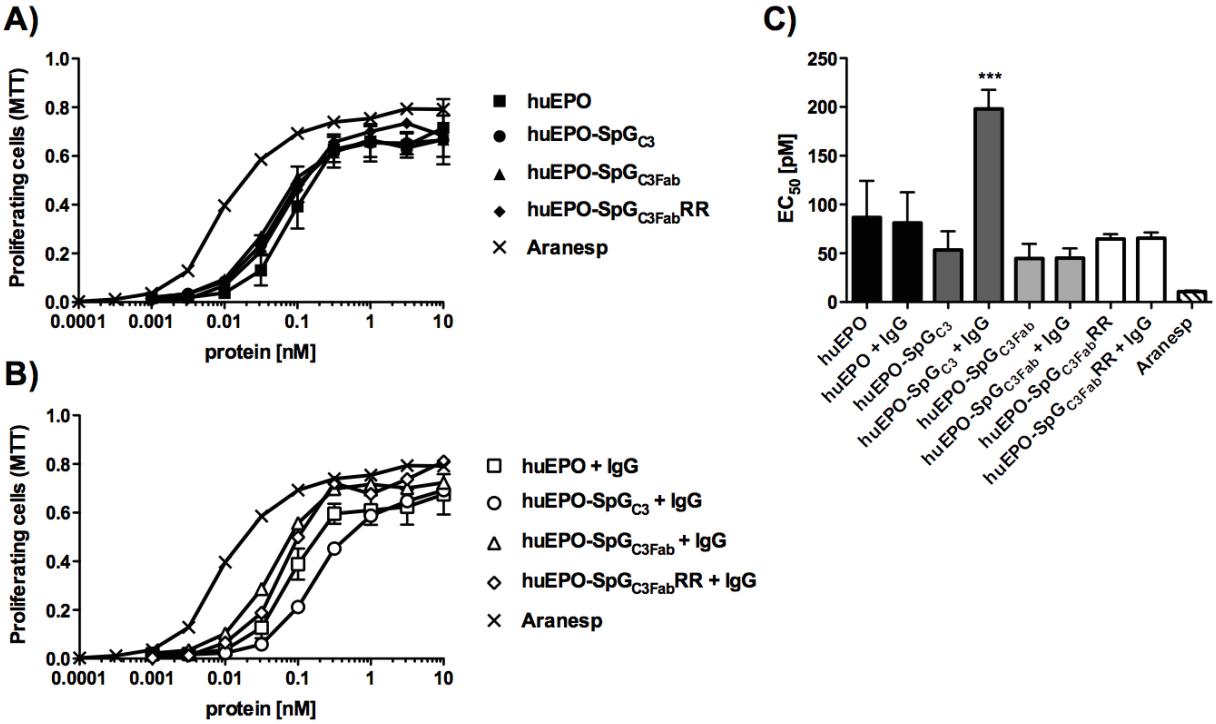

Figure 3-21: Erythropoietin dependent proliferation of UT-7/EPO cells

Previously starved UT-7/EPO cells were stimulated with indicated concentrations of huEPO fusion proteins for 4 days in the absence (A) or presence (B) of excess amounts of huIgG (100 µg/ml). Proliferation was measured via an MTT assay and EC_{50} values from three independent measurements were calculated and statistically evaluated with GraphPad Prism using one-way Anova and Tukey's post-test (C).

Table 3-10: Characterization of huEPO-IgBD fusion proteins

	Molecular mass (peptide)	Glycosylation sites	Tag	Proliferation UT-7/EPO [pM]	
				- IgG	+ IgG
huEPO	19.5 kDa	3 N / 1 O	His	87 ± 38	81 ± 32
huEPO-SpG_{C3}	26.2 kDa	3 N / 1 O	His	53 ± 19	198 ± 20
huEPO-SpG_{C3Fab}	26.0 kDa	3 N / 1 O	His	45 ± 15	45 ± 10
huEPO-SpG_{C3Fab}RR	26.1 kDa	3 N / 1 O	His	65 ± 5	65 ± 6
Aranesp	18.4 kDa	5 N / 1 O	-	11 ± 1	n.d.

3.4.2 Pharmacokinetics of huEPO-IgBD fusion proteins

After having determined the bioactivity of the huEPO-IgBD fusion proteins *in vitro*, their pharmacokinetic properties in CD1 mice were investigated. Due to the addition of an immunoglobulin-binding domain to recombinant human erythropoietin, the retention time in the bloodstream could be elongated for all variants (Figure 3-22). Already the initial half-life of the huEPO-IgBD fusion proteins could be elongated compared to the unmodified huEPO up to a factor of 3 for huEPO-SpG_{C3Fab}RR (1.2 h compared to 0.4 h of unmodified huEPO) (Table 3-11). However, this did not reach the strong improvement that could be achieved by the hyperglycosylation of Aranesp that had ameliorated the initial half-life more than 5-fold to 2.1 h. The IgBD effect became even more obvious for the terminal half-life of the huEPO fusion proteins. Whereas the unmodified huEPO exhibited a terminal half-life of only 4 h, the fusion of the SpG_{C3} domain resulted in an almost 3-fold gain in terminal circulation time and even SpG_{C3Fab} ended up in a more than 50 % longer retention endurance. These values were topped by huEPO-SpG_{C3Fab}RR that lasted in the bloodstream more than 5 times longer than the unmodified huEPO and could even significantly surpass the half-life of Aranesp. These results were also reflected in the area under the curve, where already huEPO-SpG_{C3Fab} with 167 %h reached approximately 4 times the area under the curve of the unmodified huEPO. The SpG_{C3} variant concluded in a 9-fold augmented AUC and huEPO-SpG_{C3Fab}RR managed to enhance the area by a factor of 15. Due to its high initial half-life, Aranesp showed the highest bioavailability and reached an AUC of 1028 %h.

Table 3-11: Pharmacokinetic properties of huEPO-IgBD fusion proteins

	Initial half-life [h]	Terminal half-life [h]	AUC [%h]
huEPO	0.4 ± 0.1	4.0 ± 0.1	44 ± 8
huEPO-SpG$_{C3}$	0.8 ± 0.2	11.8 ± 3.2	403 ± 42
huEPO-SpG$_{C3Fab}$	0.7 ± 0.1	6.3 ± 0.4	167 ± 31
huEPO-SpG$_{C3Fab}$RR	1.2 ± 0.2	21.5 ± 4.2	661 ± 213
Aranesp	2.1 ± 0.5	12.4 ± 1.2	1028 ± 222

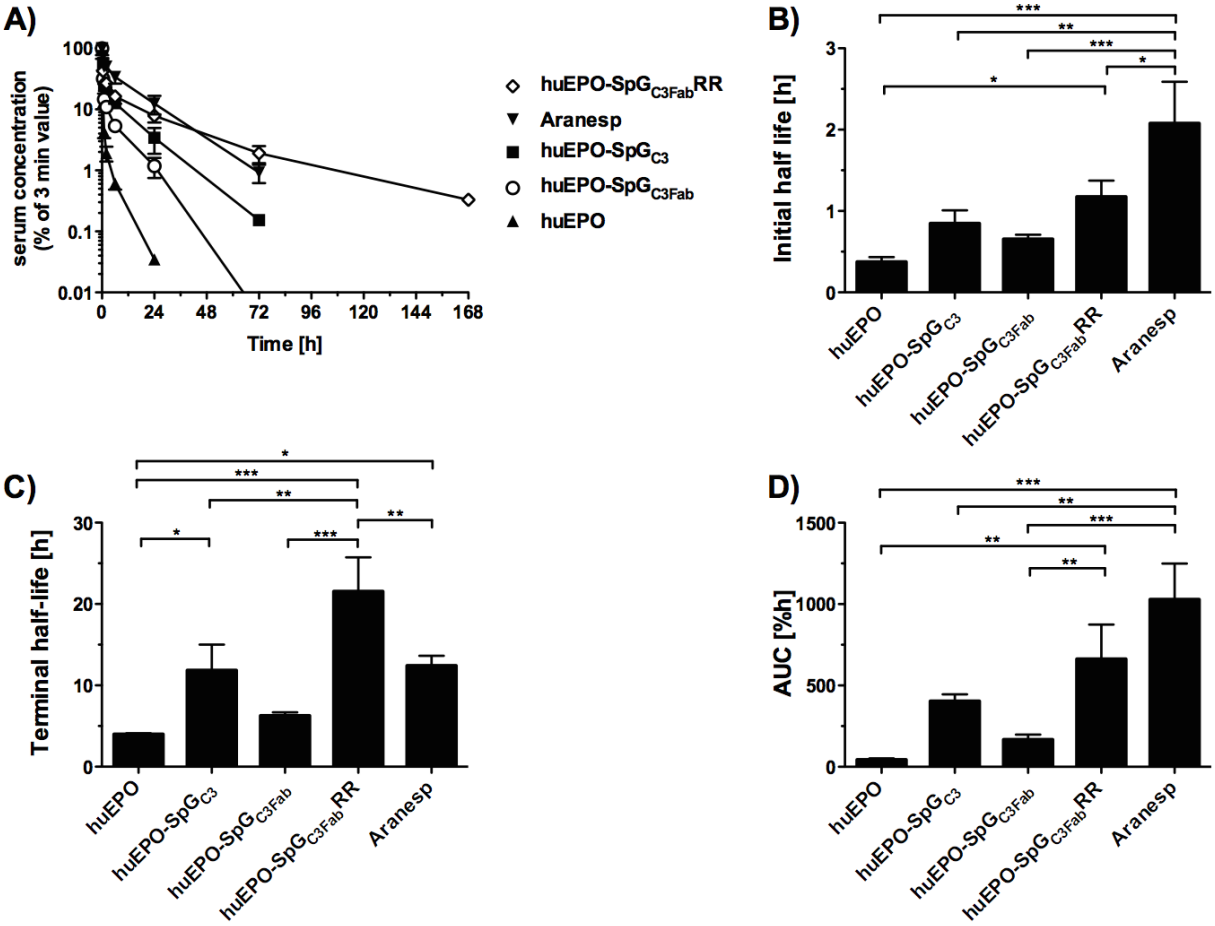

Figure 3-22: Pharmacokinetics of recombinant huEPO fusion proteins

25 µg of recombinant protein was injected i.v. into female CD1 mice. Serum concentrations were determined via MTT viability assay with erythropoietin dependent UT-7/EPO cells and subsequently normalized to the 3 minute concentration (A). Initial half-life (B), terminal half-life (C) and the area under the curve (D) were calculated using Excel and statistically analyzed with GraphPad Prism using a one-way Anova analysis with Tukey's post-test.

3.4.3 Pharmacodynamic study with huEPO-IgBDs

The pharmacodynamic properties of the huEPO-IgBD fusion proteins were examined after a single intravenous injection of huEPO fusion protein and the subsequent proliferation of erythrocytes together with the higher hemoglobin concentration in the blood of CD1 mice. For comparability, the same amount of bioactivity, based on the proliferative effect of the huEPO-IgBD fusion proteins and Aranesp from the

UT-7/EPO cell proliferation assay, was injected. This meant similar molarities for the proteins that were produced in-house (20 µg of huEPO and 26 µg of the other huEPO-IgBD fusion proteins) and one sixth of Aranesp (3.3 µg), as it was 6 times as active in the *in vitro* study. The average bodyweight of the mice was 24.4 g at the time point of injection. At day 3, no effect of treatment was detectable yet, being in well accordance to previous studies (Egrie and Browne 2002) (Figure 3-23). Starting from day 7, the hemoglobin concentration of the animals treated with huEPO-SpG$_{C3Fab}$RR and Aranesp increased, whereas no change was observed for the other huEPO fusion proteins as well as the PBS control. The hemoglobin level of Aranesp rose up to 27990 mg/dl at day 10, which is a 26.3 % improvement compared to the PBS control. huEPO-SpG$_{C3Fab}$RR already reached its peak at day 7 and could enhance the hemoglobin level 15.4 % above the control mice. These two proteins could maintain an elevated level of hemoglobin until day 21, when all levels declined back to the starting level and level of the control mice. Hence, for the calculation of the treatment benefit, the hemoglobin level was integrated over the time, starting at day 3 until day 21, resulting in the area under the curve. Over this time period, huEPO-SpG$_{C3Fab}$RR had an about 12 % increased area under the curve compared to the group that was treated with unmodified huEPO, showing a significant progress in treatment benefit. Aranesp showed the strongest beneficial effect of roughly 15 % increased AUC compared to the PBS control group.

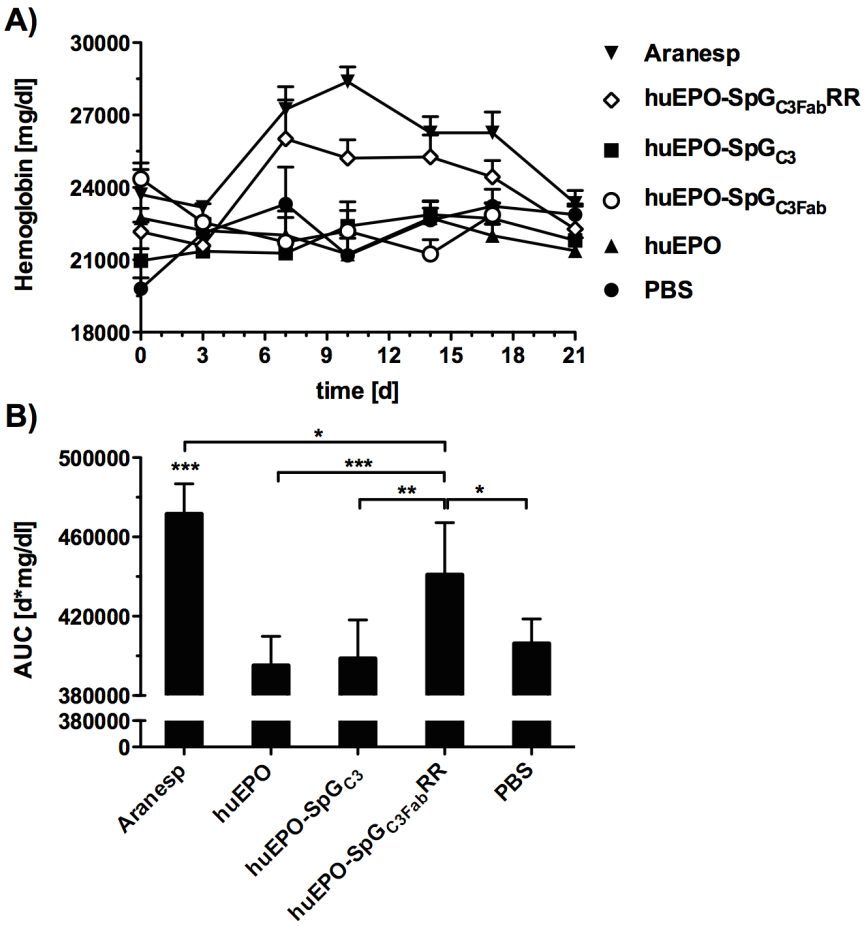

Figure 3-23: Hemoglobin level of huEPO-IgBD treated CD1 mice

20 µg of huEPO or the corresponding amount of huEPO-IgBD fusion proteins, Aranesp or PBS were injected i.v. into 7 CD1 mice per group. Blood samples were taken at indicated time points and investigated for hemoglobin concentration, shown with standard error of the mean (A). The area under the curve displays the treatment benefit by integrating the hemoglobin level over the time between day 3 and day 21 (B). AUC was statistically analyzed via GraphPad Prism's one-way Anova together with Tukey's post-test.

3.5 Pharmacokinetic properties of Fc fusion proteins

Despite all the progress that has been made on increasing the pharmacokinetics of small recombinant molecules, full-length immunoglobulins and Fc fusion proteins are state of the art for industrial production and purification of protein therapeutics. Although these proteins are above the threshold for renal filtration and incorporate the same Fc part that is responsible for the recycling via the neonatal Fc receptor, they experience strongly different elimination from the bloodstream (Hopp et al. 2010).

3.5.1 Characterization of various Fc fusion proteins

For this study, a chimeric anti-CEA IgG1 was generated, whose murine variable domains from the antibody MFE-23 (Chester et al. 2000) were fused to the human constant domains (Stork et al. 2008) (Figure 3-24). Furthermore, an scFv-Fc fusion

protein was produced, consisting of the corresponding scFv MFE-23 fused to the human γ1 Fc part, including the hinge region. Since the scFv-Fc fusion protein differed in size from the IgG, an scDb-Fc fusion protein was generated to roughly reach the size of a full-length IgG molecule. Here, instead of the scFv a bispecific single-chain diabody directed against CEA and CD3 was fused to the Fc part (Korn et al. 2004). In order to determine whether not only the size is the decisive factor, but also the C_H1 or the C_L domain are crucial for a longer half-life, a single-chain variant of a full-length IgG molecule was developed. Here, an scFv was fused to a single-chain version of the C_L and C_H1 domain that is linked to the Fc part via the hinge domain, finally resulting in scFv-scCLCH1-Fc. Furthermore, a fusion protein was generated comprising of the scDb and the IgG1 C_H2 domain without hinge region, as this domain could prove useful as half-life extension module (Gehlsen et al. 2012; Ying et al. 2014). All proteins were produced in stably transfected HEK293 cells and purified from supernatant after ammonium sulfate precipitation. Additionally, the IgG molecule was also produced in CHO-K1 cells to determine, whether its glycosylation plays a role in the pharmacokinetic properties.

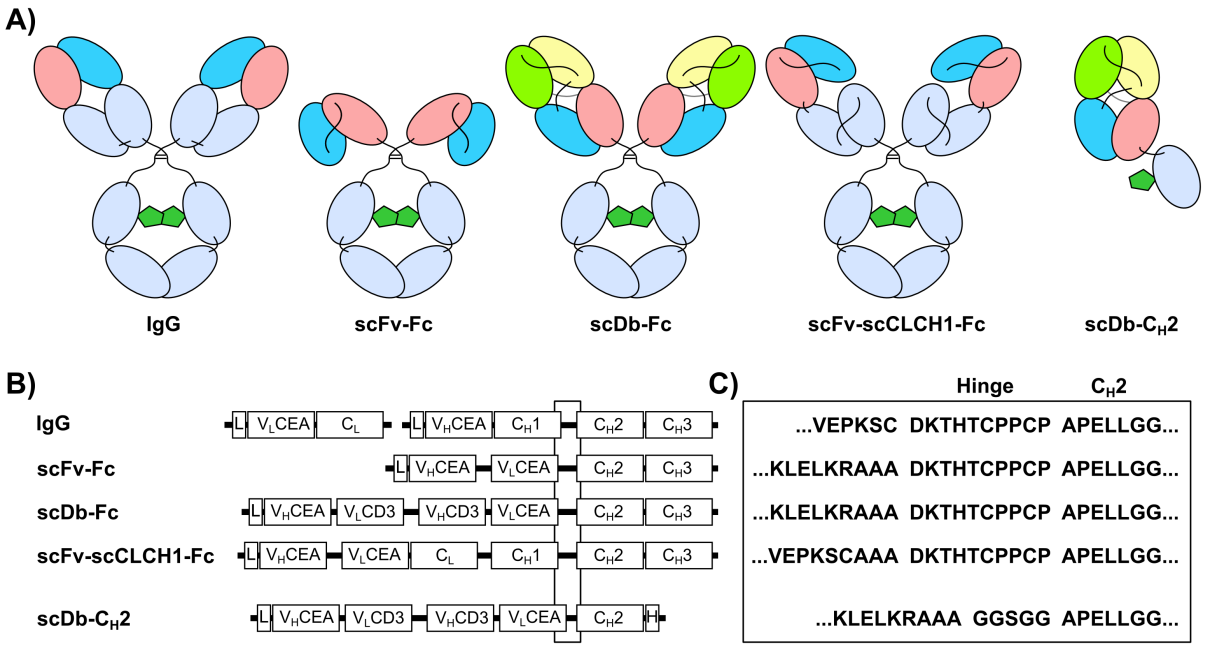

Figure 3-24: Composition of Fc fusion proteins

A) Schematic presentation of the fusion proteins used in this study. The green pentagonal structures represent the N-glycosylation at asparagine 297. Red and blue ovals represent the CEA-binding variable domains, the green and yellow ovals the CD3-binding variable domains. B) Genetic structure of the Fc fusion proteins. “L” denotes the Igκ leader sequence that is cleaved off. “H” symbolizes the hexahistidyl-tag for detection and purification. C) Sequences of the transition between antigen binding moiety and Fc part, including the hinge domain, or the C_H2 domain.

Protein A affinity chromatography was used for the purification of the proteins with Fc-part, the scDb-C_H2 was purified via its His-tag by IMAC. The Fc part including the hinge domain is also responsible for the dimerization of the Fc fusion proteins, which is verifiable under non-reducing conditions in a denaturing SDS-PAGE (Figure 3-25). All Fc fusion proteins showed bands that ran with the calculated molecular weight of the dimer under non-reducing conditions, only the scDb-C_H2 showed a band for the monomeric form, owing to the missing dimerization module (Table 3-12). Under reducing conditions, all Fc fusion proteins exhibited bands corresponding to the size of the monomeric polypeptide chain. The reduction of disulfide bonds resulted in the separation of light and heavy chain for both IgG molecules. The size exclusion demonstrated that the Fc fusion proteins eluted as a single major peak with the hydrodynamic radius of dimers. The Stokes radii of the IgG molecules (5.6 nm), both from CHO and HEK293 cells, were almost identical to the radii of the scDb-Fc (5.5 nm) and the scFv-scCLCH1-Fc (5.6 nm). The smaller scFv-Fc was detected with a hydrodynamic radius of 4.8 nm.

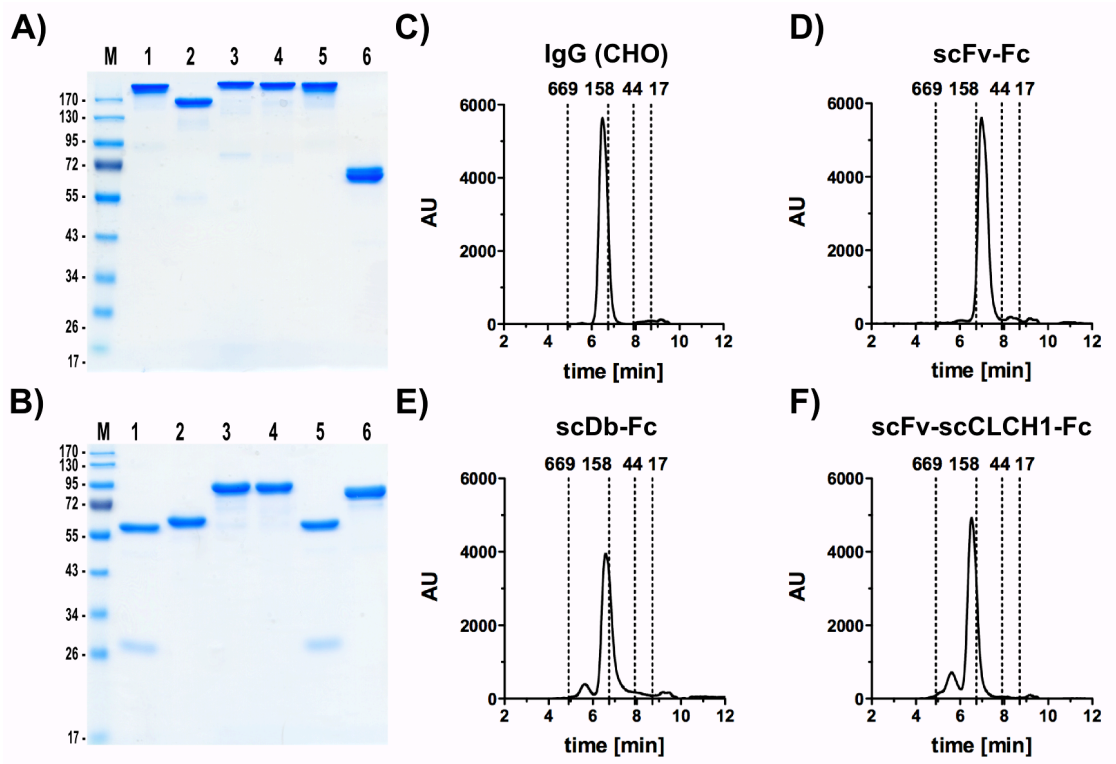

Figure 3-25: SDS-PAGE and size exclusion chromatography of Fc fusion proteins

3 µg of purified protein were run on a 10 % polyacrylamide SDS-PAGE under non-reducing conditions (A) or on a 12 % polyacrylamide SDS-PAGE under reducing conditions (B). Lane 1: IgG (CHO); 2: scFv-Fc; 3: scDb-Fc; 4: scFv-scCLCH1-Fc; 5: IgG (HEK); 6: scDb-C_H2; M: protein ladder with indicated molecular masses in kDa. C, D, E, F) Size exclusion chromatography was performed to determine purity and integrity of the Fc fusion proteins. The molecular mass of the standard proteins is indicated with the dashed lines.

Additionally, the glycosylation status of the different Fc fusion proteins was investigated via deglycosylation with N-glycosidase F. On a reducing SDS-PAGE, all treated samples run with a slightly lower apparent molecular weight than the untreated samples (Figure 3-26), which became especially obvious for the lower molecular weight bands such as the IgG molecules and the scFv-Fc.

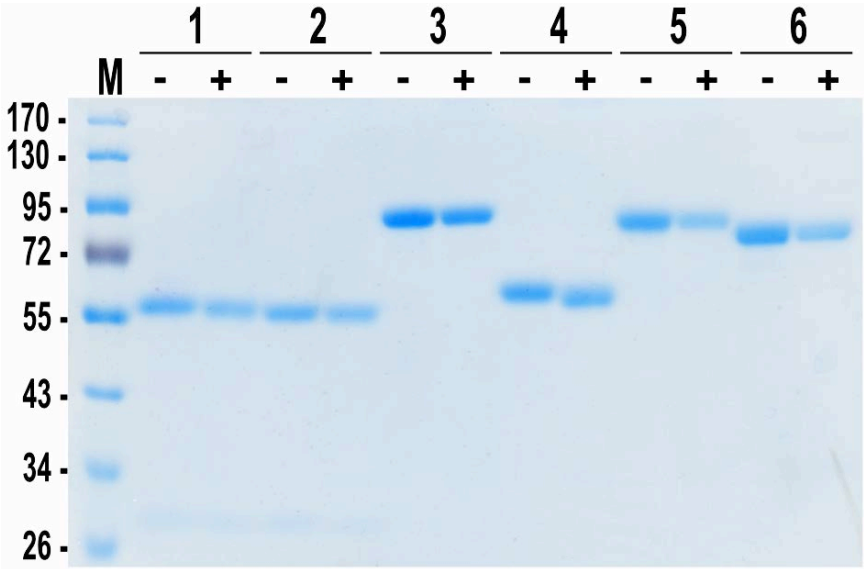

Figure 3-26: Deglycosylation of Fc fusion proteins

2 µg of purified fusion protein were boiled and subsequently incubated over night with (+) or without (-) N-glycosidase F. The protein sample was again boiled with Laemmli buffer and loaded onto a 12 % PAA-gel. Lane 1: IgG (CHO); 2: IgG (HEK293); 3: scDb-Fc; 4: scFv-Fc; 5: scFv-scCLCH1-Fc; 6: scDb-C_H2; M: molecular mass standard in kDa

The functionality in terms of antigen binding was determined in a CEA-binding ELISA for all proteins (Figure 3-27). All Fc fusion proteins bound with an EC_{50} in the same subnanomolar range. Due to being a monomeric format, the scDb-C_H2 could not reach this high binding, but showed binding that is similar to the unmodified scDb or scFv (Table 3-12).

Table 3-12: Characterization of Fc fusion proteins

	Molecular mass [kDa]	S_r [nm]	pI	Tags	Format	EC_{50} CEA [nM]
IgG	148	5.6	6.4	-	Dimer	0.12 ± 0.03
scFv-Fc	104	4.8	6.0	-	Dimer	0.14 ± 0.03
scDb-Fc	157	5.5	7.2	-	Dimer	0.15 ± 0.02
scFv-scCLCH1-Fc	151	5.6	6.5	-	Dimer	0.14 ± 0.03
scFv	27	2.5	5.9	His	Monomer	0.48 ± 0.05
scDb	53	2.6	7.7	His	Monomer	0.70 ± 0.19
scDb-C_H2	67	n.d.	7.6	His	Monomer	0.65 ± 0.10

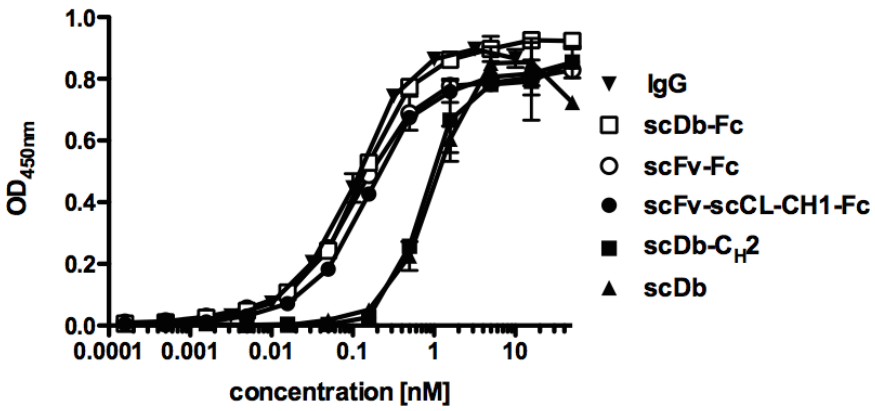

Figure 3-27: CEA-binding ELISA of Fc fusion proteins

Correct assembly and functionality of Fc fusion proteins was investigated in a CEA-binding ELISA. Serial dilutions of Fc fusion proteins were applied to immobilized CEA and binding was detected via anti-huIgG antibody (Fc specific) coupled with HRP. scDb and scDb-C_H2 were detected via anti-His-tag antibody coupled with HRP.

3.5.2 Stability determination

The stability of all Fc fusion proteins was analyzed by thermal denaturation as well as stability in serum. Dynamic light scattering was used to determine the melting temperature of the Fc fusion proteins. The scFv displayed a melting point of 46 °C (Figure 3-28, Table 3-14). Likewise, the scFv-Fc revealed a melting point of 46 °C, but also showed a second strong incline in the mean count rate at about 76 °C, likely indicating the denaturation point for the Fc part (Traxlmayr et al. 2012; Wozniak-Knopp, Stadlmann, and Rüker 2012). The low melting point of the scFv was slightly improved by the incorporating of the sequence into an scDb molecule, that has a melting temperature of 51 °C. This transition point was likewise seen for the scDb-Fc that also shows the Fc denaturation at 76 °C. The scDb-C_H2 exhibited a similar denaturation as the unmodified scDb (50 °C). By generating a single chain version of the Fab fragment together with the Fc fragment (scFv-scCLCH1-Fc), the thermal stability could be augmented to 54 °C. This stabilizing effect was even topped by the full-length IgG molecule with a regular Fab fragment and a first thermal transition point of 58 °C.

Investigation of the serum stability of the Fc proteins was performed in 50 % mouse serum over 7 days and subsequent functional detection via CEA-binding ELISA (Figure 3-29). Both IgGs as well as scFv-Fc and scDb-Fc did not show degradation after 7 days incubation in serum. On the other hand, scFv-scCLCH1-Fc already presented lower levels of intact protein after day 1 and roughly 35 % lower levels after day 7. Likewise, less active protein could be detected for the scDb-C_H2 after

day 7 by detection of the C-terminal His-tag (more than 45 % loss). Nevertheless, detection via Protein L-HRP, binding to the variable domain of the kappa light chain, revealed no significant loss in activity of scDb-C_H2 over one week.

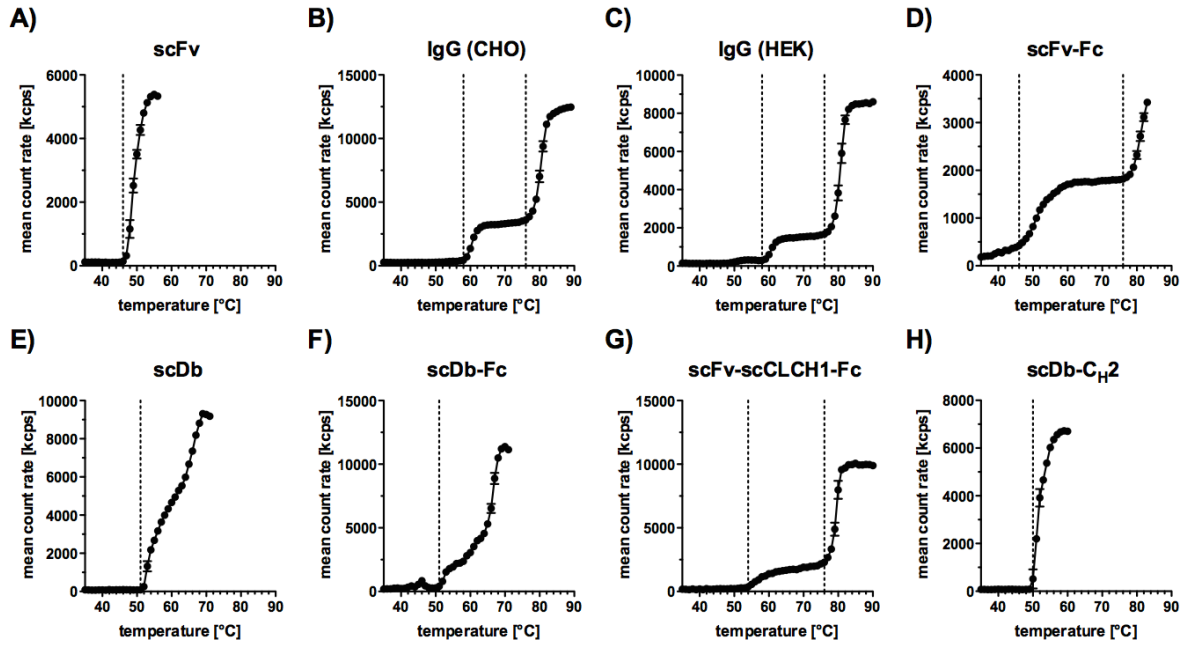

Figure 3-28: Thermal stability of Fc fusion proteins

The point of thermal denaturation was determined via dynamic light scattering. The protein sample was heated in 1 °C intervals with 2 minutes of equilibration time. The dashed vertical lines indicate the melting points, defined by an intense increase in mean count rate.

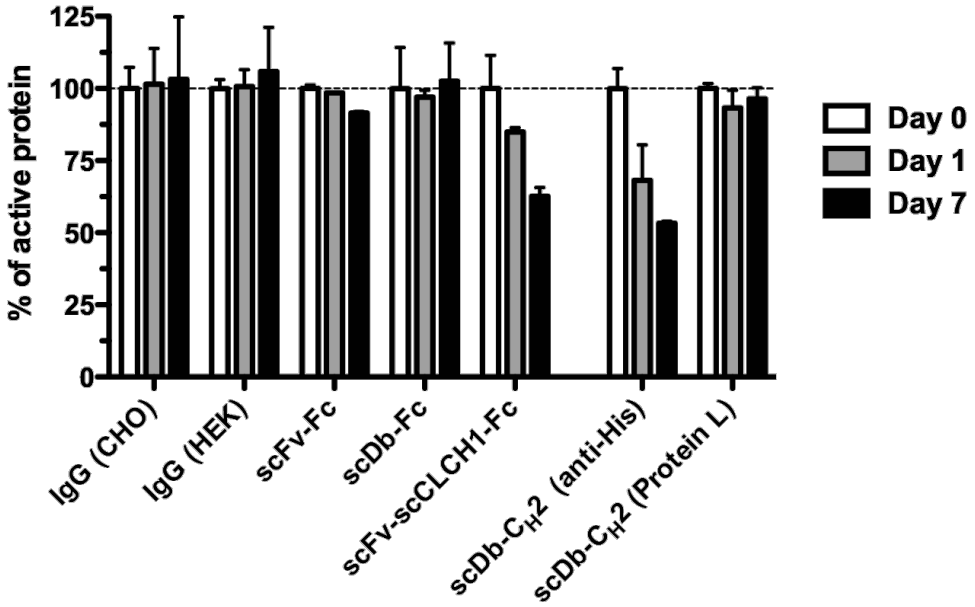

Figure 3-29: Serum stability of Fc fusion proteins

Serum stability was investigated over 7 days in 50 % mouse serum at 37 °C. Samples were frozen at -20 °C at indicated time points and subsequently tested for active protein content in a CEA-binding ELISA. Binding of Fc fusion proteins was detected by HRP conjugated anti-huIgG antibody (Fc specific), scDb-C_H2 by HRP labeled anti-His-tag antibody or Protein L.

3.5.3 Neonatal Fc receptor binding

The recycling via the neonatal Fc receptor is one of the key requirements for the long half-life of IgG molecules. Therefore the binding properties at neutral pH and in particular at acidic pH were closely investigated using an immobilized, biotinylated mouse FcRn in a quartz crystal microbalance approach (Figure 3-30). No or only negligible binding was traceable under physiological conditions. Therefore, running buffer with pH7.4 was able to regenerate the binding at pH6. Binding was detectable under acidic conditions with similar biphasic curves for all the Fc fusion proteins and K_D values for the monovalent binding around 100 nM (Table 3-13). The scDb-C_H2 only showed weak binding to the mouse FcRn at neutral pH and even less affinity under acidic conditions, although 10-fold the concentration was injected compared to the Fc fusion proteins.

Table 3-13: Affinity towards mouse FcRn at pH6

	k_{on1} [(M x s)$^{-1}$]	k_{off1} [s^{-1}]	K_{D1} [nM]	K_{D2} [M]
IgG	1.5 x 10^5	1.6 x 10^{-2}	108	1.9 x 10^{-17}
scFv-Fc	1.7 x 10^5	1.8 x 10^{-2}	107	1.8 x 10^{-16}
scDb-Fc	2.0 x 10^5	1.6 x 10^{-2}	82	1.4 x 10^{-10}
scFv-scCLCH1-Fc	1.7 x 10^5	1.2 x 10^{-2}	121	2.5 x 10^{-10}

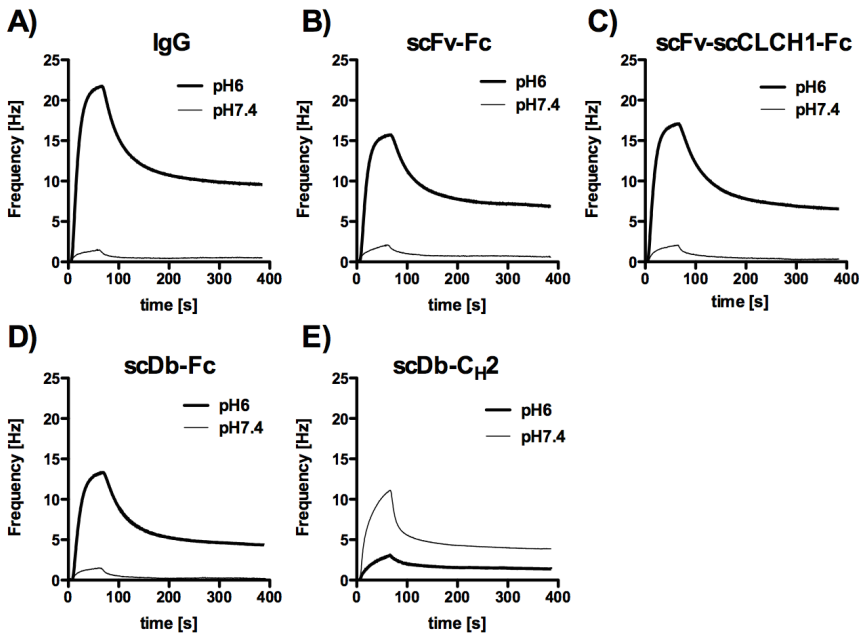

Figure 3-30: Binding to mouse FcRn

The binding of Fc fusion proteins was investigated on immobilized mouse FcRn via quartz crystal microbalance measurements. 100 nM of fusion protein was applied at pH6 and at pH7.4 and regeneration was performed twice with running buffer at pH7.4 (A-D). A concentration of 1000 nM was injected to determine the binding of scDb-C_H2 under both conditions (E). Here, regeneration was performed with 10 mM HCl pH1.95.

3.5.4 Pharmacokinetics of Fc fusion proteins

Pharmacokinetics were determined via a single injection of 25 µg protein into the tail vein of female CD1 mice. Serum concentrations were determined via CEA-binding ELISA and normalized to the 3 minute value. Both IgG1 molecules exhibited almost congruent pharmacokinetic profiles, together with a terminal half-life of about 9 days and a comparable AUC of about 8000 %h that is much higher than that of all other proteins tested (Figure 3-31, Table 3-14). The scDb-Fc with a similar molecular weight as the IgGs had a strongly reduced terminal half-life and also AUC of 140 h and 4143 %h, respectively. As seen in previous studies, the scFv-Fc also exhibited lower serum persistence than the IgG molecules (Hopp et al. 2010), with serum concentrations and an AUC that are similar to the scDb-Fc. The terminal half-life of the scFv-Fc with 104 h was somewhat inferior due to the marginally lower concentration at day 7. With 53 h, the scFv-scCLCH1-Fc had the shortest terminal half-life of all Fc fusion proteins tested and just less than a fourth of the full-length IgG molecules. This also went along with a significantly reduced area under the curve. Nevertheless, all four Fc fusion proteins demonstrated massively improved pharmacokinetic properties compared with the scDb and scFv. On the other hand, the scDb-C_H2 had a terminal half-life similar to that of the unmodified scDb, also reflected in a poor AUC.

Table 3-14: Stability and pharmacokinetic properties of Fc fusion proteins

	Melting point [°C]	Initial half-life [h]	Terminal half-life [h]	AUC [%h]
IgG (CHO)	58 / 76	7.0 ± 3.0	222 ± 8	7945 ± 222
IgG (HEK)	58 / 76	23.9 ± 15.6	236 ± 35	8349 ± 633
scFv-Fc	46 / 76	2.5 ± 0.9	104 ± 6	3966 ± 828
scDb-Fc	51	2.8 ± 1.4	140 ± 35	4143 ± 1378
scFv-scCLCH1-Fc	54 / 76	3.2 ± 0.6	53 ± 11	2349 ± 403
scFv	46	0.2 ± 0.1	0.6 ± 0.2	16 ± 4
scDb	51	0.4 ± 0.1	1.3 ± 0.2	56 ± 15
scDb-C_H2	50	0.6 ± 0.1	0.8 ± 0.1	80 ± 20

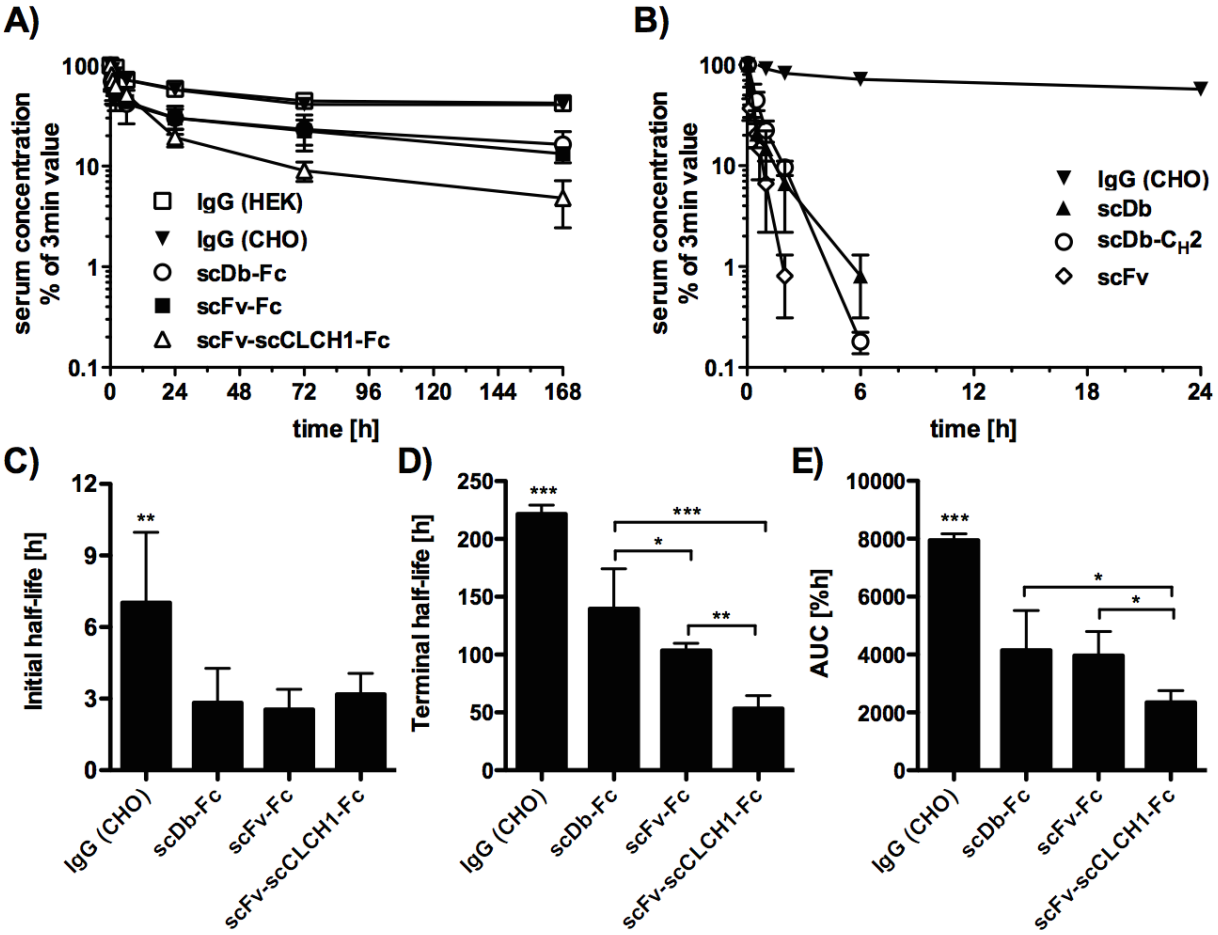

Figure 3-31: Pharmacokinetics of Fc fusion proteins

After a single injection of 25 µg protein, blood samples were collected at indicated time points. The remaining concentration was determined via CEA-binding ELISA and normalized to the 3 minute value. The pharmacokinetic properties were determined via Excel and the means were compared by one-way Anova with Tukey's post-test in GraphPad Prism (C-E).

4 Discussion

4.1 Immunoglobulin binding domains

The proteins exhibiting the longest circulation time in the blood are γ immunoglobulins and albumin with terminal half-lives of up to 21 and 19 days in humans, respectively (Morell, Terry, and Waldmann 1970; Peters 1995). This long retention time in the blood stream is influenced by many factors and one of the most important is the salvage from lysosomal degradation via the neonatal Fc receptor (Roopenian and Akilesh 2007). Exploiting the long serum persistence of these molecules therefore seems to present strong advantages, for example by fusion of an Fc part or albumin to the protein of interest (Kontermann 2012). Additionally, transient interactions via a binding moiety towards IgG or albumin also present a possibility to benefit from their long half-life. Albumin has been a target for these transient interactions for a long time and many studies have been performed using domains that can bind to albumin and successfully prolong the retention time in the bloodstream (Dennis et al. 2002; Hopp et al. 2010; Stork et al. 2009). On the other hand, the transient interaction with IgG molecules for a half-life extension purpose did not attract too much attention so far (Harmsen et al. 2005; Hoffmann et al. 2013; P Holliger et al. 1997; Hutt et al. 2012; Sockolosky, Kivimäe, and Szoka 2014; Unverdorben et al. 2012).

Some important factors have to be taken into account when generating a long lasting fusion protein with immunoglobulin-binding moieties. First, the selectivity for the IgG subclasses with long serum persistence (IgG1, IgG2 and IgG4) has to be assured (Hutt et al. 2012; Mankarious et al. 1988; Morell, Terry, and Waldmann 1970) and in particular the stability of binding under both physiological and acidic pH conditions has to be confirmed. This is necessary to maintain the high apparent hydrodynamic radius in the bloodstream (pH7.4) in order to exclude rapid renal elimination and to be able to benefit from the recycling effect in the acidified endosome. An interference with the neonatal Fc receptor, for example by occupying the same binding site on an IgG Fc part, can also negatively impact the pharmacokinetic behavior (Low and Mezo 2009; Mezo et al. 2008; Sockolosky, Kivimäe, and Szoka 2014). To avoid the formation of immune complexes, only one major binding site per IgBD-molecule would be beneficial, as otherwise the ensuing complexes might lead to a rapid

clearance of the fusion protein (Rehlaender and Cho 1998). For this reason, a monovalent use of IgBDs seems appropriate. Compared to the terminal half-life of endogenous IgG in humans (up to 21 days), the murine IgG does not have such a preferential retention time and remains in the bloodstream for 6 to 8 days (Vieira and Rajewsky 1988). This represents the maximal half-life that fusion proteins with IgBDs could exhibit in a mouse.

4.2 Novel immunoglobulin binding domains

Analogous to the well-described albumin-binding domain, the domain C3 (SpG_{C3}), also derived from *Streptococcus* Protein G, is able to bind towards IgG molecules and as a fusion partner can elongate the retention time in the bloodstream. The specificity for the long lasting IgG species was confirmed by a quartz crystal microbalance approach using both human serum IgG and purified IgG1 (Hutt et al. 2012). In accordance to previous studies, the SpG_{C3} domain was able to bind the Fab fragment as well as the Fc part of an IgG molecule (Erntell et al. 1988) with a higher affinity towards the Fc part. In order to circumvent the possible interference with the FcRn during the recycling of the IgG molecule (McDonnell et al. 2010), 3 central residues for the Fc binding were mutated into alanines to disrupt this binding site, resulting in the Fab-specific domain SpG_{C3Fab}. However, deletion of the Fc binding site resulted in reduced pharmacokinetics of scDb-SpG_{C3Fab}, compared to the corresponding SpG_{C3} fusion protein. This is presumably due to the deletion of Fc binding at neutral pH and the ensuing loss of affinity towards the full-length IgG molecules, since SpG_{C3Fab} is able to bind the Fab fragments of mouse and human with a similar or even slightly improved affinity compared to SpG_{C3}. The pH dependent changes in binding towards the Fc part were previously described for the SpG_{C3} domain, probably due to the protonation of histidine residues in the Fc part that are in close proximity to the bound domain (Sauer-Eriksson et al. 1995; Spassov and Yan 2013; Watanabe et al. 2009).

Similar to SpG_{C3Fab}, 3 residues involved in the binding towards C_H1 were substituted by alanines to generate SpG_{C3Fc}. The rationale behind this approach was to generate an IgBD that specifically binds towards the Fc parts of IgG molecules and by interference with FcRn recycling possibly lowers the serum half-life of endogenous IgG. Thus, the terminal half-life of the SpG_{C3Fc} fusion protein should be lower compared to the parental SpG_{C3} fusion protein that also binds the C_H1 domain. The

lower retention time and therefore lower serum IgG level would be advantageous in autoimmune diseases (Z. Liu et al. 1997). Conversely, the pharmacokinetic properties of the scDb-SpG_{C3Fc} exhibited an increased retention time, which cannot be correlated to the affinity determination. The performed amino acid substitutions hardly had an effect on IgG, Fc and Fab binding with comparable affinities of SpG_{C3}. Furthermore, domain C2 from Protein G was investigated for its properties in half-life extension as a fusion moiety and exhibited similar serum concentrations as well as comparable affinities towards IgG molecules as SpG_{C3}.

In order to determine the influence of the IgBD on the scDb moiety, an ELISA against the carcinoembryonic antigen and flow cytometry with CEA- or CD3-positive cells were performed. In the absence of excess amounts of IgG during the binding reaction to CEA, none of the IgBD had an impact on the binding properties, but in the presence of IgG all proteins that were able to bind the Fc part (scDb-SpG_{C3}, scDb-SpG_{C2} and scDb-SpG_{C3Fc}) showed decreased binding and a higher EC_{50} value. A plausible explanation therefore is sterical hindrance of CEA binding when the IgG molecule is bound with high affinity (up to 3 nM, Table 3-1) via its Fc part. Comparable findings were made in previous studies with the albumin-binding domain and additional albumin in the media (Stork, Müller, and Kontermann 2007; Tolmachev et al. 2007). The binding to CD3 on purified PBMCs was already altered without the addition of human serum IgG during the binding reaction, likely due to interactions with IgG that was used for the blocking of Fcγ receptors. This impact of IgG on the binding properties of the scDb moiety was also reflected in the IL-2 release. Whereas scDb-SpG_{C3Fab} showed the same activation of T-cells as the unmodified scDb, scDb-SpG_{C3} and scDb-SpG_{C3Fc} only efficiently activated the IL-2 secretion without additional IgG. Again, the binding towards the antigens of the scDb moiety could be affected as seen in ELISA and flow cytometry. Alternatively, the proper formation of a cytolytic synapse via the scDb between T-cell and target cell is disturbed by the additional IgG that could enlarge the interspace required for activation of the T-cells (Bluemel et al. 2010; Choudhuri et al. 2005).

4.3 Affinity maturation towards the C_H1 domain

Due to the lower affinity of SpG_{C3Fab} towards the complete IgG molecule and the ensuing drawback in pharmacokinetics, phage display libraries were generated in order to select for improved affinity towards the C_H1 domain. Special attention was

placed on the selection of clones that exhibit strong binding also at acidic conditions, since the dissociation from or missing association towards IgG at low pH would result in lysosomal degradation. The affinity maturation resulted in SpG_{C3Fab}RR, which presented significantly improved terminal half-life and bioavailbility as scDb fusion protein, compared to SpG_{C3Fab}. The reason for the enhancement is the improved affinity towards the IgG molecules and the Fab fragment under physiological and acidic conditions. In particular, the binding to the Fab fragment at acidic pH is increased more than 4-fold compared to SpG_{C3Fab}, indicating the formation of more stable complexes during FcRn recycling. Likewise, other studies could draw a correlation between increased affinity towards the long-lasting serum protein and half-life of the therapeutic protein, when using albumin together with albumin-binding domains or peptides (Hopp et al. 2010; Nguyen et al. 2006; Tolmachev et al. 2007). Importantly, the binding towards the Fc part at neutral pH is still eliminated. The data suggest that the partially reestablished binding to the Fc part at pH6 does not impede with the recycling via the neonatal Fc receptor, presumably due to a dominant binding to the Fab fragment. Otherwise, scDb-SpG_{C3Fab}RR could not reach its long half-life of 47.8 h and especially the high serum concentrations at day 3 and 7, as seen for scDbs fused to IgBDs originating from Protein A that only bind to the Fc part (Hutt et al. 2012; Unverdorben et al. 2012). Hereby, the maximal half-life would be determined by the half-life of IgG molecules in FcRn deficient mice, which is about 19 h (Chaudhury et al. 2003).

Apparently, residues 35 and 36 of SpG_{C3Fab} have strong influence on affinity and pharmacokinetics. Many clones derived from the error-prone PCR library (SpG_{C3Fab}E15V,YY, SpG_{C3Fab}K10Q,HNS, SpG_{C3Fab}N35Y) exhibited amino acid substitutions within this region, which was previously assigned for binding to the Fab fragment and mutated for library 3 (Figure 3-1) and could even achieve higher or comparable affinity towards mouse IgG compared to SpG_{C3Fab}RR. Nevertheless, their serum concentration after injection as scDb fusion proteins decreased more rapidly than that of scDb-SpG_{C3Fab}. Besides the mutation of the residues 35 and 36 only the SpG_{C3Fab}E15V modification showed preferential serum concentrations. This substitution is also located in a previously assigned Fab binding area that was mutated with library 1. Combining this variant with the so far best candidate SpG_{C3Fab}RR resulted in SpG_{C3Fab}RR,E15V, which could further improve the

pharmacokinetics of the scDb. Again, the slight affinity towards the Fc part apparently does not interfere with the FcRn recycling, but is negotiated by the affinity towards the C_H1 domain. The reason for these favorable pharmacokinetic properties is probably the highest affinity of all IgBDs towards mouse Fab fragment at neutral pH. In order to further highlight the effect of size on the elimination of proteins, IgBD fusion with scFvs, which have about half the molecular weight of an scDb, were created. All of these scFv fusion proteins were able to substantially improve the circulation time, but exhibited a shorter half-life than the corresponding scDb fusion protein. This is possibly due to dissociation at physiological pH and subsequent renal clearance because of an even lower hydrodynamic radius than the scDb-IgBD fusion proteins. The size effect on terminal half-life of the antibody moiety was already seen in earlier studies (Hutt et al. 2012; Müller et al. 2007). Nevertheless, the IgBDs were able to elongate the retention time in a similar manner as for the scDb, with SpG_{C3Fab}RR exhibiting the best pharmacokinetic properties, followed by SpG_{C3} and SpG_{C3Fab}.

Furthermore, these affinity-maturated mutants were characterized *in vitro* to determine whether the change in affinity also alters the behavior in binding and functionality of the fused scDb moiety. All new IgBD variants exhibited as scDb fusion proteins full binding potential to immobilized carcinoembryonic antigen as well as CEA or CD3 present of the surface of cells. These favorable binding properties were also reflected in the activation of T-cells that was seen in the IL-2 release assay for scDb-SpG_{C3Fab}RR and scDb-SpG_{C3Fab}RR,E15V. Similar to the SpG_{C3Fab} domain, the affinity maturated mutants did not interfere with the activation of T-cells in the presence of excess amounts of IgG as it was seen for the SpG_{C3} domain or an increased affinity ABD domain together with human serum albumin or even a PEGylated version of the scDb (Hopp et al. 2010; Stork et al. 2008). Therefore, the newly developed IgBDs seem to be particularly useful in extending the half-life of small bispecific T-cell engagers that need close contact between T-cell and target cell for effective retargeting and activation (Baeuerle and Reinhardt 2009; Müller and Kontermann 2010).

4.4 Deimmunization of SpG_{C3Fab}

Increasing the retention time in the bloodstream and retaining the therapeutic potential are crucial steps in improving the performance of small recombinant

proteins, but it is also important how the body reacts to the application of the drug. Even without effects of the therapeutic, the application can cause an immunologic reaction against the injected protein. Consequences can reach from neutralizing antibodies (Barbosa and Celis 2007) up to allergic reactions and anaphylactic shocks (Pedotti et al. 2001; Rosenberg 2006). Even fully human proteins can lead to the generation of anti-drug antibodies, depending on the recognition of certain sequences by antigen presenting cells with their major histocompatibility antigens of class II as foreign antigens (Rup 2003).

Since the IgBDs are derived from bacterial proteins, they will certainly not be compatible to the human self-proteins, but more important is whether their sequences are recognized by distinct HLA class II alleles (M. Baker et al. 2010). Therefore, a scanning of the sequence of SpG_{C3Fab} was performed including not only sequence, but also structure-based algorithms. Within the 8 most frequently distributed human leukocyte antigen class II alleles 9 possible T-cell epitopes were detected for SpG_{C3Fab}. The majority of the recognition patterns were concentrated within a cluster at the beginning of the sequence, between amino acids 3 and 20 (Figure 3-15). Thus, only few substitutions are necessary in order to remove these epitopes, since by one substitution multiple epitopes can be influenced. Due to the addition of the positively charged arginine residues in SpG_{C3Fab}RR, the scanning revealed three additional epitopes. Single as well as combinations of amino acid substitutions were able to disrupt possible T-cell epitopes. In order to access the quality of prediction and deimmunization from the *in silico* calculation, a validation of T-cell epitopes *in vitro* could have further determined their location and magnitude (Baker and Jones 2007). This would have been particularly useful, since *in silico* predictions often tend to over-prediction of epitopes (Perry, Jones, and Baker 2008).

In order to determine the functional binding of the deimmunized IgBDs towards IgG molecules, they were produced as scFv-IgBD fusion proteins and analyzed via quartz crystal microbalance. All combinations, but also most single amino acid mutations revealed reduced binding, indicating worse pharmacokinetic properties than the wild-type SpG_{C3Fab} due to less stable binding under physiological conditions. A combination to remove all possible epitopes would have been possible, but since the necessary mutation L12A already purged the binding completely, no combination

with that mutation was generated. For a more detailed analysis, selected domains were subcloned as scDb-IgBD fusion proteins and pharmacokinetics were investigated. Interestingly, these single mutants all showed similar serum concentrations as the SpG_{C3Fab} domain until day 1, but the concentration at day three dropped drastically. This cannot be explained by the affinity towards IgG and Fab fragment, since they are comparable or even slightly enhanced. However, the loss of affinity of the variants with multiple substitutions can explain the weak performance, which was at least partially remitted by the combination with the affinity maturated variant SpG_{C3Fab}RR.

In order to perform an *in vivo* experiment for immunogenicity of the SpG_{C3Fab} domain and its deimmunized variants, several requirements are necessary. Apart from the basic differences in human and mouse immune systems (Mestas and Hughes 2004), the mouse does not have the human set of MHC molecules, the human leukocyte antigens. Therefore, it remains unclear to what extent the mouse and human specificities overlap and whether also the murine epitopes are eliminated. The usage of transgenic mice that express the human MHC class II molecules on their cell surface might be an adequate solution (Taneja and David 1999). Since the development of immunogenicity is also dependent on the time of exposure and the dosage (Harro et al. 2010), the deimmunized version should exhibit similar half-life extension properties as the reference protein. This issue could be addressed by using the SpG_{C3Fab}RR, Y33T,DI1 variant that resembles the SpG_{C3Fab} variant most in serum concentrations. Additionally, the fusion partner of the IgBD must not contain any T-cell epitopes, as the resulting anti-drug antibodies would alter the pharmacokinetic behavior of the fusion protein. Alternatives to the here used scDb or scFv include for example deimmunized BiTEs or single-chain diabodies (Hammond et al. 2007; Vallera et al. 2010) or other therapeutic proteins (Cantor et al. 2011; Tangri et al. 2005). Even more important than these concerns is the detection of antibodies directed against the SpG_{C3Fab} domain. Since the domain has an innate affinity for IgG molecules, it is difficult to detect, whether antibodies specifically recognize the domain or whether IgGs are bound via the IgBD affinity. In a preliminary test with mouse serum, the immobilized SpG_{C3Fab} domain bound to endogenous mouse IgG in ELISA (data not shown). Furthermore, detection via an immunoblot with the denaturation of the SpG_{C3Fab} domain and subsequent incubation

with the serum of treated mice is not possible, as upon transfer to the membrane a spontaneous refolding of the domain occurs, again exhibiting binding to endogenous mouse IgG (data not shown). It also remains unclear, how the pharmacokinetic behavior of an IgBD would be altered upon binding of specific ADAs via their CDRs and not via the C_H1 domain.

4.5 Half-life extension of recombinant human erythropoietin

A therapy with small recombinant protein therapeutics offers a huge benefit to the patient, but due to their limited retention time in the bloodstream they often require multiple applications and are a very costly treatment. Using therapeutics with the same specificity and potency, but better pharmacokinetic properties will strongly reduce the burden for the patient as well as the caregivers (Powell and Gurk-Turner 2002). Therefore, the half-life extension strategy via immunoglobulin-binding domains was applied to a well-known and widely used therapeutic protein, recombinant human erythropoietin. Much effort has been placed in improving the pharmacokinetic properties so far, for example by PEGylation or hyperglycosylation of huEPO (Elliott et al. 2003; Macdougall 2008). With the use of immunoglobulin-binding domains we want to profit not only from the increased hydrodynamic radius, but also from the salvage of lysosomal degradation via the neonatal Fc receptor.

Eukaryotic production of huEPO with C-terminal addition of SpG_{C3Fab}, SpG_{C3} or SpG_{C3Fab}RR and subsequent purification via IMAC resulted in highly glycosylated proteins that exhibited single bands in an SDS-PAGE analysis after removal of the glycosylation. Their activity and proliferative potential was investigated with UT-7/EPO-cells, revealing that the addition of the IgBDs did not influence the activity per se, as was seen for other protein modifications like PEGylation and hyperglycosylation (Sinclair 2013). This reduced *in vitro* activity is due to a lower affinity towards the EPO receptor, presumably as consequence to sterical hindrance or charge effects (Egrie and Browne 2001). Analogous to the activity of the scDb-IgBD fusion proteins, the addition of excess amounts of human IgG to the medium changed the activity of huEPO-SpG_{C3}, but did neither influence unmodified huEPO, nor huEPO-SpG_{C3Fab} and huEPO-SpG_{C3Fab}RR. This effect could on the one hand be mediated by decreased binding towards the EPO receptor (Gross and Lodish 2006), like it was previously seen for IgBD-fused scDb and its antigens CEA and CD3. On the other hand, the steric hindrance could prevent the EPO receptor

dimer from undergoing conformational changes, suppressing signal transduction and proliferation (Hodges et al. 2007). Nevertheless, the pharmacokinetic studies were performed with all huEPO-IgBD fusion proteins, since the 4-fold decreased activity of huEPO-SpG_{C3} is similar to the 3-fold decreased activity of Aranesp, which can be overcome by the strong increase in half-life (Egrie and Browne 2001). Aranesp was also included in this proliferation assay and displayed favorable activation compared to all huEPO fusion proteins that were produced in-house. This is probably due to the higher product quality of the clinic material or owing to the additional poly-histidine tag for purification of the in-house produced fusion proteins.

Since the serum concentrations have been normalized to the serum concentration at the 3 minute time point, the product quality does not play the key role for the pharmacokinetic parameters. For both, huEPO and Aranesp previously reported terminal half-lives have been confirmed, with Aranesp showing a three times higher terminal half-life (Egrie and Browne 2001; Powell and Gurk-Turner 2002). By adding the immunoglobulin-binding domains, the terminal half-life of huEPO could be elongated, which is also reflected in a higher bioavailability. Similar to the previous studies, SpG_{C3Fab}RR was the IgBD that provided the best pharmacokinetic effect with a 5-fold increased terminal elimination time and also 15-fold higher area under the curve. Although the terminal half-life of huEPO-SpG_{C3Fab}RR exceeds Aranesp, the AUC is lower due to the higher initial half-life of Aranesp. Several other authors suggest that the recycling via the neonatal Fc receptor reveals its potential primarily in the terminal elimination phase (Datta-Mannan et al. 2007; Hinton et al. 2006; Medesan et al. 1998), well corresponding to the here obtained data. An additional issue is the way of clearance of huEPO from the bloodstream. With its nonlinear pharmacokinetics, huEPO is not mainly cleared via liver or kidney (Dinkelaar et al. 1981; Yoon et al. 1997), but the EPO receptor and its turnover seem to have strong influence on the serum concentration of huEPO. It was shown that upon binding and activation a rapid degradation of receptor and cytokine occurs. If the dissociation happens fast enough, only the receptor will be internalized and degraded after activation, leading to a longer serum persistence of those huEPO variants that exhibit less affinity towards the receptor, like Aranesp (Gross and Lodish 2006; Walrafen et al. 2005). Thus, apart from the direct effects of the hyperglycosylation to the pharmacokinetics, also the decreased affinity and activation of the EPO receptor

increase the serum concentrations of Aranesp compared to the other huEPO fusion proteins. Since huEPO-SpG_{C3} also displayed decreased activity in the presence of excess amounts of IgG during the proliferation assay, the pharmacokinetics could possibly also be influenced by diminished receptor binding, similar to Aranesp. In order to evaluate this hypothesis, an internalization study of all huEPO fusion proteins would have been necessary (Gross and Lodish 2006).

The augmented terminal half-life and bioavailability of Aranesp also translated into a higher efficacy of treatment, resulting in an about 13-fold higher biological activity when administered once a week, compared to unmodified huEPO (Egrie et al. 2003; Sasu et al. 2005). Whereas huEPO, huEPO-SpG_{C3Fab} and huEPO-SpG_{C3} did not increase the hemoglobin level of CD1 mice by a single injection, Aranesp and huEPO-SpG_{C3Fab}RR could benefit from their better pharmacokinetic properties and strongly increase the hemoglobin concentration for 18 days. The differences in biological activity can mostly be explained by the bioavailability of the huEPO fusion proteins. The concentration of huEPO, together with SpG_{C3Fab} and SpG_{C3}, apparently has not been within a therapeutic window for a sufficient amount of time to promote the onset of additional erythrocyte production. On the other side, Aranesp and huEPO-SpG_{C3Fab}RR maintained a high serum concentration and increased the hemoglobin concentration. The reason for the better performance of Aranesp compared to huEPO-SpG_{C3Fab}RR is probably the higher initial half-life and thus also higher AUC, as well as reduced receptor affinity, which presumably lead to less degradation after activation. For comparison reasons, all fusion proteins should be manufactured with the same product quality to exclude differences in bioactivity and therefore different effects during pharmacodynamic studies.

A very interesting issue is the translation of these results into human patients. Apart from the question of half-life elongation via the immunoglobulin-binding domains, the retention time for both unmodified and hyperglycosylated huEPO is about twice as high in humans as in the murine system (Macdougall et al. 1999). Moreover, there is a drastic difference in receptor affinity. Whereas the affinity in mice, rats and monkeys is similar with about 0.11 - 0.15 nM, the affinity of the human EPO receptor is 10-fold higher with 0.012 nM (Todokoro et al. 1987; Woo et al. 2007). Other approaches with EPO have been launched that utilize FcRn recycling, for example

Fusion of huEPO towards an Fc part. However, the permanent increase in size (112 kDa) results in lower bioavailability, since moving through endothelial cells is probably limited (Bitonti et al. 2004).

4.6 Fc fusion proteins

Monoclonal antibodies of the gamma immunoglobulin class are amongst the most widely used recombinant therapeutic proteins, due to their high producibility, stability and long serum half-life (Carter 2011). In accordance to earlier studies, the pharmacokinetic performance of a full-length IgG molecule exceeded other Fc fusion proteins, although an identical IgG1 Fc part was used for all fusion proteins (Suzuki et al. 2010). The effect of differing half-lives is already prominent for various IgG molecules like Trastuzumab and Daclizumab, where the terminal half-life ranges from 2.7 days to 20 days (Tokuda et al. 1999; Vincenti et al. 1998). Among other factors, the non-linear clearance with internalization and subsequent degradation of the antigen together with the antibody plays an important role and is jointly responsible for the weak pharmacokinetics of Trastuzumab (Mould and Sweeney 2007). For this reason, the carcinoembryonic antigen was chosen as target antigen for all Fc fusion proteins, since CEA does not get actively internalized upon antibody binding and it is not endogenous in mice and will therefore not impact the pharmacokinetics by unwanted side effects (Schmidt, Thurber, and Wittrup 2008). After the first exploration that the scFv-Fc exhibits a lower terminal half-life than the parental full-length antibody, we decided to investigate the size effect of the Fc fusion proteins by generating an scDb-Fc matching the molecular weight and additionally an scFv-scCLCH1-Fc to have a similar amino acid composition as the unmodified IgG. Apart from the CEA binding, scDb-Fc can also bind to the epsilon chain of human CD3 (Arnett et al. 2004), but as the parental antibody UCHT-1 is species-specific, no interference in the mouse system should occur. The integrity and purity of the Fc fusion proteins was determined via size exclusion chromatography, revealing a single elution peak for all proteins and a hydrodynamic radius of 5.6 nm for the IgG that is in well accordance to previous determinations (Stork et al. 2008). Both scDb-Fc and scFv-scCLCH1-Fc fulfilled the requirement to resemble the IgG molecule in size, only scFv-Fc had a smaller hydrodynamic radius reflecting the lower molecular weight. Increasing the size from the scFv-Fc towards the scDb-Fc hardly had an influence on the pharmacokinetic properties, with both proteins revealing an area under the curve about half of the unmodified IgG. Introduction of the constant domains of the Fab

fragment as a single chain variant (scFv-scCLCH1-Fc) also resulted in the same size as an IgG, but the bioavailability deteriorated to just 30 % of the aimed AUC.

A further factor for the elimination of proteins from the serum is the net charge of circulating molecules (Igawa et al. 2010). A protein with a low isoelectric point will be negatively charged under physiological conditions and possibly be repulsed from the likewise negatively charged cell surface (Boswell et al. 2010), as well as the glomerular fenestrations of the kidney (Kontos and Hubbell 2012). Hence, rapid renal degradation is avoided and the protein will not undergo fluid phase endocytosis and can avoid possible degradation in the lysosome, independent of the FcRn recycling (Gurbaxani, Dostalek, and Gardner 2013). The IgG molecule has a low isoelectric point, but with scFv-Fc having a lower, scDb-Fc having a higher and scFv-scCLCH1-Fc having a similar pI, no correlation concerning the half-life can be drawn. The susceptibility of recombinant proteins to serum proteases also affects the potency and retention time of the therapeutic in the blood stream. In particular, linker sequences between the immunoglobulin domains that are exposed to surrounding media can often be subject to proteolytic cleavage (Le Gall et al. 2004; Holliger and Hudson 2005). After 7 days of incubation with mouse serum neither the IgG molecules, nor scFv-Fc or scDb-Fc displayed a decreased level of active protein. In contrast, scFv-scCLCH1-Fc only showed about 65 % of the starting activity, denoting that one or more of the linker sequences between the scFv and the Fc part are not resistant to proteolytic cleavage. Furthermore, scDb-C_H2 is prone to serum protease digestion, since after serum incubation only about half of the protein was completely intact. Of note, after detection of the binding of scDb-C_H2 not via His-tag, but via Protein L (binding directly to the scDb via the variable domain of the kappa light chain), no loss in activity was noticeable, meaning that the linker sequences between the scDb and the C_H2 domain or the subsequent sequence must be affected, since the scDb moiety is still able to fully bind CEA.

Since all Fc fusion proteins are endowed with the identical Fc part of human IgG1, the capability to bind to the neonatal Fc receptor at acidic conditions should be comparable if no sterical hindrance prevents the correct complex formation. The assays were performed using the mouse FcRn to assess the *in vitro* binding kinetics as well as the *in vivo* pharmacokinetics in the same species system. With an affinity

of around 100 nM for all Fc fusion proteins, the binding, but also association and dissociation constants are in well accordance to previous studies, suggesting that intact FcRn binding is crucial, but not sufficient to reach the long half-life of a full-length IgG molecule (Gurbaxani et al. 2006). Thus, the poor binding properties of the scDb-C_H2 towards moFcRn, especially under acidic conditions, explain the rapid elimination from the bloodstream and the missing recycling effect. The ratio of association and dissociation rate also plays a role for the pharmacokinetic behavior of the Fc fusion proteins. Slowing down the dissociation rate at acidic pH translates into better serum half-life (Datta-Mannan et al. 2007). However, the kinetic rates of all Fc fusion proteins are comparable and therefore not the key factor for the differences in the pharmacokinetics. Additionally, the kinetics, i.e. the dissociation of bound Fc fusion protein from the FcRn, upon returning to a physiological pH, accompany with a longer *in vivo* half-life (Wang et al. 2011). Other studies highlight the importance of the Fab fragment for the recycling effect of the FcRn. An interaction between the Fab fragment and the FcRn was detected by hydrogen-deuterium exchange studies and subsequent mass spectrometry (Jensen et al. 2015). Although using full-length antibodies with identical Fc region, the Fab fragment was responsible for differences in FcRn binding and subsequently also pharmacokinetics (Wang et al. 2011). Since the affinity of all Fc fusion proteins towards the FcRn is similar, the fusion partner of the Fc part does not seem to have a strong impact on the *in vitro* interaction, but the question to what extent the N-terminal domains of the Fc part contribute to the recycling process or obstruct it remains unsolved. The high affinity calculated for K_{D2} is far from physiologically reasonable data and can be considered as artifact.

Besides the fluid phase endocytosis, binding of the Fc part towards Fcγ receptors on immune effector cells like macrophages, neutrophils, dendritic cells or natural killer cells can also cause the internalization and subsequent degradation of Fc fusion proteins (Comber et al. 1989; Gillies et al. 1999). Fc fusion proteins have to be glycosylated at asparagine 297 for the binding towards Fcγ receptors (Clark 1997). Therefore, also the glycosylation status influences the pharmacokinetic profile of Fc fusion proteins and the content of negatively charged sialic acid is even able to modify FcRn affinity. Although a high content of sialic acid decreases the affinity towards FcRn, the pharmacokinetic properties are enhanced (L. Liu et al. 2012). The issue of varying glycosylation was addressed by the generation of the CHO-produced

IgG molecule, but this did neither alter the *in vitro* properties, nor the serum concentration during the pharmacokinetic study. In accordance to literature, no single *in vitro* parameter could be isolated to accurately predict the *in vivo* pharmacokinetic behavior (Datta-Mannan and Wroblewski 2014). Rather an interplay of many factors, including size, stability, net charge, FcRn binding and others is necessary to explain the exceeding performance of the IgG molecule compared to other Fc formats.

4.7 Translation of animal results

In order to translate the pharmacokinetic findings of this study into the human situation, further studies are necessary using the human FcRn for binding studies, as well as evaluation in a more human-like system, like transgenic mice endowed with the human FcRn (Proetzel and Roopenian 2014). In general, the principles of allometric scaling calculated for small molecules used in an animal system into the human system is not appropriate for recombinant proteins, since many additional factors influence the performance of biotherapeutics (Deng et al. 2011). These parameters include, besides the biological effect of the therapeutic, likewise oxygen utilization, caloric expenditure, basal metabolism, blood volume, circulating plasma proteins, renal function and FcRn recycling (Reagan-Shaw et al. 2008). There are methods to roughly predict the pharmacokinetic behavior of protein drugs in humans, but a lot of effort and different animal models are necessary in order to reliably precalculate these parameters (Mahmood 2009).

4.8 Conclusion and outlook

The present study could demonstrate that immunoglobulin-binding domains represent a versatile tool for the half-life extension of small recombinant therapeutic proteins. Via affinity maturation of the C_H1 specific domain SpG_{C3Fab}, resulting in $SpG_{C3Fab}RR$, the terminal half-life of fusion proteins with antibody fragments (scFv and scDb), but also human erythropoietin could be significantly elongated. In the mean time, full functionality like IL-2 secretion for the scDb and proliferative effect of huEPO could be retained upon fusion of $SpG_{C3Fab}RR$, in contrast to other half-life extension strategies like PEGylation, hyperglycosylation or addition of an albumin-binding domain (Sinclair 2013; Stork et al. 2008; Tolmachev et al. 2007).

A pharmacodynamic study with a single injection of huEPO fusion proteins showed the beneficial properties of huEPO-$SpG_{C3Fab}RR$, only exceeded by Aranesp due to its

long initial half-life and lower receptor affinity. A combination of hyperglycosylation together with IgBDs could further enhance the pharmacokinetic and pharmacodynamic potential and simultaneously retain a low hydrodynamic radius for tissue penetration. Another pharmacodynamic study with the scDb could reinforce the potential of the IgBDs. For this purpose, a syngeneic mouse model with an scDb that is targeting a tumor antigen and the murine CD3 has to be established. A possible setup could be generated with an scDb against Fibroblast activation protein (FAP) combined with the scFv 2C11 against mouse CD3 in a B16-FAP tumor model in C57BL/6 mice (Brocks et al. 2001; Kermer et al. 2012; Liao et al. 2000) or with other antigens like EpCAM in a 4T1 breast cancer model (Amann et al. 2008).

By application of sequence and structure-based algorithms, T-cell epitopes in the sequence of SpG_{C3Fab} were identified and eliminated via a combination of amino acid substitutions. These deimmunized IgBDs exhibited the potential to increase the half-life as scDb fusion proteins, but the affinity maturated SpG_{C3Fab}RR could not be reached. In order to improve the affinity towards the Fab fragment and also the pharmacokinetics, a phage display approach could be used, generating a library that is only comprised of deimmunized SpG_{C3Fab} mutants. Since the residues that are responsible for immunogenicity are known, the corresponding amino acids can be substituted to amino acids that do not form epitopes. Such a library had been generated during this study with a diversity of 36×10^6 clones (6.7×10^6 different possible sequences), but the selection was not yet performed.

Full-length IgG has shown to have advantages in pharmacokinetic behavior compared to other Fc fusion proteins due to factors like size, net charge and stability. Redesigning linkers, especially for scFv-scCLCH1-Fc and scDb-C_H2, could eliminate the susceptibility of the recombinant fusion proteins to serum proteases and further stabilize the biotherapeutics in the bloodstream. Various substitutions in the Fc part have been described to improve the pharmacokinetic behavior by increasing the affinity towards the FcRn at acidic pH with simultaneous release at pH7.4. Those mutations include for example the substitution of asparagine 434 by alanine (N434A) or the triple mutation M252Y/S254T/T256E (YTE) that generate a new hydrophobic interaction site and the creation of salt-bridges, respectively (Dall'Acqua et al. 2006; Deng et al. 2010; Oganesyan et al. 2014).

5 Bibliography

Akerström, B, and L Björck. 1986. “A Physicochemical Study of Protein G, a Molecule with Unique Immunoglobulin G-Binding Properties.” *The Journal of biological chemistry* 261(22): 10240–47.

Alberts, Bruce, Alexander Johnson, Julian Lewis, Martin Raff, Keith Roberts, and Peter Walter. 2002. “T Cells and MHC Proteins.” In *Molecular Biology of the Cell*,.

Amann, Maria, Klaus Brischwein, Petra Lutterbuese, Larissa Parr, Laetitia Petersen, Grit Lorenczewski, Eva Krinner, Sandra Bruckmeier, Sandra Lippold, Roman Kischel, Ralf Lutterbuese, Peter Kufer, Patrick a. Baeuerle, and Bernd Schlereth. 2008. “Therapeutic Window of MuS110, a Single-Chain Antibody Construct Bispecific for Murine EpCAM and Murine CD3.” *Cancer Research* 68(1): 143–51.

Andersen, Jan Terje, Rikard Pehrson, Vladimir Tolmachev, Muluneh Bekele Daba, Lars Abrahmsén, and Caroline Ekblad. 2011. “Extending Half-Life by Indirect Targeting of the Neonatal Fc Receptor (FcRn) Using a Minimal Albumin Binding Domain.” *Journal of Biological Chemistry* 286(7): 5234–41.

Arnett, Kelly L, Stephen C Harrison, and Don C Wiley. 2004. “Crystal Structure of a Human CD3-Epsilon/delta Dimer in Complex with a UCHT1 Single-Chain Antibody Fragment.” *Proceedings of the National Academy of Sciences of the United States of America* 101(46): 16268–73.

Baeuerle, Patrick A, and Jerry A Murry. 2014. “Human Therapies as a Successful Liaison between Chemistry and Biology.” *Chemistry & biology* 21(9): 1046–54.

Baeuerle, Patrick A., and Carsten Reinhardt. 2009. “Bispecific T-Cell Engaging Antibodies for Cancer Therapy.” *Cancer Research* 69(12): 4941–44.

Baker, Matthew P, and Timothy D Jones. 2007. “Identification and Removal of Immunogenicity in Therapeutic Proteins.” *Current opinion in drug discovery & development* 10(2): 219–27.

Baker, Matthew, Helen M. Reynolds, Brooke Lumicisi, and Christine J. Bryson. 2010. “Immunogenicity of Protein Therapeutics: The Key Causes, Consequences and Challenges.” *Self/Nonself* 1(4): 314–22.

Barbosa, Maria D F S, and Esteban Celis. 2007. “Immunogenicity of Protein Therapeutics and the Interplay between Tolerance and Antibody Responses.” *Drug Discovery Today* 12(15-16): 674–81.

Beck, Alain, and Janice M Reichert. 2011. “Therapeutic Fc-Fusion Proteins and Peptides as Successful Alternatives to Antibodies.” *mAbs* 3(5): 415–16.

Berger, Verena, Fabian Richter, Kirstin Zettlitz, Felix Unverdorben, Peter Scheurich, Andreas Herrmann, Klaus Pfizenmaier, and Roland E Kontermann. 2013. “An Anti-TNFR1 scFv-HSA Fusion Protein as Selective Antagonist of TNF Action.” *Protein engineering, design & selection : PEDS* 26(10): 581–87.

Bertolotto, A, A Sala, S Malucchi, F Marnetto, M Caldano, A Di Sapio, M Capobianco, and F Gilli. 2004. 75 Journal of neurology, neurosurgery, and psychiatry *Biological Activity of Interferon Betas in Patients with Multiple Sclerosis Is Affected by Treatment Regimen and Neutralising Antibodies.*

Bitonti, Alan J, Jennifer A Dumont, Susan C Low, Robert T Peters, Keith E Kropp, Vito J Palombella, James M Stattel, Yichun Lu, Cristina a Tan, Jeffrey J Song, Ana Maria Garcia, Neil E Simister, Gerburg M Spiekermann, Wayne I Lencer, and Richard S Blumberg. 2004. “Pulmonary Delivery of an Erythropoietin Fc Fusion Protein in Non-Human Primates through an Immunoglobulin Transport Pathway.” *Proceedings of the National Academy of Sciences of the United States of America* 101(26): 9763–68.

Bluemel, Claudia, Susanne Hausmann, Petra Fluhr, Mirnalini Sriskandarajah, William B Stallcup, Patrick a Baeuerle, and Peter Kufer. 2010. “Epitope Distance to the Target Cell Membrane and Antigen Size Determine the Potency of T Cell-Mediated Lysis by BiTE Antibodies Specific for a Large Melanoma Surface Antigen.” *Cancer immunology, immunotherapy : CII* 59(8): 1197–1209.

Borrok, M Jack, Yanli Wu, Nurten Beyaz, Xiang-qing Yu, Vaheh Oganesyan, F Dall Acqua, Ping Tsui, M Jack Borrok, Yanli Wu, Nurten Beyaz, Xiang-qing Yu, Vaheh Oganesyan, F Dall Acqua, and Ping Tsui. 2014. “Immunology : pH-Dependent Binding Engineering Reveals An FcRn Affinity Threshold Which Governs IgG Recycling pH-Dependent FcRn Binding and IgG Clearance pH-Dependent Binding Engineering Reveals An FcRn Affinity Threshold Which Governs IgG Recycling Runnin.”

Boswell, C Andrew, Devin B Tesar, Kiran Mukhyala, Frank-Peter Theil, Paul J Fielder, and Leslie a Khawli. 2010. “Effects of Charge on Antibody Tissue Distribution and Pharmacokinetics.” *Bioconjugate chemistry* 21(12): 2153–63.

Brinks, Vera, Daniel Weinbuch, Matthew Baker, Yann Dean, Philippe Stas, Stefan Kostense, Bonita Rup, and Wim Jiskoot. 2013. “Preclinical Models Used for Immunogenicity Prediction of Therapeutic Proteins.” *Pharmaceutical research* 30(7): 1719–28.

Brocks, B, P Garin-Chesa, E Behrle, J E Park, W J Rettig, K Pfizenmaier, and D Moosmayer. 2001. “Species-Crossreactive scFv against the Tumor Stroma Marker ‘Fibroblast Activation Protein’ Selected by Phage Display from an Immunized FAP-/- Knock-out Mouse.” *Molecular medicine (Cambridge, Mass.)* 7(7): 461–69.

Bunn, H Franklin. 2013. “Erythropoietin.” *Cold Spring Harbor Perspectives in Medicine* 3(3): a011619.

Burmeister, W P, A H Huber, and P J Bjorkman. 1994. “Crystal Structure of the Complex of Rat Neonatal Fc Receptor with Fc.” *Nature* 372: 379–83.

Cantor, Jason R, Tae Hyeon Yoo, Aakanksha Dixit, Brent L Iverson, Thomas G Forsthuber, and George Georgiou. 2011. “Therapeutic Enzyme Deimmunization by Combinatorial T-Cell Epitope Removal Using Neutral Drift.” *Proceedings of the National Academy of Sciences of the United States of America* 108(4): 1272–77.

Carter, Paul J. 2011. “Introduction to Current and Future Protein Therapeutics: A Protein Engineering Perspective.” *Experimental cell research* 317(9): 1261–69.

Casadevall, Nicole, Joelle Nataf, Beatrice Viron, Amir Kolta, Patrick Michaud, Jean-Jacques Kiladjian, Patrick Mayeux, and Irene Teyssandier. 2002. “In Patients Treated With Recombinant Erythropoietin.” *The New England Journal of Medicine* 346(7): 469–75.

Chaudhury, Chaity, Charles L Brooks, Daniel C Carter, John M Robinson, and Clark L Anderson. 2006. “Albumin Binding to FcRn: Distinct from the FcRn-IgG Interaction.” *Biochemistry* 45(15): 4983–90.

Chaudhury, Chaity, Samina Mehnaz, John M Robinson, William L Hayton, Dennis K Pearl, Derry C Roopenian, and Clark L Anderson. 2003. “The Major Histocompatibility Complex-Related Fc Receptor for IgG (FcRn) Binds Albumin and Prolongs Its Lifespan.” *Journal of Experimental Medicine* 197(3): 315–22.

Chester, K A, A Mayer, J Bhatia, L Robson, D I Spencer, S P Cooke, A A Flynn, S K Sharma, G Boxer, R B Pedley, and R H Begent. 2000. “Recombinant Anti-Carcinoembryonic Antigen Antibodies for Targeting Cancer.” *Cancer chemotherapy and pharmacology* 46 Suppl: S8–12.

Chirmule, Narendra, Vibha Jawa, and Bernd Meibohm. 2012. “Immunogenicity to Therapeutic Proteins: Impact on PK/PD and Efficacy.” *The AAPS Journal* 14(2): 296–302.

Choudhuri, Kaushik, David Wiseman, Marion H Brown, Keith Gould, and P Anton van der Merwe. 2005. “T-Cell Receptor Triggering Is Critically Dependent on the Dimensions of Its Peptide-MHC Ligand.” *Nature* 436(7050): 578–82.

Clark, Michael R. 1997. “IgG Effector Mechanisms.” *Chemical immunology* 65: 88–110.

Comber, P G, F Gomez, M D Rossman, and A D Schreiber. 1989. “Receptors for the Fc Portion of Immunoglobulin G (Fc Gamma R) on Human Monocytes and Macrophages.” *Progress in clinical and biological research* 297: 273–85.

Czajkowsky, Daniel M, Jun Hu, Zhifeng Shao, and Richard J Pleass. 2012. “Fc-Fusion Proteins: New Developments and Future Perspectives.” *EMBO Molecular Medicine* 4(10): 1015–28.

Dall’Acqua, William F, Peter A Kiener, and Herren Wu. 2006. “Properties of Human IgG1s Engineered for Enhanced Binding to the Neonatal Fc Receptor (FcRn).” *Journal of Biological Chemistry* 281(33): 23514–24.

Datta-Mannan, Amita, Derrick R Witcher, Ying Tang, Jeffry Watkins, and Victor J Wroblewski. 2007. “Monoclonal Antibody Clearance. Impact of Modulating the Interaction of IgG with the Neonatal Fc Receptor.” *The Journal of biological chemistry* 282(3): 1709–17.

Datta-Mannan, Amita, and Victor J Wroblewski. 2014. “Application of FcRn Binding Assays To Guide mAb Development.” *Drug metabolism and disposition: the biological fate of chemicals*: 1–25.

DeLano, W. L., M H Ultsch, A M de Vos, and J A Wells. 2000. “Convergent Solutions to Binding at a Protein-Protein Interface.” *Science (New York, N.Y.)* 287(5456): 1279–83.

Deng, Rong, Suhasini Iyer, Frank-Peter Theil, Deborah L. Mortensen, Paul J. Fielder, and Saileta Prabhu. 2011. “Projecting Human Pharmacokinetics of Therapeutic Antibodies from Nonclinical Data: What Have We Learned?” *mAbs* 3(1): 61–66.

Deng, Rong, Kelly M Loyet, Samantha Lien, Suhasini Iyer, Laura E DeForge, Frank Peter Theil, Henry B Lowman, Paul J Fielder, and Saileta Prabhu. 2010. “Pharmacokinetics of Humanized Monoclonal Anti-Tumor Necrosis Factor-A Antibody and Its Neonatal Fc Receptor Variants in Mice and Cynomolgus Monkeys.” *Drug Metabolism and Disposition* 38(4): 600–605.

Dennis, Mark S, Min Zhang, Y. Gloria Meng, Miryam Kadkhodayan, Daniel Kirchhofer, Dan Combs, and Lisa A Damico. 2002. “Albumin Binding as a General Strategy for Improving the Pharmacokinetics of Proteins.” *Journal of Biological Chemistry* 277(38): 35035–43.

Derrick, Jeremy P., and Dale B. Wigley. 1994. “The Third IgG-Binding Domain from Streptococcal Protein G. An Analysis by X-Ray Crystallography of the Structure Alone and in a Complex with Fab.” *Journal of molecular biology* 243(5): 906–18.

Dinkelaar, R B, E Y Engels, A A Hart, L P Schoemaker, E Bosch, and R A Chamuleau. 1981. “Metabolic Studies on Erythropoietin (EP): II. The Role of Liver and Kidney in the Metabolism of Ep.” *Experimental hematology* 9(7): 796–803.

Egrie, J C, and J K Browne. 2001. “Development and Characterization of Novel Erythropoiesis Stimulating Protein (NESP).” *Nephrology, dialysis, transplantation : official publication of the European Dialysis and Transplant Association - European Renal Association* 16 Suppl 3: 3–13.

Egrie, Joan C, and Jeffrey K Browne. 2002. “Development and Characterization of Darbepoetin Alfa.” *Oncology (Williston Park, N.Y.)* 16(10 Suppl 11): 13–22.

Egrie, Joan C, Erik Dwyer, Jeffrey K Browne, Anna Hitz, and Michele a Lykos. 2003. “Darbepoetin Alfa Has a Longer Circulating Half-Life and Greater in Vivo Potency than Recombinant Human Erythropoietin.” *Experimental Hematology* 31(4): 290–99.

Elliott, Steve, Tony Lorenzini, Sheilah Asher, Ken Aoki, David Brankow, Lynette Buck, Leigh Busse, David Chang, Janis Fuller, James Grant, Natasha Hernday, Martha Hokum, Sylvia Hu, Andrew Knudten, Nancy Levin, Renee Komorowski, Frank Martin, Rachell Navarro, Timothy Osslund, Gary Rogers, Norma Rogers, Geri Trail, and Joan Egrie. 2003. “Enhancement of Therapeutic Protein in Vivo Activities through Glycoengineering.” *Nature biotechnology* 21(April): 414–21.

Elliott, Steve, and Angus M Sinclair. 2012. “The Effect of Erythropoietin on Normal and Neoplastic Cells.” *Biologics : targets & therapy* 6: 163–89.

Enever, Carrie, Thil Batuwangala, Chris Plummer, and Armin Sepp. 2009. “Next Generation Immunotherapeutics--Honing the Magic Bullet.” *Current opinion in biotechnology* 20(4): 405–11.

Erntell, Mats, Erling B Myhre, U Sjöbring, and L Björck. 1988. “Streptococcal Protein G Has Affinity for Both Fab- and Fc-Fragments of Human IgG.” *Molecular immunology* 25(2): 121–26.

Ezan, Eric. 2013. “Pharmacokinetic Studies of Protein Drugs: Past, Present and Future.” *Advanced drug delivery reviews* 65(8): 1065–73.

Finnern, R, E Pedrollo, I Fisch, J Wieslander, J D Marks, C M Lockwood, and W H Ouwehand. 1997. “Human Autoimmune Anti-Proteinase 3 scFv from a Phage Display Library.” *Clinical and experimental immunology* 107(2): 269–81.

Le Gall, Fabrice, Uwe Reusch, Melvyn Little, and Sergey M Kipriyanov. 2004. “Effect of Linker Sequences between the Antibody Variable Domains on the Formation, Stability and Biological Activity of a Bispecific Tandem Diabody.” *Protein engineering, design & selection : PEDS* 17(4): 357–66.

Gehlsen, Kurt, Rui Gong, Dave Bramhill, David Wiersma, Shaun Kirkpatrick, Yangping Wang, Yang Feng, and Dimiter S Dimitrov. 2012. “Pharmacokinetics of Engineered Human Monomeric and Dimeric CH2 Domains.” *mAbs* 4(4): 466–74.

Gieffers, Christian, Michael Kluge, Christian Merz, Jaromir Sykora, Meinolf Thiemann, René Schaal, Carmen Fischer, Marcus Branschädel, Behnaz Ahangarian Abhari, Peter Hohenberger, Simone Fulda, Harald Fricke, and Oliver Hill. 2013. “APG350 Induces Superior Clustering of TRAIL Receptors and Shows Therapeutic Antitumor Efficacy Independent of Cross-Linking via Fcγ Receptors.” *Molecular cancer therapeutics* 12(12): 2735–47.

Gillies, Stephen D, Yan Lan, Bea Brunkhorst, Wai-Keung Wong, Yue Li, and Kin-Ming Lo. 2002. “Bi-Functional Cytokine Fusion Proteins for Gene Therapy and Antibody-Targeted Treatment of Cancer.” *Cancer immunology, immunotherapy : CII* 51(8): 449–60.

Gillies, Stephen D, Yan Lan, K M Lo, Michael Super, and John Wesolowski. 1999. “Improving the Efficacy of Antibody-Interleukin 2 Fusion Proteins by Reducing Their Interaction with Fc Receptors.” *Cancer research* 59(9): 2159–66.

Gragert, Loren, Abeer Madbouly, John Freeman, and Martin Maiers. 2013. “Six-Locus High Resolution HLA Haplotype Frequencies Derived from Mixed-Resolution DNA Typing for the Entire US Donor Registry.” *Human Immunology* 74(10): 1313–20.

Gregoriadis, Gregory, Sanjay Jain, Ioannis Papaioannou, and Peter Laing. 2005. “Improving the Therapeutic Efficacy of Peptides and Proteins: A Role for Polysialic Acids.” *International Journal of Pharmaceutics* 300: 125–30.

De Groot, Anne S., and David W. Scott. 2007. “Immunogenicity of Protein Therapeutics.” *Trends in Immunology* 28(11): 482–90.

Gross, Alec W, and Harvey F Lodish. 2006. “Cellular Trafficking and Degradation of Erythropoietin and Novel Erythropoiesis Stimulating Protein (NESP).” *The Journal of biological chemistry* 281(4): 2024–32.

Gurbaxani, Brian, Linh L Dela Cruz, Koteswara Chintalacharuvu, and Sherie L Morrison. 2006. “Analysis of a Family of Antibodies with Different Half-Lives in Mice Fails to Find a Correlation between Affinity for FcRn and Serum Half-Life.” *Molecular immunology* 43(9): 1462–73.

Gurbaxani, Brian, Miroslav Dostalek, and Iain Gardner. 2013. “Are Endosomal Trafficking Parameters Better Targets for Improving mAb Pharmacokinetics than FcRn Binding Affinity?” *Molecular immunology* 56(4): 660–74.

Hammond, Scott a., Ralf Lutterbuese, Shannon Roff, Petra Lutterbuese, Bernd Schlereth, Elizabeth Bruckheimer, Michael S. Kinch, Steve Coats, Patrick a. Baeuerle, Peter Kufer, and Peter a. Kiener. 2007. “Selective Targeting and Potent Control of Tumor Growth Using an EphA2/CD3-Bispecific Single-Chain Antibody Construct.” *Cancer Research* 67(8): 3927–35.

Haraldsson, Börje, and Jenny Sörensson. 2004. “Why Do We Not All Have Proteinuria? An Update of Our Current Understanding of the Glomerular Barrier.” *News in physiological sciences : an international journal of physiology produced jointly by the International Union of Physiological Sciences and the American Physiological Society* 19(1): 7–10.

Harmsen, Michiel M, Conny B Van Solt, Helmi P D Fijten, and Marga C Van Setten. 2005. “Prolonged in Vivo Residence Times of Llama Single-Domain Antibody Fragments in Pigs by Binding to Porcine Immunoglobulins.” *Vaccine* 23(41): 4926–34.

Harro, Clayton, Robert Betts, Walter Orenstein, Eun Jeong Kwak, Howard E. Greenberg, Matthew T. Onorato, Jon Hartzel, Joy Lipka, Mark J. DiNubile, and Nicholas Kartsonis. 2010. “Safety and Immunogenicity of a Novel Staphylococcus Aureus Vaccine: Results from the First Study of the Vaccine Dose Range in Humans.” *Clinical and Vaccine Immunology* 17(12): 1868–74.

Havelund, Svend, Anne Plum, Ulla Ribel, Ib Jonassen, Aage Vølund, Jan Markussen, and Peter Kurtzhals. 2004. “The Mechanism of Protraction of Insulin Detemir, a Long-Acting, Acylated Analog of Human Insulin.” *Pharmaceutical Research* 21(8): 1498–1504.

Hermeling, Suzanne, Daan J a Crommelin, Huub Schellekens, and Wim Jiskoot. 2004. “Structure-Immunogenicity Relationships of Therapeutic Proteins.” *Pharmaceutical Research* 21(6): 897–903.

Hinton, Paul R, Joanna M Xiong, Mary G Johlfs, Meina Tao Tang, Stephen Keller, and Naoya Tsurushita. 2006. “An Engineered Human IgG1 Antibody with Longer Serum Half-Life.” *Journal of immunology (Baltimore, Md. : 1950)*.

Hodges, Vivien M, Susan Rainey, Terence R Lappin, and a Peter Maxwell. 2007. “Pathophysiology of Anemia and Erythrocytosis.” *Critical Reviews in Oncology/Hematology* 64(2): 139–58.

Hoffmann, Eike, Anish Konkar, Sebastian Dziadek, Hans-Peter Josel, Karin Conde-Knape, Holger Kropp, Lothar Kling, Kay Stubenrauch, Irmgard Thorey, Stefan Dengl, and Ulrich Brinkmann. 2013. “PK Modulation of Haptenylated Peptides via Non-Covalent Antibody Complexation.” *Journal of controlled release : official journal of the Controlled Release Society* 171(1): 48–56.

Holliger, P, M Wing, J D Pound, H Bohlen, and G Winter. 1997. “Retargeting Serum Immunoglobulin with Bispecific Diabodies.” *Nature biotechnology* 15: 632–36.

Holliger, Philipp, and Peter J Hudson. 2005. “Engineered Antibody Fragments and the Rise of Single Domains.” *Nature biotechnology* 23(9): 1126–36.

Hombach, Andreas, Claudia Heuser, and Hinrich Abken. 2005. “Simultaneous Targeting of IL2 and IL12 to Hodgkin’s Lymphoma Cells Enhances Activation of Resting NK Cells and Tumor Cell Lysis.” *International journal of cancer. Journal international du cancer* 115(2): 241–47.

Hopp, Jonas, Nora Hornig, Kirstin A Zettlitz, Aline Schwarz, Nadine Fuß, Dafne Müller, and Roland E Kontermann. 2010. “The Effects of Affinity and Valency of an Albumin-Binding Domain (ABD) on the Half-Life of a Single-Chain Diabody-ABD Fusion Protein.” *Protein engineering, design & selection : PEDS* 23(11): 827–34.

Hörl, Walter H. 2013. “Differentiating Factors between Erythropoiesis-Stimulating Agents: An Update to Selection for Anaemia of Chronic Kidney Disease.” *Drugs* 73(2): 117–30.

Hutt, Meike, Aline Färber-Schwarz, Felix Unverdorben, Fabian Richter, and Roland E Kontermann. 2012. “Plasma Half-Life Extension of Small Recombinant Antibodies by Fusion to Immunoglobulin-Binding Domains.” *Journal of Biological Chemistry* 287(7): 4462–69.

Igawa, T, H Tsunoda, T Tachibana, A Maeda, F Mimoto, C Moriyama, M Nanami, Y Sekimori, Y Nabuchi, Y Aso, and K Hattori. 2010. “Reduced Elimination of IgG Antibodies by Engineering the Variable Region.” *Protein engineering, design & selection : PEDS* 23(5): 385–92.

Ishino, Tetsuya, Mengmeng Wang, Lidia Mosyak, Amy Tam, Weili Duan, Kristine Svenson, Alison Joyce, Denise M O’Hara, Laura Lin, William S Somers, and Ronald Kriz. 2013. “Engineering a Monomeric Fc Domain Modality by N-Glycosylation for the Half-Life Extension of Biotherapeutics.” *The Journal of biological chemistry* 288(23): 16529–37.

Jelkmann, Wolfgang. 2007. “Recombinant EPO Production--Points the Nephrologist Should Know.” *Nephrology, dialysis, transplantation : official publication of the European Dialysis and Transplant Association - European Renal Association* 22(10): 2749–53.

Jensen, Pernille Foged, Vincent Larraillet, Tilman Schlothauer, Hubert Kettenberger, Maximiliane Hilger, and Kasper D. Rand. 2015. “Investigating the Interaction between the Neonatal Fc Receptor and Monoclonal Antibody Variants by Hydrogen/Deuterium Exchange Mass Spectrometry.” *Molecular & Cellular Proteomics* 14(1): 148–61.

Jones, Kevin B, David W Anderson, and Gregory D Longmore. 2005. “Effects of Recombinant Hematopoietins on Blood-Loss Anemia in Mice.” *The Iowa orthopaedic journal* 25: 129–34.

Kang, Jung Seok, Patrick P Deluca, and Kang Choon Lee. 2009. “Emerging PEGylated Drugs.” *Expert opinion on emerging drugs* 14: 363–80.

Kapur, Rick, Helga K Einarsdottir, and Gestur Vidarsson. 2014. “IgG-Effector Functions: ‘The Good, The Bad and The Ugly.’” *Immunology letters*: 1–6.

Kenanova, Vania, Tove Olafsen, Desiree M Crow, Gobalakrishnan Sundaresan, Murugesan Subbarayan, Nora H Carter, David N Ikle, Paul J Yazaki, Arion F Chatziioannou, Sanjiv S Gambhir, Lawrence E Williams, John E Shively, David Colcher, Andrew A Raubitschek, and Anna M Wu. 2005. “Tailoring the Pharmacokinetics and Positron Emission Tomography Imaging Properties of Anti-Carcinoembryonic Antigen Single-Chain Fv-Fc Antibody Fragments.” *Cancer research* 65(2): 622–31.

Kermer, V., V. Baum, N. Hornig, R. E. Kontermann, and D. Muller. 2012. “An Antibody Fusion Protein for Cancer Immunotherapy Mimicking IL-15 Trans-Presentation at the Tumor Site.” *Molecular Cancer Therapeutics* 11(13): 1279–88.

Kim, Jonghan, William L Hayton, John M Robinson, and Clark L Anderson. 2007. “Kinetics of FcRn-Mediated Recycling of IgG and Albumin in Human: Pathophysiology and Therapeutic Implications Using a Simplified Mechanism-Based Model.” *Clinical Immunology* 122: 146–55.

Kontermann, Roland E. 2009. “Strategies to Extend Plasma Half-Lives of Recombinant Antibodies.” *BioDrugs* 23(6): 93–109.

Kontermann, Roland E. 2011. “Strategies for Extended Serum Half-Life of Protein Therapeutics.” *Current Opinion in Biotechnology* 22(6): 868–76.

Kontermann, Roland E. 2012. “Half-Life Modulating Strategies-An Introduction.” In *Therapeutic Proteins: Strategies to Modulate Their Plasma Half-Lives*, , 1–21.

Kontos, Stephan, and Jeffrey a Hubbell. 2012. “Drug Development: Longer-Lived Proteins.” *Chemical Society reviews* 41(7): 2686–95.

Korn, Tina, Dirk M Nettelbeck, Tina Völkel, Rolf Müller, and Roland E Kontermann. 2004. “Recombinant Bispecific Antibodies for the Targeting of Adenoviruses to CEA-Expressing Tumour Cells: A Comparative Analysis of Bacterially Expressed Single-Chain Diabody and Tandem scFv.” *The journal of gene medicine* 6(6): 642–51.

Koury, Mark J. 2005. “Erythropoietin: The Story of Hypoxia and a Finely Regulated Hematopoietic Hormone.” *Experimental hematology* 33(11): 1263–70.

Lencer, Wayne I., and Richard S. Blumberg. 2005. “A Passionate Kiss, Then Run: Exocytosis and Recycling of IgG by FcRn.” *Trends in Cell Biology* 15(1): 5–9.

Levin, Ditza, Basil Golding, Scott E. Strome, and Zuben E. Sauna. 2014. “Fc Fusion as a Platform Technology: Potential for Modulating Immunogenicity.” *Trends in Biotechnology* 33(1): 27–34.

Liao, K W, Y C Lo, and S R Roffler. 2000. “Activation of Lymphocytes by Anti-CD3 Single-Chain Antibody Dimers Expressed on the Plasma Membrane of Tumor Cells.” *Gene therapy* 7: 339–47.

Liebner, Robert, Roman Mathaes, Martin Meyer, Thomas Hey, Gerhard Winter, and Ahmed Besheer. 2014. “Protein HESylation for Half-Life Extension: Synthesis, Characterization and Pharmacokinetics of HESylated Anakinra.” *European journal of pharmaceutics and biopharmaceutics : official journal of Arbeitsgemeinschaft fur Pharmazeutische Verfahrenstechnik e.V*.

Liu, Liming, Sujatha Gomathinayagam, Lora Hamuro, Thomayant Prueksaritanont, Weirong Wang, Terrance a Stadheim, and Stephen R Hamilton. 2012. “The Impact of Glycosylation on the Pharmacokinetics of a TNFR2:Fc Fusion Protein Expressed in Glycoengineered Pichia Pastoris.” *Pharmaceutical research* (1).

Liu, Z, D C Roopenian, X Zhou, G J Christianson, L a Diaz, D D Sedmak, and C L Anderson. 1997. “Beta2-Microglobulin-Deficient Mice Are Resistant to Bullous Pemphigoid.” *The Journal of experimental medicine* 186(5): 777–83.

Low, Susan C, and Adam R Mezo. 2009. “Inhibitors of the FcRn:IgG Protein-Protein Interaction.” *The AAPS journal* 11(3): 432–34.

Macdougall, I C, S J Gray, O Elston, C Breen, B Jenkins, J Browne, and J Egrie. 1999. “Pharmacokinetics of Novel Erythropoiesis Stimulating Protein Compared with Epoetin Alfa in Dialysis Patients.” *Journal of the American Society of Nephrology : JASN* 10: 2392–95.

Macdougall, Iain C. 2008. “Novel Erythropoiesis-Stimulating Agents: A New Era in Anemia Management.” *Clinical Journal of the American Society of Nephrology* 3: 200–207.

Mahmood, Iftekhar. 2009. “Pharmacokinetic Allometric Scaling of Antibodies: Application to the First-in-Human Dose Estimation.” *Journal of Pharmaceutical Sciences* 98(10): 3850–61.

Maiers, Martin, Loren Gragert, and William Klitz. 2007. “High-Resolution HLA Alleles and Haplotypes in the United States Population.” *Human Immunology* 68: 779–88.

Mankarious, S, M Lee, S Fischer, K H Pyun, H D Ochs, V A Oxelius, and R J Wedgwood. 1988. “The Half-Lives of IgG Subclasses and Specific Antibodies in Patients with Primary Immunodeficiency Who Are Receiving Intravenously Administered Immunoglobulin.” *The Journal of laboratory and clinical medicine* 112(5): 634–40.

Martin, W L, A P West, L Gan, and P J Bjorkman. 2001. “Crystal Structure at 2.8 A of an FcRn/heterodimeric Fc Complex: Mechanism of pH-Dependent Binding.” *Molecular cell* 7(4): 867–77.

Matsumura, Y, and H Maeda. 1986. “A New Concept for Macromolecular Therapeutics in Cancer Chemotherapy: Mechanism of Tumoritropic Accumulation of Proteins and the Antitumor Agent Smancs.” *Cancer Research* 46(December): 6387–92.

Mayer, A, K A Chester, A A Flynn, and R H Begent. 1999. “Taking Engineered Anti-CEA Antibodies to the Clinic.” *Journal of immunological methods* 231(1-2): 261–73.

McDonnell, Kevin A, Susan C Low, Todd Hoehn, Ryan Donnelly, Holly Palmieri, Cara Fraley, Paul Sakorafas, and Adam R Mezo. 2010. “Synthesis and Structure-Activity Relationships of Dimeric Peptide Antagonists of the Human Immunoglobulin G-Human Neonatal Fc Receptor (IgG-FcRn) Interaction.” *Journal of Medicinal Chemistry* 53(4): 1587–96.

Medesan, Corneliu, Petru Cianga, Mark Mummert, Diana Stanescu, Victor Ghetie, and E. Sally Ward. 1998. “Comparative Studies of Rat IgG to Further Delineate the Fc:FcRn Interaction Site.” *European Journal of Immunology* 28: 2092–2100.

Melder, Robert J, Blaire L Osborn, Todd Riccobene, Palanisamy Kanakaraj, Ping Wei, Guoxian Chen, David Stolow, Wendy Green Halpern, Thi-Sau Migone, Qi Wang, Krzysztof J Grzegorzewski, and Gilles Gallant. 2005. “Pharmacokinetics and in Vitro and in Vivo Anti-Tumor Response of an Interleukin-2-Human Serum Albumin Fusion Protein in Mice.” *Cancer immunology, immunotherapy : CII* 54(6): 535–47.

Mestas, Javier, and Christopher C W Hughes. 2004. “Of Mice and Not Men: Differences between Mouse and Human Immunology.” *Journal of immunology (Baltimore, Md. : 1950)* 172: 2731–38.

Mezo, Adam R, Kevin A McDonnell, Cristina a Tan Hehir, Susan C Low, Vito J Palombella, James M Stattel, George D Kamphaus, Cara Fraley, Yixia Zhang, Jennifer a Dumont, and Alan J Bitonti. 2008. “Reduction of IgG in Nonhuman Primates by a Peptide Antagonist of the Neonatal Fc Receptor FcRn.” *Proceedings of the National Academy of Sciences of the United States of America* 105(7): 2337–42.

Morell, Andreas, William D Terry, and Thomas A Waldmann. 1970. “Metabolic Properties of IgG Subclasses in Man.” *The Journal of clinical investigation* 49(4): 673–80.

Mould, Diane R, and Kevin R D Sweeney. 2007. “The Pharmacokinetics and Pharmacodynamics of Monoclonal Antibodies--Mechanistic Modeling Applied to Drug Development.” *Current opinion in drug discovery & development* 10: 84–96.

Müller, Dafne, Anette Karle, Bettina Meissburger, Ines Höfig, Roland Stork, and Roland E Kontermann. 2007. “Improved Pharmacokinetics of Recombinant Bispecific Antibody Molecules by Fusion to Human Serum Albumin.” *The Journal of biological chemistry* 282(17): 12650–60.

Müller, Dafne, and Roland E. Kontermann. 2010. “Bispecific Antibodies for Cancer Immunotherapy: Current Perspectives.” *BioDrugs* 24(2): 89–98.

Nguyen, Allen, Arthur E Reyes, Min Zhang, Paul McDonald, Wai Lee T Wong, Lisa A Damico, and Mark S Dennis. 2006. “The Pharmacokinetics of an Albumin-Binding Fab (AB.Fab) Can Be Modulated as a Function of Affinity for Albumin.” *Protein engineering, design & selection : PEDS* 19(7): 291–97.

Oganesyan, Vaheh, Melissa M Damschroder, Kimberly E Cook, Qing Li, Changshou Gao, Herren Wu, and William F Dall’Acqua. 2014. “Structural Insights into Neonatal Fc Receptor-Based Recycling Mechanisms.” *The Journal of biological chemistry* 289(11): 7812–24.

Parker, Andrew S, Wei Zheng, Karl E Griswold, and Chris Bailey-Kellogg. 2010. “Optimization Algorithms for Functional Deimmunization of Therapeutic Proteins.” *BMC bioinformatics* 11: 180.

Pedotti, R, D Mitchell, J Wedemeyer, M Karpuj, D Chabas, E M Hattab, M Tsai, S J Galli, and L Steinman. 2001. “An Unexpected Version of Horror Autotoxicus: Anaphylactic Shock to a Self-Peptide.” *Nature immunology* 2(3): 216–22.

Perry, Laura C a, Timothy D. Jones, and Matthew P. Baker. 2008. “New Approaches to Prediction of Immune Responses to Therapeutic Proteins during Preclinical Development.” *Drugs in R and D* 9(6): 385–96.

Peters, Theodore Jr. 1995. *All About Albumin: Biochemistry, Genetics, and Medical Applications*.

Powell, John, and Cheryle Gurk-Turner. 2002. “Darbepoetin Alfa (Aranesp).” *Proceedings (Baylor University. Medical Center)* 15(3): 332–35.

Proetzel, Gabriele, and Derry C Roopenian. 2014. “Humanized FcRn Mouse Models for Evaluating Pharmacokinetics of Human IgG Antibodies.” *Methods (San Diego, Calif.)* 65(1): 148–53.

Prümmer, O. 1997. “Treatment-Induced Antibodies to Interleukin-2.” *Biotherapy (Dordrecht, Netherlands)* 10(1): 15–24.

Radstake, T R D J, M Svenson, a M Eijsbouts, F H J van den Hoogen, C Enevold, P L C M van Riel, and K Bendtzen. 2009. “Formation of Antibodies against Infliximab and Adalimumab Strongly Correlates with Functional Drug Levels and Clinical Responses in Rheumatoid Arthritis.” *Annals of the rheumatic diseases* 68: 1739–45.

Rammensee, H G. 1995. “Chemistry of Peptides Associated with MHC Class I and Class II Molecules.” *Current opinion in immunology* 7: 85–96.

Rath, Timo, Kristi Baker, Jennifer A Dumont, Robert T Peters, Haiyan Jiang, Shuo-Wang Qiao, Wayne I Lencer, Glenn F Pierce, and Richard S Blumberg. 2013. “Fc-Fusion Proteins and FcRn: Structural Insights for Longer-Lasting and More Effective Therapeutics.” *Critical reviews in biotechnology* 8551: 1–20.

Reagan-Shaw, Shannon, Minakshi Nihal, and Nihal Ahmad. 2008. “Dose Translation from Animal to Human Studies Revisited.” *The FASEB journal : official publication of the Federation of American Societies for Experimental Biology* 22(3): 659–61.

Rehlaender, B N, and M J Cho. 1998. “Antibodies as Carrier Proteins.” *Pharmaceutical research* 15(11): 1652–56.

Roopenian, Derry C, and Shreeram Akilesh. 2007. “FcRn: The Neonatal Fc Receptor Comes of Age.” *Nature reviews. Immunology* 7(9): 715–25.

Rosenberg, Amy S. 2006. “Effects of Protein Aggregates: An Immunologic Perspective.” *The AAPS journal* 8(3): E501–7.

Rup, B. 2003. “Immunogenicity and Immune Tolerance Coagulation Factors VIII and IX.” *Developments in biologicals* 112: 55–59.

Sasu, Barbra J, Cynthia Hartley, Henry Schultz, Patricia McElroy, Raheemuddin Khaja, Steven Elliott, Joan C Egrie, Jeffrey K Browne, C Glenn Begley, and Graham Molineux. 2005. “Comparison of Epoetin Alfa and Darbepoetin Alfa Biological Activity under Different Administration Schedules in Normal Mice.” *Acta haematologica* 113(3): 163–74.

Sauer-Eriksson, A E, G J Kleywegt, M Uhlén, and T A Jones. 1995. “Crystal Structure of the C2 Fragment of Streptococcal Protein G in Complex with the Fc Domain of Human IgG.” *Structure (London, England : 1993)* 3(3): 265–78.

Sauerborn, Melody, Vera Brinks, Wim Jiskoot, and Huub Schellekens. 2010. “Immunological Mechanism Underlying the Immune Response to Recombinant Human Protein Therapeutics.” *Trends in pharmacological sciences* 31(2): 53–59.

Schellenberger, Volker, Chia-wei Wang, Nathan C Geething, Benjamin J Spink, Andrew Campbell, Wayne To, Michael D Scholle, Yong Yin, Yi Yao, Oren Bogin, Jeffrey L Cleland, Joshua Silverman, and Willem P C Stemmer. 2009. “A Recombinant Polypeptide Extends the in Vivo Half-Life of Peptides and Proteins in a Tunable Manner.” *Nature biotechnology* 27(12): 1186–90.

Schlapschy, Martin, Uli Binder, Claudia Börger, Ina Theobald, Klaus Wachinger, Sigrid Kisling, Dirk Haller, and Arne Skerra. 2013. “PASylation: A Biological Alternative to PEGylation for Extending the Plasma Half-Life of Pharmaceutically Active Proteins.” *Protein Engineering, Design and Selection* 26(8): 489–501.

Schmidt, Michael M, Greg M. Thurber, and K Dane Wittrup. 2008. “Kinetics of Anti-Carcinoembryonic Antigen Antibody Internalization: Effects of Affinity, Bivalency, and Stability.” *Cancer Immunology, Immunotherapy* 57(12): 1879–90.

Schmidt, Michael M, Sharon A Townson, Amy J Andreucci, Bracken M King, Emily B Schirmer, Alec J Murillo, Christian Dombrowski, Alison W Tisdale, Patricia a Lowden, Allyson L Masci, Joseph T Kovalchin, David V Erbe, K Dane Wittrup, Eric S Furfine, and Thomas M Barnes. 2013. “Crystal Structure of an HSA/FcRn Complex Reveals Recycling by Competitive Mimicry of HSA Ligands at a pH-Dependent Hydrophobic Interface.” *Structure* 21(11): 1966–78.

Scott, D W, and Anne S. De Groot. 2010. “Can We Prevent Immunogenicity of Human Protein Drugs?” *Annals of the rheumatic diseases* 69 Suppl 1(Suppl I): i72–76.

Seifert, Oliver, Aline Plappert, Sina Fellermeier, Martin Siegemund, Klaus Pfizenmaier, and Roland E Kontermann. 2014. “Tetravalent Antibody-scTRAIL Fusion Proteins with Improved Properties.” *Molecular cancer therapeutics* 13(1): 101–11.

Sinclair, Angus M. 2013. “Erythropoiesis Stimulating Agents: Approaches to Modulate Activity.” *Biologics : targets & therapy* 7: 161–74.

Sleep, Darrell, Jason Cameron, and Leslie R Evans. 2013. “Albumin as a Versatile Platform for Drug Half-Life Extension.” *Biochimica et biophysica acta* 1830(12): 5526–34.

Sockolosky, Jonathan T, Saul Kivimäe, and Francis C Szoka. 2014. “Fusion of a Short Peptide That Binds Immunoglobulin G to a Recombinant Protein Substantially Increases Its Plasma Half-Life in Mice.” *PloS one* 9(7): e102566.

Spassov, Velin Z, and Lisa Yan. 2013. “pH-Selective Mutagenesis of Protein-Protein Interfaces: In Silico Design of Therapeutic Antibodies with Prolonged Half-Life.” *Proteins* 81(4): 704–14.

Stork, Roland, Emmanuelle Campigna, Bruno Robert, Dafne Müller, and Roland E Kontermann. 2009. “Biodistribution of a Bispecific Single-Chain Diabody and Its Half-Life Extended Derivatives.” *The Journal of biological chemistry* 284(38): 25612–19.

Stork, Roland, Dafne Müller, and Roland E Kontermann. 2007. “A Novel Tri-Functional Antibody Fusion Protein with Improved Pharmacokinetic Properties Generated by Fusing a Bispecific Single-Chain Diabody with an Albumin-Binding Domain from Streptococcal Protein G.” *Protein engineering, design & selection : PEDS* 20(11): 569–76.

Stork, Roland, Kirstin A Zettlitz, Dafne Müller, Miriam Rether, Franz-Georg Hanisch, and Roland E Kontermann. 2008. “N-Glycosylation as Novel Strategy to Improve Pharmacokinetic Properties of Bispecific Single-Chain Diabodies.” *The Journal of biological chemistry* 283(12): 7804–12.

Sturniolo, T, E Bono, J Ding, L Raddrizzani, O Tuereci, U Sahin, M Braxenthaler, F Gallazzi, M P Protti, F Sinigaglia, and J Hammer. 1999. “Generation of Tissue-Specific and Promiscuous HLA Ligand Databases Using DNA Microarrays and Virtual HLA Class II Matrices.” *Nature biotechnology* 17: 555–61.

Suzuki, Takuo, Akiko Ishii-Watabe, Minoru Tada, Tetsu Kobayashi, Toshie Kanayasu-Toyoda, Toru Kawanishi, and Teruhide Yamaguchi. 2010. “Importance of Neonatal FcR in Regulating the Serum Half-Life of Therapeutic Proteins Containing the Fc Domain of Human IgG1: A Comparative Study of the Affinity of Monoclonal Antibodies and Fc-Fusion Proteins to Human Neonatal FcR.” *Journal of immunology (Baltimore, Md. : 1950)* 184(4): 1968–76.

Szlachcic, Anna, Malgorzata Zakrzewska, and Jacek Otlewski. 2011. “Longer Action Means Better Drug: Tuning up Protein Therapeutics.” *Biotechnology advances* 29(4): 436–41.

Taneja, V, and C S David. 1999. “HLA Class II Transgenic Mice as Models of Human Diseases.” *Immunological reviews* 169: 67–79.

Tangri, S., B. R. Mothe, J. Eisenbraun, J. Sidney, S. Southwood, K. Briggs, J. Zinckgraf, P. Bilsel, M. Newman, R. Chesnut, C. LiCalsi, and a. Sette. 2005. “Rationally Engineered Therapeutic Proteins with Reduced Immunogenicity.” *The Journal of Immunology* 174(6): 3187–96.

Tashiro, Mitsuru, and Gaetano T Montelione. 1995. “Structures of Bacterial Immunoglobulin-Binding Domains and Their Complexes with Immunoglobulins.” *Current opinion in structural biology* 5(4): 471–81.

Ternant, David, Alexandre Aubourg, Charlotte Magdelaine-Beuzelin, Danielle Degenne, Hervé Watier, Laurence Picon, and Gilles Paintaud. 2008. “Infliximab Pharmacokinetics in Inflammatory Bowel Disease Patients.” *Therapeutic drug monitoring* 30(4): 523–29.

Todokoro, K, S Kanazawa, H Amanuma, and Y Ikawa. 1987. “Specific Binding of Erythropoietin to Its Receptor on Responsive Mouse Erythroleukemia Cells.” *Proceedings of the National Academy of Sciences of the United States of America* 84(June): 4126–30.

Tokuda, Y, T Watanabe, Y Omuro, M Ando, N Katsumata, A Okumura, M Ohta, H Fujii, Y Sasaki, and T Niwa. 1999. “Dose Escalation and Pharmacokinetic Study of a Humanized Anti-HER2 Monoclonal Antibody in Patients with HER2 / Neu-Overexpressing Metastatic Breast Cancer.” 81(May): 1419–25.

Tolmachev, Vladimir, Anna Orlova, Rikard Pehrson, Joakim Galli, Barbro Baastrup, Karl Andersson, Mattias Sandström, Daniel Rosik, Jörgen Carlsson, Hans Lundqvist, Anders Wennborg, and Fredrik Y Nilsson. 2007. “Radionuclide Therapy of HER2-Positive Microxenografts Using a 177Lu-Labeled HER2-Specific Affibody Molecule.” *Cancer research* 67(6): 2773–82.

Topp, Max S, Nicola Gökbuget, Anthony S Stein, Gerhard Zugmaier, Susan O’Brien, Ralf C Bargou, Hervé Dombret, Adele K Fielding, Leonard Heffner, Richard a Larson, Svenja Neumann, Robin Foà, Mark Litzow, Josep-Maria Ribera, Alessandro Rambaldi, Gary Schiller, Monika Brüggemann, Heinz a Horst, Chris Holland, Catherine Jia, Tapan Maniar, Birgit Huber, Dirk Nagorsen, Stephen J Forman, and Hagop M Kantarjian. 2015. “Safety and Activity of Blinatumomab for Adult Patients with Relapsed or Refractory B-Precursor Acute Lymphoblastic Leukaemia: A Multicentre, Single-Arm, Phase 2 Study.” *The Lancet Oncology* 16: 57–66.

Traxlmayr, Michael W, Maximilian Faissner, Gerhard Stadlmayr, Christoph Hasenhindl, Bernhard Antes, Florian Rüker, and Christian Obinger. 2012. “Directed Evolution of Stabilized IgG1-Fc Scaffolds by Application of Strong Heat Shock to Libraries Displayed on Yeast.” *Biochimica et biophysica acta* 1824(4): 542–49.

Tryggvason, Karl, and Jorma Wartiovaara. 2005. “How Does the Kidney Filter Plasma?” *Physiology (Bethesda, Md.)* 20: 96–101.

Unverdorben, Felix, Aline Färber-Schwarz, Fabian Richter, Meike Hutt, and Roland E Kontermann. 2012. “Half-Life Extension of a Single-Chain Diabody by Fusion to Domain B of Staphylococcal Protein A.” *Protein engineering, design & selection : PEDS* 25(2): 81–88.

Vallera, Daniel A, Seunguk Oh, Hua Chen, Yanqun Shu, and Arthur E Frankel. 2010. “Bioengineering a Unique Deimmunized Bispecific Targeted Toxin That Simultaneously Recognizes Human CD22 and CD19 Receptors in a Mouse Model of B-Cell Metastases.” *Molecular cancer therapeutics* 9(June): 1872–83.

Vieira, P, and K Rajewsky. 1988. “The Half-Lives of Serum Immunoglobulins in Adult Mice.” *European journal of immunology* 18: 313–16.

Vincenti, F, R Kirkman, S Light, G Bumgardner, M Pescovitz, P Halloran, J Neylan, A Wilkinson, H Ekberg, R Gaston, L Backman, and J Burdick. 1998. “Interleukin-2-Receptor Blockade with Daclizumab to Prevent Acute Rejection in Renal Transplantation. Daclizumab Triple Therapy Study Group.” *The New England journal of medicine* 338(3): 161–65.

Walrafen, Pierre, Frédérique Verdier, Zahra Kadri, Stany Chrétien, Catherine Lacombe, and Patrick Mayeux. 2005. “Both Proteasomes and Lysosomes Degrade the Activated Erythropoietin Receptor.” *Blood* 105(2): 600–608.

Wang, Weirong, Ping Lu, Yulin Fang, Lora Hamuro, Tamara Pittman, Brian Carr, Jerome Hochman, and Thomayant Prueksaritanont. 2011. “Monoclonal Antibodies with Identical Fc Sequences Can Bind to FcRn Differentially with Pharmacokinetic Consequences.” *Drug metabolism and disposition: the biological fate of chemicals* 39(9): 1469–77.

Watanabe, Hideki, Hiroyuki Matsumaru, Ayako Ooishi, Yanwen Feng, Takayuki Odahara, Kyoko Suto, and Shinya Honda. 2009. “Optimizing pH Response of Affinity between Protein G and IgG Fc: How Electrostatic Modulations Affect Protein-Protein Interactions.” *The Journal of biological chemistry* 284(18): 12373–83.

Way, Jeffrey C, Scott Lauder, Beatrice Brunkhorst, Su-Ming Kong, An Qi, Gordon Webster, Islay Campbell, Sue McKenzie, Yan Lan, Bo Marelli, Lieu Anh Nguyen, Steven Degon, Kin-Ming Lo, and Stephen D Gillies. 2005. “Improvement of Fc-Erythropoietin Structure and Pharmacokinetics by Modification at a Disulfide Bond.” *Protein engineering, design & selection : PEDS* 18(3): 111–18.

Weflen, Andrew W, Nina Baier, Qing-Juan Tang, Malon Van den Hof, Richard S Blumberg, Wayne I Lencer, and Ramiro H Massol. 2013. “Multivalent Immune Complexes Divert FcRn to Lysosomes by Exclusion from Recycling Sorting Tubules.” *Molecular biology of the cell* 24(15): 2398–2405.

Woo, Sukyung, Wojciech Krzyzanski, and William J. Jusko. 2007. “Target-Mediated Pharmacokinetic and Pharmacodynamic Model of Recombinant Human Erythropoietin (rHuEPO).” *Journal of Pharmacokinetics and Pharmacodynamics* 34: 849–68.

Wozniak-Knopp, Gordana, Johannes Stadlmann, and Florian Rüker. 2012. “Stabilisation of the Fc Fragment of Human IgG1 by Engineered Intradomain Disulfide Bonds.” *PloS one* 7(1): e30083.

Ying, Tianlei, Tina W Ju, Yanping Wang, Ponraj Prabakaran, and Dimiter S Dimitrov. 2014. “Interactions of IgG1 CH2 and CH3 Domains with FcRn.” *Frontiers in immunology* 5(April): 146.

Yip, Victor, Enzo Palma, Devin Tesar, Eduardo Mundo, Daniela Bumbaca, Elizabeth Torres, Noe Reyes, Ben-Quan Shen, Paul J Fielder, Saileta Prabhu, Leslie a Khawli, and Charles Boswell. 2014. “Quantitative Cumulative Biodistribution of Antibodies in Mice: Effect of Modulating Binding Affinity to the Neonatal Fc Receptor.” *mAbs* 6(3): 689–96.

Yoon, W H, S J Park, I C Kim, and M G Lee. 1997. “Pharmacokinetics of Recombinant Human Erythropoietin in Rabbits and 3/4 Nephrectomized Rats.” *Research communications in molecular pathology and pharmacology* 96(2): 227–40.

Yoshida, Kenji, Adam L. Corper, Rana Herro, Bana Jabri, Ian A. Wilson, and Luc Teyton. 2010. “The Diabetogenic Mouse MHC Class II Molecule I-Ag7 Is Endowed with a Switch That Modulates TCR Affinity.” *Journal of Clinical Investigation* 120(5): 1578–90.

6 Sequences

pSecTagA scDb-IgBD

```
                                                                                SfiI
                                                                                |
ATG GAG ACA GAC ACA CTC CTG CTA TGG GTA CTG CTG CTC TGG GTT CCA GGT TCC ACT GGT GAC GCG GCC CAG CCG GCC ATG GCC CAG GTG AAA CTG CAG C  < 100
 M   E   T   D   T   L   L   L   W   V   L   L   L   W   V   P   G   S   T   G   D   A   A   Q   P   A   M   A   Q   V   K   L   Q
            10          20          30          40          50          60          70          80          90

AG TCT GGG GCA GAA CTT GTG AGG TCA GGG ACC TCA GTC AAG TTG TCC TGC ACA GCT TCT GGC TTC AAC ATT AAA GAC TCC TAT ATG CAC TGG TTG AGG CA  < 200
Q   S   G   A   E   L   V   R   S   G   T   S   V   K   L   S   C   T   A   S   G   F   N   I   K   D   S   Y   M   H   W   L   R   Q
            110         120         130         140         150         160         170         180         190

G GGG CCT GAA CAG GGC CTG GAG TGG ATT GGA TGG ATT GAT CCT GAG AAT GGT GAT ACT GAA TAT GCC CCG AAG TTC CAG GGC AAG GCC ACT TTT ACT ACA  < 300
  G   P   E   Q   G   L   E   W   I   G   W   I   D   P   E   N   G   D   T   E   Y   A   P   K   F   Q   G   K   A   T   F   T   T
            210         220         230         240         250         260         270         280         290

GAC ACA TCC TCC AAC ACA GCC TAC CTG CAG CTC AGC AGC CTG ACA TCT GAG GAC ACT GCC GTC TAT TAT TGT AAT GAG GGG ACT CCG ACT GGG CCG TAC T  < 400
 D   T   S   S   N   T   A   Y   L   Q   L   S   S   L   T   S   E   D   T   A   V   Y   Y   C   N   E   G   T   P   T   G   P   Y
            310         320         330         340         350         360         370         380         390

AC TTT GAC TAC TGG GGC CAA GGG ACC ACG GTC ACC GTC TCC TCA GGC GGT GGC GGA TCG GAT ATC CAG ATG ACC CAG TCC CCG AGT TCC CTG TCC GCC TC  < 500
Y   F   D   Y   W   G   Q   G   T   T   V   T   V   S   S   G   G   G   G   S   D   I   Q   M   T   Q   S   P   S   S   L   S   A   S
            410         420         430         440         450         460         470         480         490

T GTG GGC GAT AGA GTC ACC ATC ACC TGT CGT GCC AGT CAG GAC ATC CGT AAT TAT CTG AAC TGG TAT CAA CAG AAA CCA GGA AAA GCT CCG AAA CTA CTG  < 600
  V   G   D   R   V   T   I   T   C   R   A   S   Q   D   I   R   N   Y   L   N   W   Y   Q   Q   K   P   G   K   A   P   K   L   L
            510         520         530         540         550         560         570         580         590

ATT TAC TAT ACC TCC CGC CTG GAG TCT GGA GTC CCT TCT CGC TTC TCT GGT TCT GGT TCT GGG ACG GAT TAC ACT CTC ACC ATC AGC AGT CTG CAA CCG G  < 700
 I   Y   Y   T   S   R   L   E   S   G   V   P   S   R   F   S   G   S   G   S   G   T   D   Y   T   L   T   I   S   S   L   Q   P
            610         620         630         640         650         660         670         680         690

AG GAC TTC GCA ACC TAT TAC TGT CAG CAA GGT AAT ACT CTG CCG TGG ACG TTC GGA CAG GGC ACC AAG GTG GAG ATC AAA CGT GGA GGC GGT GGC AGC GG  < 800
E   D   F   A   T   Y   Y   C   Q   Q   G   N   T   L   P   W   T   F   G   Q   G   T   K   V   E   I   K   R   G   G   G   G   S   G
            710         720         730         740         750         760         770         780         790

T GGG CGC GCC TCG GCC GGA GGT GGC TCA GAG GTT CAG CTG GTG GAG TCT GGC GGT GGC CTG GTG CAG CCA GGG GGC TCA CTC CGT TTG TCC TGT GCA GCT  < 900
  G   R   A   S   A   G   G   G   S   E   V   Q   L   V   E   S   G   G   G   L   V   Q   P   G   G   S   L   R   L   S   C   A   A
            810         820         830         840         850         860         870         880         890

TCT GGC TAC TCC TTT ACC GGC TAC ACT ATG AAC TGG GTG CGT CAG GCC CCA GGT AAG GGC CTG GAA TGG GTT GCA CTG ATT AAT CCT TAT AAA GGT GTT T  < 1000
 S   G   Y   S   F   T   G   Y   T   M   N   W   V   R   Q   A   P   G   K   G   L   E   W   V   A   L   I   N   P   Y   K   G   V
            910         920         930         940         950         960         970         980         990

CC ACC TAT AAC CAG AAA TTC AAG GAT CGT TTC ACG ATA TCC GTA GAT AAA TCC AAA AAC ACA GCC TAC CTG CAA ATG AAC AGC CTG CGT GCT GAG GAC AC  < 1100
S   T   Y   N   Q   K   F   K   D   R   F   T   I   S   V   D   K   S   K   N   T   A   Y   L   Q   M   N   S   L   R   A   E   D   T
           1010        1020        1030        1040        1050        1060        1070        1080        1090

T GCA GTC TAT TAT TGT GCT AGA AGC GGA TAC TAC GGC GAT AGC GAC TGG TAT TTT GAC GTC TGG GGT CAA GGA ACC CTA GTC ACC GTC TCC TCG GGA GGC  < 1200
  A   V   Y   Y   C   A   R   S   G   Y   Y   G   D   S   D   W   Y   F   D   V   W   G   Q   G   T   L   V   T   V   S   S   G   G
           1110        1120        1130        1140        1150        1160        1170        1180        1190

GGG GGT TCG GAC ATC GAG CTC ACC CAG TCT CCA GCA ATC ATG TCT GCA TCT CCA GGG GAG AAA GTC ACC ATA ACC TGC AGT GCC AGC TCA AGT GTA AGT T  < 1300
 G   G   S   D   I   E   L   T   Q   S   P   A   I   M   S   A   S   P   G   E   K   V   T   I   T   C   S   A   S   S   S   V   S
           1210        1220        1230        1240        1250        1260        1270        1280        1290

AC ATG CAC TGG TTC CAG CAG AAG CCA GGC ACT TCT CCC AAA CTC TGG ATT TAT AGC ACA TCC AAC CTG GCT TCT GGA GTC CCT GCT CGC TTC AGT GGC AG  < 1400
Y   M   H   W   F   Q   Q   K   P   G   T   S   P   K   L   W   I   Y   S   T   S   N   L   A   S   G   V   P   A   R   F   S   G   S
           1310        1320        1330        1340        1350        1360        1370        1380        1390

T GGA TCT GGG ACC TCT TAC TCT CTC ACA ATC AGC CGA ATG GAG GCT GAA GAT GCT GCC ACT TAT TAC TGC CAG CAA AGG AGT AGT TAC CCA CTC ACG TTC  < 1500
  G   S   G   T   S   Y   S   L   T   I   S   R   M   E   A   E   D   A   A   T   Y   Y   C   Q   Q   R   S   S   Y   P   L   T   F
           1410        1420        1430        1440        1450        1460        1470        1480        1490

                                   NotI                                   BamHI                                   EcoRI      XbaI
                                   |                                      |                                       |          |
GGT GCT GGC ACC AAG CTG GAG CTG AAA CGG GCG GCC GCA GGC GGA TCT GGC GGA ... ... GGC GGA TCC CAC CAC CAC CAT CAC CAC TGA TGA GAA TTC CGC TCT AGA ...
 G   A   G   T   K   L   E   L   K   R   A   A   A   G   G   S   G   G ... ... G   G   S   H   H   H   H   H   H   *
           1510        1520        1530        1540
```

pAB1 scFv-IgBD

```
                                                   SfiI
                                                   |
ATG AAA TAC CTA TTG CCT ACG GCA GCC GCT GGA TTG TTA TTA CTC GCG GCC CAG CCG GCC ATG GCC CAG GTG AAA CTG CAG CAG TCT GGG GCA GAA CTT G  < 100
 M   K   Y   L   L   P   T   A   A   A   G   L   L   L   L   A   A   Q   P   A   M   A   Q   V   K   L   Q   Q   S   G   A   E   L
           10          20          30          40          50          60          70          80          90

TG AGG TCA GGG ACC TCA GTC AAG TTG TCC TGC ACA GCT TCT GGC TTC AAC ATT AAA GAC TCC TAT ATG CAC TGG TTG AGG CAG GGG CCT GAA CAG GGC CT  < 200
V   R   S   G   T   S   V   K   L   S   C   T   A   S   G   F   N   I   K   D   S   Y   M   H   W   L   R   Q   G   P   E   Q   G   L
           110         120         130         140         150         160         170         180         190

G GAG TGG ATT GGA TGG ATT GAT CCT GAG AAT GGT GAT ACT GAA TAT GCC CCG AAG TTC CAG GGC AAG GCC ACT TTT ACT ACA GAC ACA TCC TCC AAC ACA  < 300
  E   W   I   G   W   I   D   P   E   N   G   D   T   E   Y   A   P   K   F   Q   G   K   A   T   F   T   T   D   T   S   S   N   T
           210         220         230         240         250         260         270         280         290

GCC TAC CTG CAG CTC AGC AGC CTG ACA TCT GAG GAC ACT GCC GTC TAT TAT TGT AAT GAG GGG ACT CCG ACT GGG CCG TAC TAC TTT GAC TAC TGG GGC C  < 400
 A   Y   L   Q   L   S   S   L   T   S   E   D   T   A   V   Y   Y   C   N   E   G   T   P   T   G   P   Y   Y   F   D   Y   W   G
           310         320         330         340         350         360         370         380         390

AA GGG ACC ACG GTC ACC GTC TCC TCA GGT GGA GGC GGT TCA GGG GGA GGT GGA TCC GGT GGA GGC GGT TCA GAC ATC GAG CTC ACC CAG TCT CCA GCA AT  < 500
Q   G   T   T   V   T   V   S   S   G   G   G   G   S   G   G   G   G   S   G   G   G   G   S   D   I   E   L   T   Q   S   P   A   I
           410         420         430         440         450         460         470         480         490

C ATG TCT GCA TCT CCA GGG GAG AAA GTC ACC ATA ACC TGC AGT GCC AGC TCA AGT GTA AGT TAC ATG CAC TGG TTC CAG CAG AAG CCA GGC ACT TCT CCC  < 600
  M   S   A   S   P   G   E   K   V   T   I   T   C   S   A   S   S   S   V   S   Y   M   H   W   F   Q   Q   K   P   G   T   S   P
           510         520         530         540         550         560         570         580         590

AAA CTC TGG ATT TAT AGC ACA TCC AAC CTG GCT TCT GGA GTC CCT GCT CGC TTC AGT GGC AGT GGA TCT GGG ACC TCT TAC TCT CTC ACA ATC AGC CGA A  < 700
 K   L   W   I   Y   S   T   S   N   L   A   S   G   V   P   A   R   F   S   G   S   G   S   G   T   S   Y   S   L   T   I   S   R
           610         620         630         640         650         660         670         680         690

                                                                                                                   NotI
                                                                                                                   |
TG GAG GCT GAA GAT GCT GCC ACT TAT TAC TGC CAG CAA AGG AGT AGT TAC CCA CTC ACG TTC GGT GCT GGC ACC AAG CTG GAG CTG AAA CGG GCG GCC GC  < 800
M   E   A   E   D   A   A   T   Y   Y   C   Q   Q   R   S   S   Y   P   L   T   F   G   A   G   T   K   L   E   L   K   R   A   A   A
           710         720         730         740         750         760         770         780         790

                                                                  EcoRI
                                                                  |
A GGC GGA TCT GGC ... ... GGC GGC GGA TCC CAC CAC CAC CAT CAC CAC TGA TGA GAA TTC
  G   G   S   G ... ...  G   G   G   S   H   H   H   H   H   H   *   *
```

Novel immunoglobulin-binding domains

SpG_{C3}

```
ACC ACC TAC AAG CTG GTG ATC AAC GGC AAG ACC CTG AAG GGC GAG ACA ACC ACC AAG GCC GTG GAC GCC GAG ACA GCC GAG AAG GCC
 T   T   Y   K   L   V   I   N   G   K   T   L   K   G   E   T   T   T   K   A   V   D   A   E   T   A   E   K   A

TTC AAG CAG TAC GCC AAC GAC AAC GGC GTG GAC GGC GTG TGG ACC TAC GAC GAC GCC ACC AAG ACC TTC ACC GTG ACC GAG
 F   K   Q   Y   A   N   D   N   G   V   D   G   V   W   T   Y   D   D   A   T   K   T   F   T   V   T   E
```

SpG_{C3Fab}

```
ACA ACA TAC AAG CTC GTG ATC AAC GGC AAG ACC CTG AAG GGC GAG ACA ACC ACC AAA GCC GTC GAC GCC GAA ACA GCC GCC GCT GCC
 T   T   Y   K   L   V   I   N   G   K   T   L   K   G   E   T   T   T   K   A   V   D   A   E   T   A   A   A   A

TTT GCC CAG TAC GCC AAC GAT AAT GGC GTG GAC GGC GTG TGG ACC TAC GAC GAC GCC ACC AAG ACC TTC ACC GTG ACC GAA
 F   A   Q   Y   A   N   D   N   G   V   D   G   V   W   T   Y   D   D   A   T   K   T   F   T   V   T   E
```

SpG_{C3Fc}

```
ACA ACA TAC AAG CTC GTG ATC AAC GGC AAG GCC CTG GCT GGC GCC ACC ACA ACA AAA GCC GTC GAC GCC GAG ACA GCC GAG AAG GCC
 T   T   Y   K   L   V   I   N   G   K   A   L   A   G   A   T   T   T   K   A   V   D   A   E   T   A   E   K   A

TTT AAG CAG TAC GCC AAC GAC AAC GGC GTG GAC GGC GTG TGG ACC TAC GAC GAT GCC ACC AAG ACC TTC ACC GTG ACC GAG
 F   K   Q   Y   A   N   D   N   G   V   D   G   V   W   T   Y   D   D   A   T   K   T   F   T   V   T   E
```

SpG_{C2}

```
ACA ACA TAC AAG CTC GTG ATC AAC GGC AAG ACC CTG AAG GGC GAG ACA ACC ACC GAA GCC GTC GAC GCC GCC ACA GCC GAG AAG GTG
 T   T   Y   K   L   V   I   N   G   K   T   L   K   G   E   T   T   T   E   A   V   D   A   A   T   A   E   K   V

TTC AAG CAG TAC GCC AAC GAC AAC GGC GTG GAC GGC GAG TGG ACC TAC GAC GAT GCC ACC AAG ACC TTC ACC GTG ACC GAG
 F   K   Q   Y   A   N   D   N   G   V   D   G   E   W   T   Y   D   D   A   T   K   T   F   T   V   T   E
```

Affinity maturated IgBDs

Amino acids of the determined Fab binding site are colored according to their use for the generation of phage display libraries (Library 1: blue, library 2: red, library 3: green) (Figure 3-1).

SpG_{C3Fab}TTR

```
ACA ACA TAC AAG CTC GTG ATC AAC GGC AAG ACC CTG AAG GGC ACT ACG CGT ACC AAA GCC GTC GAC GCC GAA ACA GCC GCC GCT GCC
 T   T   Y   K   L   V   I   N   G   K   T   L   K   G   T   T   R   T   K   A   V   D   A   E   T   A   A   A   A

TTT GCC CAG TAC GCC AAC GAT AAT GGC GTG GAC GGC GTG TGG ACC TAC GAC GAC GCC ACC AAG ACC TTC ACC GTG ACC GAA
 F   A   Q   Y   A   N   D   N   G   V   D   G   V   W   T   Y   D   D   A   T   K   T   F   T   V   T   E
```

SpG_{C3Fab}HTM

```
ACA ACA TAC AGG CTC GTG ATC AAC GGC AAG ACC CTG AAG GGC CAT ACG ATG ACC AAA GCC GTC GAC GCC GAA ACA GCC GCC GCT GCC
 T   T   Y   R   L   V   I   N   G   K   T   L   K   G   H   T   M   T   K   A   V   D   A   E   T   A   A   A   A

TTT GCC CAG TAC GCC AAC GAT AAT GGC GTG GAC GGC GTG TGG ACC TAC GAC GAC GCC ACC AAG ACC TTC ACC GTG ACC GAA
 F   A   Q   Y   A   N   D   N   G   V   D   G   V   W   T   Y   D   D   A   T   K   T   F   T   V   T   E
```

SpG_{C3Fab}K13S

```
ACA ACA TAC AAG CTC GTG ATC AAC GGC AAG ACC CTG TCT GGC GAG ACA ACC ACC AAA GCC GTC GAC GCC GAA ACA GCC GCC GCT GCC
 T   T   Y   K   L   V   I   N   G   K   T   L   S   G   E   T   T   T   K   A   V   D   A   E   T   A   A   A   A

TTT GCC CAG TAC GCC AAC GAT AAT GGC GTG GAC GGC GTG TGG ACC TAC GAC GAC GCC ACC AAG ACC TTC ACC GTG ACC GAG
 F   A   Q   Y   A   N   D   N   G   V   D   G   V   W   T   Y   D   D   A   T   K   T   F   T   V   T   E
```

SpG_{C3Fab}FRQ

```
ACA ACA TAC AAG CTC GTG ATC AAC GGC AAG ACC CTG AAG GGC GAG ACA ACC ACC AAA GCC GTC GAC GCC GAA ACA GCC GCC GCT GCC
 T   T   Y   K   L   V   I   N   G   K   T   L   K   G   E   T   T   T   K   A   V   D   A   E   T   A   A   A   A

TTT GCC CAG TGG GCC TTT AGG CAG GGC GTG GAC GGC GTG TGG ACC TAC GAC GAC GCC ACC AAG ACC TTC ACC GTG ACC GAG
 F   A   Q   W   A   F   R   Q   G   V   D   G   V   W   T   Y   D   D   A   T   K   T   F   T   V   T   E
```

SpG_{C3Fab}RR

```
ACA ACA TAC AAG CTC GTG ATC AAC GGC AAG ACC CTG AAG GGC GAG ACA ACC ACC AAA GCC GTC GAC GCC GAA ACA GCC GCC GCT GCC
 T   T   Y   K   L   V   I   N   G   K   T   L   K   G   E   T   T   T   K   A   V   D   A   E   T   A   A   A   A

TTT GCC CAG TAT GCC AGG AGG AAT GGC GTG GAC GGC GTG TGG ACC TAC GAC GAC GCC ACC AAG ACC TTC ACC GTG ACC GAG
 F   A   Q   Y   A   R   R   N   G   V   D   G   V   W   T   Y   D   D   A   T   K   T   F   T   V   T   E
```

SpG_{C3Fab}T1A,E15Q

```
GCA ACA TAC AAG CTC GTG ATC AAC GGC AAG ACC CTG AAG GGC CAG ACA ACC ACC AAA GCC GTC GAC GCC GAA ACA GCC GCC GCT GCC
 A   T   Y   K   L   V   I   N   G   K   T   L   K   G   Q   T   T   T   K   A   V   D   A   E   T   A   A   A   A

TTT GCC CAG TAC GCC AAC GAT AAT GGC GTG GAC GGC GTG TGG ACC TAC GAC GAC GCC ACC AAG ACC TTC ACC GTG ACC GAG
 F   A   Q   Y   A   N   D   N   G   V   D   G   V   W   T   Y   D   D   A   T   K   T   F   T   V   T   E
```

SpG_{C3Fab}E15V

```
ACA ACA TAC AAG CTC GTG ATC AAC GGC AAG ACC CTG AAG GGC GTG ACA ACC ACC AAA GCC GTC GAC GCC GAA ACA GCC GCC GCT GCC
 T   T   Y   K   L   V   I   N   G   K   T   L   K   G   V   T   T   T   K   A   V   D   A   E   T   A   A   A   A

TTT GCC CAG TAC GCC AAC GAT AAT GGC GTG GAC GGC GTG TGG ACC TAC GAC GAC GCC ACC AAG ACC TTC ACC GTG ACC GAG
 F   A   Q   Y   A   N   D   N   G   V   D   G   V   W   T   Y   D   D   A   T   K   T   F   T   V   T   E
```

SpG_{C3Fab}E15V,YY

```
ACA ACA TAC AAG CTC GTG ATC AAC GGC AAG ACC CTG AAG GGC GTG ACA ACC ACC AAA GCC GTC GAC GCC GAA ACA GCC GCC GCT GCC
 T   T   Y   K   L   V   I   N   G   K   T   L   K   G   V   T   T   T   K   A   V   D   A   E   T   A   A   A   A

TTT GCC CAG TAC GCC TAC TAT AAT GGC GTG GAC GGC GTG TGG ACC TAC GAC GAC GCC ACC AAG ACC TTC ACC GTG ACC GAG
 F   A   Q   Y   A   Y   Y   N   G   V   D   G   V   W   T   Y   D   D   A   T   K   T   F   T   V   T   E
```

SpG_{C3Fab}K10Q,HNS

```
ACA ACA TAC AAG CTC GTG ATC AAC GGC CAG ACC CTG AAG GGC GAG ACA ACC ACC AAA GCC GTC GAC GCC GAA ACA GCC GCC GCT GCC
 T   T   Y   K   L   V   I   N   G   Q   T   L   K   G   E   T   T   T   K   A   V   D   A   E   T   A   A   A   A

TTT GCC CAG TAC GCC CAC AAT AAT GGC GTG GAC GGC GTG TGG ACC TAC GAC GAC GCC TCC AAG ACC TTC ACC GTG ACC GAG
 F   A   Q   Y   A   H   N   N   G   V   D   G   V   W   T   Y   D   D   A   S   K   T   F   T   V   T   E
```

SpG_{C3Fab}N35Y

```
ACA ACA TAC AAG CTC GTG ATC AAC GGC AAG ACC CTG AAG GGA GAG ACA ACC ACC AAA GCC GTC GAC GCC GAA ACA GCC GCC GCT GCC
 T   T   Y   K   L   V   I   N   G   K   T   L   K   G   E   T   T   T   K   A   V   D   A   E   T   A   A   A   A

TTT GCC CAG TAC GCC TAC GAT AAT GGC GTG GAC GGC GTG TGG ACC TAC GAC GAC GCC ACC AAG ACC TTC ACC GTG ACC GAG
 F   A   Q   Y   A   Y   D   N   G   V   D   G   V   W   T   Y   D   D   A   T   K   T   F   T   V   T   E
```

SpG_{C3Fab}K50Q

```
ACA ACA TAC AAG CTC GTG ATC AAC GGC AAG ACC CTG AAG GGC GAG ACA ACC ACC AAA GCC GTC GAC GCC GAA ACA GCC GCC GCT GCC
 T   T   Y   K   L   V   I   N   G   K   T   L   K   G   E   T   T   T   K   A   V   D   A   E   T   A   A   A   A

TTT GCC CAG TAC GCC AAC GAT AAT GGC GTG GAC GGC GTG TGG ACC TAC GAC GAC GCC ACC CAG ACC TTC ACC GTG ACC GAG
 F   A   Q   Y   A   N   D   N   G   V   D   G   V   W   T   Y   D   D   A   T   Q   T   F   T   V   T   E
```

SpG_{C3Fab}RR,E15V

```
ACA ACA TAC AAG CTC GTG ATC AAC GGC AAG ACC CTG AAG GGC GTG ACA ACC ACC AAA GCC GTC GAC GCC GAA ACA GCC GCC GCT GCC
 T   T   Y   K   L   V   I   N   G   K   T   L   K   G   V   T   T   T   K   A   V   D   A   E   T   A   A   A   A

TTT GCC CAG TAT GCC AGG AGG AAT GGC GTG GAC GGC GTG TGG ACC TAC GAC GAC GCC ACC AAG ACC TTC ACC GTG ACC GAG
 F   A   Q   Y   A   R   R   N   G   V   D   G   V   W   T   Y   D   D   A   T   K   T   F   T   V   T   E
```

Deimmunized IgBDs

SpG_{C3Fab}K4E

```
ACA ACA TAC GAG CTC GTG ATC AAC GGC AAG ACC CTG AAG GGC GAG ACA ACC ACC AAA GCC GTC GAC GCC GAA ACA GCC GCC GCT GCC
 T   T   Y   E   L   V   I   N   G   K   T   L   K   G   E   T   T   T   K   A   V   D   A   E   T   A   A   A   A

TTT GCC CAG TAC GCC AAC GAT AAT GGC GTG GAC GGC GTG TGG ACC TAC GAC GAC GCC ACC AAG ACC TTC ACC GTG ACC GAA
 F   A   Q   Y   A   N   D   N   G   V   D   G   V   W   T   Y   D   D   A   T   K   T   F   T   V   T   E
```

SpG_{C3Fab}L5A

```
ACA ACA TAC AAG GCC GTG ATC AAC GGC AAG ACC CTG AAG GGC GAG ACA ACC ACC AAA GCC GTC GAC GCC GAA ACA GCC GCC GCT GCC
 T   T   Y   K   A   V   I   N   G   K   T   L   K   G   E   T   T   T   K   A   V   D   A   E   T   A   A   A   A

TTT GCC CAG TAC GCC AAC GAT AAT GGC GTG GAC GGC GTG TGG ACC TAC GAC GAC GCC ACC AAG ACC TTC ACC GTG ACC GAA
 F   A   Q   Y   A   N   D   N   G   V   D   G   V   W   T   Y   D   D   A   T   K   T   F   T   V   T   E
```

SpG_{C3Fab}V6A

```
ACA ACA TAC AAG CTC GCG ATC AAC GGC AAG ACC CTG AAG GGC GAG ACA ACC ACC AAA GCC GTC GAC GCC GAA ACA GCC GCC GCT GCC
 T   T   Y   K   L   A   I   N   G   K   T   L   K   G   E   T   T   T   K   A   V   D   A   E   T   A   A   A   A

TTT GCC CAG TAC GCC AAC GAT AAT GGC GTG GAC GGC GTG TGG ACC TAC GAC GAC GCC ACC AAG ACC TTC ACC GTG ACC GAA
 F   A   Q   Y   A   N   D   N   G   V   D   G   V   W   T   Y   D   D   A   T   K   T   F   T   V   T   E
```

SpG_{C3Fab}I7L

```
ACA ACA TAC AAG CTC GTG CTC AAC GGC AAG ACC CTG AAG GGC GAG ACA ACC ACC AAA GCC GTC GAC GCC GAA ACA GCC GCC GCT GCC
 T   T   Y   K   L   V   L   N   G   K   T   L   K   G   E   T   T   T   K   A   V   D   A   E   T   A   A   A   A

TTT GCC CAG TAC GCC AAC GAT AAT GGC GTG GAC GGC GTG TGG ACC TAC GAC GAC GCC ACC AAG ACC TTC ACC GTG ACC GAA
 F   A   Q   Y   A   N   D   N   G   V   D   G   V   W   T   Y   D   D   A   T   K   T   F   T   V   T   E
```

SpG_{C3Fab}N8D

```
ACA ACA TAC AAG CTC GTG ATC GAC GGC AAG ACC CTG AAG GGC GAG ACA ACC ACC AAA GCC GTC GAC GCC GAA ACA GCC GCC GCT GCC
 T   T   Y   K   L   V   I   D   G   K   T   L   K   G   E   T   T   T   K   A   V   D   A   E   T   A   A   A   A

TTT GCC CAG TAC GCC AAC GAT AAT GGC GTG GAC GGC GTG TGG ACC TAC GAC GAC GCC ACC AAG ACC TTC ACC GTG ACC GAA
 F   A   Q   Y   A   N   D   N   G   V   D   G   V   W   T   Y   D   D   A   T   K   T   F   T   V   T   E
```

SpG_{C3Fab}K10Q

```
ACA ACA TAC AAG CTC GTG ATC AAC GGC CAG ACC CTG AAG GGC GAG ACA ACC ACC AAA GCC GTC GAC GCC GAA ACA GCC GCC GCT GCC
 T   T   Y   K   L   V   I   N   G   Q   T   L   K   G   E   T   T   T   K   A   V   D   A   E   T   A   A   A   A

TTT GCC CAG TAC GCC AAC GAT AAT GGC GTG GAC GGC GTG TGG ACC TAC GAC GAC GCC ACC AAG ACC TTC ACC GTG ACC GAA
 F   A   Q   Y   A   N   D   N   G   V   D   G   V   W   T   Y   D   D   A   T   K   T   F   T   V   T   E
```

SpG_{C3Fab}L12A

```
ACA ACA TAC AAG CTC GTG ATC AAC GGC AAG ACC GCG AAG GGC GAG ACA ACC ACC AAA GCC GTC GAC GCC GAA ACA GCC GCC GCT GCC
 T   T   Y   K   L   V   I   N   G   K   T   A   K   G   E   T   T   T   K   A   V   D   A   E   T   A   A   A   A

TTT GCC CAG TAC GCC AAC GAT AAT GGC GTG GAC GGC GTG TGG ACC TAC GAC GAC GCC ACC AAG ACC TTC ACC GTG ACC GAA
 F   A   Q   Y   A   N   D   N   G   V   D   G   V   W   T   Y   D   D   A   T   K   T   F   T   V   T   E
```

SpG_{C3Fab}T44S

```
ACA ACA TAC AAG CTC GTG ATC AAC GGC AAG ACC CTG AAG GGC GAG ACA ACC ACC AAA GCC GTC GAC GCC GAA ACA GCC GCC GCT GCC
 T   T   Y   K   L   V   I   N   G   K   T   L   K   G   E   T   T   T   K   A   V   D   A   E   T   A   A   A   A

TTT GCC CAG TAC GCC AAC GAT AAT GGC GTG GAC GGC GTG TGG TCC TAC GAC GAC GCC ACC AAG ACC TTC ACC GTG ACC GAA
 F   A   Q   Y   A   N   D   N   G   V   D   G   V   W   S   Y   D   D   A   T   K   T   F   T   V   T   E
```

SpG_{C3Fab}A48G

```
ACA ACA TAC AAG CTC GTG ATC AAC GGC AAG ACC CTG AAG GGC GAG ACA ACC ACC AAA GCC GTC GAC GCC GAA ACA GCC GCC GCT GCC
 T   T   Y   K   L   V   I   N   G   K   T   L   K   G   E   T   T   T   K   A   V   D   A   E   T   A   A   A   A

TTT GCC CAG TAC GCC AAC GAT AAT GGC GTG GAC GGC GTG TGG ACC TAC GAC GAC GGC ACC AAG ACC TTC ACC GTG ACC GAA
 F   A   Q   Y   A   N   D   N   G   V   D   G   V   W   T   Y   D   D   G   T   K   T   F   T   V   T   E
```

SpG_{C3Fab}DI1

```
ACA ACA TAC GAG CTC GCG ATC AAC GGC CAG ACC CTG AAG GGC GAG ACA ACC ACC AAA GCC GTC GAC GCC GAA ACA GCC GCC GCT GCC
 T   T   Y   E   L   A   I   N   G   Q   T   L   K   G   E   T   T   T   K   A   V   D   A   E   T   A   A   A   A

TTT GCC CAG TAC GCC AAC GAT AAT GGC GTG GAC GGC GTG TGG ACC TAC GAC GAC GGC ACC AAG ACC TTC ACC GTG ACC GAA
 F   A   Q   Y   A   N   D   N   G   V   D   G   V   W   T   Y   D   D   G   T   K   T   F   T   V   T   E
```

SpG_{C3Fab}DI2

```
ACA ACA TAC AAG GTC GCG ATC AAC GGC CAG ACC CTG AAG GGC GAG ACA ACC ACC AAA GCC GTC GAC GCC GAA ACA GCC GCC GCT GCC
 T   T   Y   K   V   A   I   N   G   Q   T   L   K   G   E   T   T   T   K   A   V   D   A   E   T   A   A   A   A

TTT GCC CAG TAC GCC AAC GAT AAT GGC GTG GAC GGC GTG TGG ACC TAC GAC GAC GGC ACC AAG ACC TTC ACC GTG ACC GAA
 F   A   Q   Y   A   N   D   N   G   V   D   G   V   W   T   Y   D   D   G   T   K   T   F   T   V   T   E
```

SpG_{C3Fab}DI3

```
ACA ACA TAC AAG CTC ACG ATC GAC GGC AAG ACC CTG AAG GGC GAG ACA ACC ACC AAA GCC GTC GAC GCC GAA ACA GCC GCC GCT GCC
 T   T   Y   K   L   T   I   D   G   K   T   L   K   G   E   T   T   T   K   A   V   D   A   E   T   A   A   A   A

TTT GCC CAG TAC GCC AAC GAT AAT GGC GTG GAC GGC GTG TGG TCC TAC GAC GAC GCC ACC AAG ACC TTC ACC GTG ACC GAA
 F   A   Q   Y   A   N   D   N   G   V   D   G   V   W   S   Y   D   D   A   T   K   T   F   T   V   T   E
```

SpG_{C3Fab}DI4

```
ACA ACA TAC AAG CTC ACG ATC AAC GGC GAG ACC CTG AAG GGC GAG ACA ACC ACC AAA GCC GTC GAC GCC GAA ACA GCC GCC GCT GCC
 T   T   Y   K   L   T   I   N   G   E   T   L   K   G   E   T   T   T   K   A   V   D   A   E   T   A   A   A   A

TTT GCC CAG TAC GCC AAC GAT AAT GGC GTG GAC GGC GTG TGG TCC TAC GAC GAC GCC ACC AAG ACC TTC ACC GTG ACC GAA
 F   A   Q   Y   A   N   D   N   G   V   D   G   V   W   S   Y   D   D   A   T   K   T   F   T   V   T   E
```

SpG_{C3Fab}DI5

```
ACA ACA TAC AAG CTC GTG CTC AAC GGC GAG ACC CTG AAG GGC GAG ACA ACC ACC AAA GCC GTC GAC GCC GAA ACA GCC GCC GCT GCC
 T   T   Y   K   L   V   L   N   G   E   T   L   K   G   E   T   T   T   K   A   V   D   A   E   T   A   A   A   A

TTT GCC CAG TAC GCC AAC GAT AAT GGC GTG GAC GGC GTG TGG TCC TAC GAC GAC GCC ACC AAG ACC TTC ACC GTG ACC GAA
 F   A   Q   Y   A   N   D   N   G   V   D   G   V   W   S   Y   D   D   A   T   K   T   F   T   V   T   E
```

SpG_{C3Fab}RR,Y33A

```
ACA ACA TAC AAG CTC GTG ATC AAC GGC AAG ACC CTG AAG GGC GAG ACA ACC ACC AAA GCC GTC GAC GCC GAA ACA GCC GCC GCT GCC
 T   T   Y   K   L   V   I   N   G   K   T   L   K   G   E   T   T   T   K   A   V   D   A   E   T   A   A   A   A

TTT GCC CAG GCT GCC AGG AGG AAT GGC GTG GAC GGC GTG TGG ACC TAC GAC GAC GCC ACC AAG ACC TTC ACC GTG ACC GAA
 F   A   Q   A   A   R   R   N   G   V   D   G   V   W   T   Y   D   D   A   T   K   T   F   T   V   T   E
```

SpG_{C3Fab}RR,Y33T,DI1

```
ACA ACA TAC GAG CTC GCG ATC AAC GGC CAG ACC CTG AAG GGC GAG ACA ACC ACC AAA GCC GTC GAC GCC GAA ACA GCC GCC GCT GCC
 T   T   Y   E   L   A   I   N   G   Q   T   L   K   G   E   T   T   T   K   A   V   D   A   E   T   A   A   A   A

TTT GCC CAG ACT GCC AGG AGG AAT GGC GTG GAC GGC GTG TGG TCC TAC GAC GAC GCC ACC AAG ACC TTC ACC GTG ACC GAA
 F   A   Q   T   A   R   R   N   G   V   D   G   V   W   S   Y   D   D   A   T   K   T   F   T   V   T   E
```

huEPO fusion proteins

pSecTagAL1 huEPO

```
                                                                                AgeI
                                                                                |
ATG GAG ACA GAC ACA CTC CTG CTA TGG GTA CTG CTG CTC TGG GTT CCA GGT TCC ACC GGT GAC GCC CCC CCT AGA CTG ATC TGC GAC AGC CGG GTG CTG G  < 100
 M   E   T   D   T   L   L   L   W   V   L   L   L   W   V   P   G   S   T   G   D   A   P   P   R   L   I   C   D   S   R   V   L
            10          20          30          40          50          60          70          80          90

AA AGA TAC CTG CTG GAA GCC AAA GAG GCC GAG AAC ATC ACC ACC GGC TGC GCC GAG CAC TGC TCC CTG AAC GAG AAT ATC ACC GTG CCC GAC ACC AAA GT  < 200
E   R   Y   L   L   E   A   K   E   A   E   N   I   T   T   G   C   A   E   H   C   S   L   N   E   N   I   T   V   P   D   T   K   V
            110         120         130         140         150         160         170         180         190

G AAC TTC TAC GCC TGG AAG CGG ATG GAA GTG GGC CAG CAG GCT GTG GAA GTG TGG CAG GGA CTG GCC CTG CTG TCT GAG GCT GTG CTG AGA GGA CAG GCT  < 300
N   F   Y   A   W   K   R   M   E   V   G   Q   Q   A   V   E   V   W   Q   G   L   A   L   L   S   E   A   V   L   R   G   Q   A
210         220         230         240         250         260         270         280         290

CTG CTC GTG AAC AGC AGC CAG CCT TGG GAG CCT CTC CAG CTG CAC GTG GAC AAG GCC GTG TCT GGC CTG AGA AGC CTG ACC ACC CTG CTG AGA GCA CTG G  < 400
 L   L   V   N   S   S   Q   P   W   E   P   L   Q   L   H   V   D   K   A   V   S   G   L   R   S   L   T   T   L   L   R   A   L
            310         320         330         340         350         360         370         380         390

GA GCC CAG AAA GAG GCC ATC AGC CCT CCA GAT GCC GCC TCT GCT GCC CCC CTG AGA ACC ATC ACC GCC GAC ACC TTC AGA AAG CTG TTC CGG GTG TAC AG  < 500
G   A   Q   K   E   A   I   S   P   P   D   A   A   S   A   A   P   L   R   T   I   T   A   D   T   F   R   K   L   F   R   V   Y   S
            410         420         430         440         450         460         470         480         490
                                                                            NotI                                    XbaI
                                                                            |                                       |
C AAC TTC CTG AGA GGC AAG CTG AAG CTG TAC ACA GGC GAG GCC TGT CGG ACC GGC GAC AGA GCG GCC GCC CAC CAT CAT CAC CAT CAC TAA TCT AGA ...
  N   F   L   R   G   K   L   K   L   Y   T   G   E   A   C   R   T   G   D   R   A   A   A   H   H   H   H   H   H   *
            510         520         530         540         550         560         570         580         590
```

Fc fusion proteins

The sequence of the Fc fusion proteins is shown until the beginning of domain C_H2. The subsequent Fc part is identical to the Fc part of IgG CEA.

IgG CEA – Heavy chain

```
ATG GAG ACA GAC ACA CTC CTG CTA TGG GTA CTG CTG CTC TGG GTT CCA GGT TCC ACT GGT GAC GCG GCC CAG CCG GCC ATG GCC CAG GTG AAA CTG CAG C  < 100
 M   E   T   D   T   L   L   L   W   V   L   L   L   W   V   P   G   S   T   G   D   A   A   Q   P   A   M   A   Q   V   K   L   Q
            10          20          30          40          50          60          70          80          90

AG TCT GGG GCA GAA CTT GTG AGG TCA GGG ACC TCA GTC AAG TTG TCC TGC ACA GCT TCT GGC TTC AAC ATT AAA GAC TCC TAT ATG CAC TGG TTG AGG CA  < 200
Q   S   G   A   E   L   V   R   S   G   T   S   V   K   L   S   C   T   A   S   G   F   N   I   K   D   S   Y   M   H   W   L   R   Q
            110         120         130         140         150         160         170         180         190

G GGG CCT GAA CAG GGC CTG GAG TGG ATT GGA TGG ATT GAT CCT GAG AAT GGT GAT ACT GAA TAT GCC CCG AAG TTC CAG GGC AAG GCC ACT TTT ACT ACA  < 300
  G   P   E   Q   G   L   E   W   I   G   W   I   D   P   E   N   G   D   T   E   Y   A   P   K   F   Q   G   K   A   T   F   T   T
            210         220         230         240         250         260         270         280         290

GAC ACA TCC TCC AAC ACA GCC TAC CTG CAG CTC AGC AGC CTG ACA TCT GAG GAC ACT GCC GTC TAT TAT TGT AAT GAG GGG ACT CCG ACT GGG CCG TAC T  < 400
 D   T   S   S   N   T   A   Y   L   Q   L   S   S   L   T   S   E   D   T   A   V   Y   Y   C   N   E   G   T   P   T   G   P   Y
            310         320         330         340         350         360         370         380         390

AC TTT GAC TAC TGG GGC CAA GGG ACC ACG GTC ACC GTC TCG AGT GCC TCC ACC AAG GGC CCA TCG GTC TTC CCC CTG GCA CCC TCC TCC AAG AGC ACC TC  < 500
Y   F   D   Y   W   G   Q   G   T   T   V   T   V   S   S   A   S   T   K   G   P   S   V   F   P   L   A   P   S   S   K   S   T   S
            410         420         430         440         450         460         470         480         490

T GGG GGC ACA GCG GCC CTG GGC TGC CTG GTC AAG GAC TAC TTC CCC GAA CCG GTG ACG GTG TCG TGG AAC TCA GGC GCC CTG ACC AGC GGC GTG CAC ACC  < 600
  G   G   T   A   A   L   G   C   L   V   K   D   Y   F   P   E   P   V   T   V   S   W   N   S   G   A   L   T   S   G   V   H   T
            510         520         530         540         550         560         570         580         590

TTC CCG GCT GTC CTA CAG TCC TCA GGA CTC TAC TCC CTC AGC AGC GTG GTG ACC GTG CCC TCC AGC AGC TTG GGC ACC CAG ACC TAC ATC TGC AAC GTG A  < 700
 F   P   A   V   L   Q   S   S   G   L   Y   S   L   S   S   V   V   T   V   P   S   S   S   L   G   T   Q   T   Y   I   C   N   V
            610         620         630         640         650         660         670         680         690

AT CAC AAG CCC AGC AAC ACC AAG GTG GAC AAA CGC GTT GAG CCC AAA TCT TGT GAC AAA ACT CAC ACA TGC CCA CCG TGC CCA GCA CCT GAA CTC CTG GG  < 800
N   H   K   P   S   N   T   K   V   D   K   R   V   E   P   K   S   C   D   K   T   H   T   C   P   P   C   P   A   P   E   L   L   G
            710         720         730         740         750         760         770         780         790

G GGA CCG TCA GTC TTC CTC TTC CCC CCA AAA CCC AAG GAC ACC CTC ATG ATC TCC CGG ACC CCT GAG GTC ACA TGC GTG GTG GTG GAC GTG AGC CAC GAA  < 900
  G   P   S   V   F   L   F   P   P   K   P   K   D   T   L   M   I   S   R   T   P   E   V   T   C   V   V   V   D   V   S   H   E
            810         820         830         840         850         860         870         880         890

GAC CCT GAG GTC AAG TTC AAC TGG TAC GTG GAC GGC GTG GAG GTG CAT AAT GCC AAG ACA AAG CCG CGG GAG GAG CAG TAC AAC AGC ACG TAC CGG GTG G  < 1000
 D   P   E   V   K   F   N   W   Y   V   D   G   V   E   V   H   N   A   K   T   K   P   R   E   E   Q   Y   N   S   T   Y   R   V
            910         920         930         940         950         960         970         980         990

TC AGC GTC CTC ACC GTC CTG CAC CAG GAC TGG CTG AAT GGC AAG GAG TAC AAG TGC AAG GTC TCC AAC AAA GCC CTC CCA GCC CCC ATC GAG AAA ACC AT  < 1100
V   S   V   L   T   V   L   H   Q   D   W   L   N   G   K   E   Y   K   C   K   V   S   N   K   A   L   P   A   P   I   E   K   T   I
            1010        1020        1030        1040        1050        1060        1070        1080        1090

C TCC AAA GCC AAA GGG CAG CCC CGA GAA CCA CAG GTG TAC ACC CTG CCC CCA TCC CGG GAT GAG CTG ACC AAG AAC CAG GTC AGC CTG ACC TGC CTG GTC  < 1200
  S   K   A   K   G   Q   P   R   E   P   Q   V   Y   T   L   P   P   S   R   D   E   L   T   K   N   Q   V   S   L   T   C   L   V
            1110        1120        1130        1140        1150        1160        1170        1180        1190

AAA GGC TTC TAT CCC AGC GAC ATC GCC GTG GAG TGG GAG AGC AAT GGG CAG CCG GAG AAC AAC TAC AAG ACC ACG CCT CCC GTG CTG GAC TCC GAC GGC T  < 1300
 K   G   F   Y   P   S   D   I   A   V   E   W   E   S   N   G   Q   P   E   N   N   Y   K   T   T   P   P   V   L   D   S   D   G
            1210        1220        1230        1240        1250        1260        1270        1280        1290

CC TTC TTC CTC TAC AGC AAG CTC ACC GTG GAC AAG AGC AGG TGG CAG CAG GGG AAC GTC TTC TCA TGC TCC GTG ATG CAT GAG GCT CTG CAC AAC CAC TA  < 1400
S   F   F   L   Y   S   K   L   T   V   D   K   S   R   W   Q   Q   G   N   V   F   S   C   S   V   M   H   E   A   L   H   N   H   Y
            1310        1320        1330        1340        1350        1360        1370        1380        1390

C ACG CAG AAG AGC CTC TCC CTG TCT CCG GGT AAA TAA ...
  T   Q   K   S   L   S   L   S   P   G   K   *
            1410        1420        1430
```

IgG CEA – Light chain

```
ATG GAG ACA GAC ACA CTC CTG CTA TGG GTA CTG CTG CTC TGG GTT CCA GGT TCC ACT GGT GAC GCG GCC CAG CCG GCC GAC ATC GAG CTC ACC CAG TCT C  < 100
 M   E   T   D   T   L   L   L   W   V   L   L   L   W   V   P   G   S   T   G   D   A   A   Q   P   A   D   I   E   L   T   Q   S
           10          20          30          40          50          60          70          80          90

CA GCA ATC ATG TCT GCA TCT CCA GGG GAG AAA GTC ACC ATA ACC TGC AGT GCC AGC TCA AGT GTA AGT TAC ATG CAC TGG TTC CAG CAG AAG CCA GGC AC  < 200
P   A   I   M   S   A   S   P   G   E   K   V   T   I   T   C   S   A   S   S   S   V   S   Y   M   H   W   F   Q   Q   K   P   G   T
           110         120         130         140         150         160         170         180         190

T TCT CCC AAA CTC TGG ATT TAT AGC ACA TCC AAC CTG GCT TCT GGA GTC CCT GCT CGC TTC AGT GGC AGT GGA TCT GGG ACC TCT TAC TCT CTC ACA ATC  < 300
  S   P   K   L   W   I   Y   S   T   S   N   L   A   S   G   V   P   A   R   F   S   G   S   G   S   G   T   S   Y   S   L   T   I
           210         220         230         240         250         260         270         280         290

AGC CGA ATG GAG GCT GAA GAT GCT GCC ACT TAT TAC TGC CAG CAA AGG AGT AGT TAC CCA CTC ACG TTC GGT GCT GGC ACC AAG CTG GAG CTG AAA CGG A  < 400
 S   R   M   E   A   E   D   A   A   T   Y   Y   C   Q   Q   R   S   S   Y   P   L   T   F   G   A   G   T   K   L   E   L   K   R
           310         320         330         340         350         360         370         380         390

CT GTG GGC GCG CCA TCT GTC TTC ATC TTC CCG CCA TCT GAT GAG CAG TTG AAA TCT GGA ACT GCC TCT GTT GTG TGC CTG CTG AAT AAC TTC TAT CCC AG  < 500
  T   V   G   A   P   S   V   F   I   F   P   P   S   D   E   Q   L   K   S   G   T   A   S   V   V   C   L   L   N   N   F   Y   P   R
             410         420         430         440         450         460         470         480         490

A GAG GCC AAA GTA CAG TGG AAG GTG GAT AAC GCC CTC CAA TCG GGT AAC TCC CAG GAG AGT GTC ACA GAG CAG GAC AGC AAG GAC AGC ACC TAC AGC CTC  < 600
    E   A   K   V   Q   W   K   V   D   N   A   L   Q   S   G   N   S   Q   E   S   V   T   E   Q   D   S   K   D   S   T   Y   S   L
             510         520         530         540         550         560         570         580         590

AGC AGC ACC CTG ACG CTG AGC AAA GCA GAC TAC GAG AAA CAC AAA GTC TAC GCC TGC GAA GTC ACC CAT CAG GGC CTG AGC TCG CCC GTC ACA AAG AGC T  < 700
 S   S   T   L   T   L   S   K   A   D   Y   E   K   H   K   V   Y   A   C   E   V   T   H   Q   G   L   S   S   P   V   T   K   S
           610         620         630         640         650         660         670         680         690

TC AAC AGG GGA GAG TGT TAA ...
F   N   R   G   E   C   *
           710         720
```

scFv-Fc

```
ATG GAG ACA GAC ACA CTC CTG CTA TGG GTA CTG CTG CTC TGG GTT CCA GGT TCC ACT GGT GAC GCG GCC CAG CCG GCC ATG GCC CAG GTG AAA CTG CAG C  < 100
 M   E   T   D   T   L   L   L   W   V   L   L   L   W   V   P   G   S   T   G   D   A   A   Q   P   A   M   A   Q   V   K   L   Q
           10          20          30          40          50          60          70          80          90

AG TCT GGG GCA GAA CTT GTG AGG TCA GGG ACC TCA GTC AAG TTG TCC TGC ACA GCT TCT GGC TTC AAC ATT AAA GAC TCC TAT ATG CAC TGG TTG AGG CA  < 200
Q   S   G   A   E   L   V   R   S   G   T   S   V   K   L   S   C   T   A   S   G   F   N   I   K   D   S   Y   M   H   W   L   R   Q
           110         120         130         140         150         160         170         180         190

G GGG CCT GAA CAG GGC CTG GAG TGG ATT GGA TGG ATT GAT CCT GAG AAT GGT GAT ACT GAA TAT GCC CCG AAG TTC CAG GGC AAG GCC ACT TTT ACT ACA  < 300
  G   P   E   Q   G   L   E   W   I   G   W   I   D   P   E   N   G   D   T   E   Y   A   P   K   F   Q   G   K   A   T   F   T   T
             210         220         230         240         250         260         270         280         290

GAC ACA TCC TCC AAC ACA GCC TAC CTG CAG CTC AGC AGC CTG ACA TCT GAG GAC ACT GCC GTC TAT TAT TGT AAT GAG GGG ACT CCG ACT GGG CCG TAC T  < 400
 D   T   S   S   N   T   A   Y   L   Q   L   S   S   L   T   S   E   D   T   A   V   Y   Y   C   N   E   G   T   P   T   G   P   Y
           310         320         330         340         350         360         370         380         390

AC TTT GAC TAC TGG GGC CAA GGG ACC ACG GTC ACC GTC TCC TCA GGT GGA GGC GGT TCA GGG GGA GGT GGA TCC GGT GGA GGC GGT TCA GAC ATC GAG CT  < 500
Y   F   D   Y   W   G   Q   G   T   T   V   T   V   S   S   G   G   G   G   S   G   G   G   G   S   G   G   G   G   S   D   I   E   L
           410         420         430         440         450         460         470         480         490

C ACC CAG TCT CCA GCA ATC ATG TCT GCA TCT CCA GGG GAG AAA GTC ACC ATA ACC TGC AGT GCC AGC TCA AGT GTA AGT TAC ATG CAC TGG TTC CAG CAG  < 600
  T   Q   S   P   A   I   M   S   A   S   P   G   E   K   V   T   I   T   C   S   A   S   S   S   V   S   Y   M   H   W   F   Q   Q
             510         520         530         540         550         560         570         580         590

AAG CCA GGC ACT TCT CCC AAA CTC TGG ATT TAT AGC ACA TCC AAC CTG GCT TCT GGA GTC CCT GCT CGC TTC AGT GGC AGT GGA TCT GGG ACC TCT TAC T  < 700
 K   P   G   T   S   P   K   L   W   I   Y   S   T   S   N   L   A   S   G   V   P   A   R   F   S   G   S   G   S   G   T   S   Y
           610         620         630         640         650         660         670         680         690

CT CTC ACA ATC AGC CGA ATG GAG GCT GAA GAT GCT GCC ACT TAT TAC TGC CAG CAA AGG AGT AGT TAC CCA CTC ACG TTC GGT GCT GGC ACC AAG CTG GA  < 800
S   L   T   I   S   R   M   E   A   E   D   A   A   T   Y   Y   C   Q   Q   R   S   S   Y   P   L   T   F   G   A   G   T   K   L   E
           710         720         730         740         750         760         770         780         790

G CTG AAA CGG GCg gcc GCA GAC AAA ACT CAC ACA TGC CCA CCG TGC CCA GCA CCT GAA CTC CTG GGG GGA ...
  L   K   R   A   A   A   D   K   T   H   T   C   P   P   C   P   A   P   E   L   L   G   G ...
           810         820         830         840         850         860         870
```

scDb-Fc

```
ATG GAG ACA GAC ACA CTC CTG CTA TGG GTA CTG CTG CTC TGG GTT CCA GGT TCC ACT GGT GAC GCG GCC Cag cCG GCC ATG GCC CAG GTG AAA CTG CAG C  < 100
 M   E   T   D   T   L   L   L   W   V   L   L   L   W   V   P   G   S   T   G   D   A   A   Q   P   A   M   A   Q   V   K   L   Q
            10          20          30          40          50          60          70          80          90

AG TCT GGG GCA GAA CTT GTG AGG TCA GGG ACC TCA GTC AAG TTG TCC TGC ACA GCT TCT GGC TTC AAC ATT AAA GAC TCC TAT ATG CAC TGG TTG AGG CA  < 200
Q   S   G   A   E   L   V   R   S   G   T   S   V   K   L   S   C   T   A   S   G   F   N   I   K   D   S   Y   M   H   W   L   R   Q
            110         120         130         140         150         160         170         180         190

G GGG CCT GAA CAG GGC CTG GAG TGG ATT GGA TGG ATT GAT CCT GAG AAT GGT GAT ACT GAA TAT GCC CCG AAG TTC CAG GGC AAG GCC ACT TTT ACT ACA  < 300
  G   P   E   Q   G   L   E   W   I   G   W   I   D   P   E   N   G   D   T   E   Y   A   P   K   F   Q   G   K   A   T   F   T   T
            210         220         230         240         250         260         270         280         290

GAC ACA TCC TCC AAC ACA GCC TAC CTG CAG CTC AGC AGC CTG ACA TCT GAG GAC ACT GCC GTC TAT TAT TGT AAT GAG GGG ACT CCG ACT GGG CCG TAC T  < 400
 D   T   S   S   N   T   A   Y   L   Q   L   S   S   L   T   S   E   D   T   A   V   Y   Y   C   N   E   G   T   P   T   G   P   Y
            310         320         330         340         350         360         370         380         390

AC TTT GAC TAC TGG GGC CAA GGG ACC ACG GTC ACC GTC TCC TCA GGC GGT GGC GGA TCG GAT ATC CAG ATG ACC CAG TCC CCG AGT TCC CTG TCC GCC TC  < 500
Y   F   D   Y   W   G   Q   G   T   T   V   T   V   S   S   G   G   G   G   S   D   I   Q   M   T   Q   S   P   S   S   L   S   A   S
            410         420         430         440         450         460         470         480         490

T GTG GGC GAT AGA GTC ACC ATC ACC TGT CGT GCC AGT CAG GAC ATC CGT AAT TAT CTG AAC TGG TAT CAA CAG AAA CCA GGA AAA GCT CCG AAA CTA CTG  < 600
  V   G   D   R   V   T   I   T   C   R   A   S   Q   D   I   R   N   Y   L   N   W   Y   Q   Q   K   P   G   K   A   P   K   L   L
            510         520         530         540         550         560         570         580         590

ATT TAC TAT ACC TCC CGC CTG GAG TCT GGA GTC CCT TCT CGC TTC TCT GGT TCT GGT TCT GGG ACG GAT TAC ACT CTC ACC ATC AGC AGT CTG CAA CCG G  < 700
 I   Y   Y   T   S   R   L   E   S   G   V   P   S   R   F   S   G   S   G   S   G   T   D   Y   T   L   T   I   S   S   L   Q   P
            610         620         630         640         650         660         670         680         690

AG GAC TTC GCA ACC TAT TAC TGT CAG CAA GGT AAT ACT CTG CCG TGG ACG TTC GGA CAG GGC ACC AAG GTG GAG ATC AAA CGT GGA GGC GGT GGC AGC GG  < 800
E   D   F   A   T   Y   Y   C   Q   Q   G   N   T   L   P   W   T   F   G   Q   G   T   K   V   E   I   K   R   G   G   G   G   S   G
            710         720         730         740         750         760         770         780         790

T GGG CGC GCC TCG GGC GGA GGT GGC TCA GAG GTT CAG CTG GTG GAG TCT GGC GGT GGC CTG GTG CAG CCA GGG GGC TCA CTC CGT TTG TCC TGT GCA GCT  < 900
  G   R   A   S   G   G   G   G   S   E   V   Q   L   V   E   S   G   G   G   L   V   Q   P   G   G   S   L   R   L   S   C   A   A
            810         820         830         840         850         860         870         880         890

TCT GGC TAC TCC TTT ACC GGC TAC ACT ATG AAC TGG GTG CGT CAG GCC CCA GGT AAG GGC CTG GAA TGG GTT GCA CTG ATT AAT CCT TAT AAA GGT GTT T  < 1000
 S   G   Y   S   F   T   G   Y   T   M   N   W   V   R   Q   A   P   G   K   G   L   E   W   V   A   L   I   N   P   Y   K   G   V
            910         920         930         940         950         960         970         980         990

CC ACC TAT AAC CAG AAA TTC AAG GAT CGT TTC ACG ATA TCC GTA GAT AAA TCC AAA AAC ACA GCC TAC CTG CAA ATG AAC AGC CTG CGT GCT GAG GAC AC  < 1100
S   T   Y   N   Q   K   F   K   D   R   F   T   I   S   V   D   K   S   K   N   T   A   Y   L   Q   M   N   S   L   R   A   E   D   T
            1010        1020        1030        1040        1050        1060        1070        1080        1090

T GCA GTC TAT TAT TGT GCT AGA AGC GGA TAC TAC GGC GAT AGC GAC TGG TAT TTT GAC GTC TGG GGT CAA GGA ACC CTA GTC ACC GTC TCC TCG GGA GGC  < 1200
  A   V   Y   Y   C   A   R   S   G   Y   Y   G   D   S   D   W   Y   F   D   V   W   G   Q   G   T   L   V   T   V   S   S   G   G
            1110        1120        1130        1140        1150        1160        1170        1180        1190

GGG GGT TCG GAC ATC GAG CTC ACC CAG TCT CCA GCC ATC ATG TCT GCA TCT CCA GGG GAG AAG GTC ACC ATA ACC TGC AGT GCC AGC TCA AGT GTA AGT T  < 1300
 G   G   S   D   I   E   L   T   Q   S   P   A   I   M   S   A   S   P   G   E   K   V   T   I   T   C   S   A   S   S   S   V   S
            1210        1220        1230        1240        1250        1260        1270        1280        1290

AC ATG CAC TGG TTC CAG CAG AAG CCA GGC ACT TCT CCC AAA CTC TGG ATT TAT AGC ACA TCC AAC CTG GCT TCT GGA GTC CCT GCT CGC TTC AGT GGC AG  < 1400
Y   M   H   W   F   Q   Q   K   P   G   T   S   P   K   L   W   I   Y   S   T   S   N   L   A   S   G   V   P   A   R   F   S   G   S
            1310        1320        1330        1340        1350        1360        1370        1380        1390

T GGA TCT GGG ACC TCT TAC TCT CTC ACA ATC AGC CGA ATG GAG GCT GAA GAT GCT GCC ACT TAT TAC TGC CAG CAA AGG AGT AGT TAC CCA CTC ACG TTC  < 1500
  G   S   G   T   S   Y   S   L   T   I   S   R   M   E   A   E   D   A   A   T   Y   Y   C   Q   Q   R   S   S   Y   P   L   T   F
            1410        1420        1430        1440        1450        1460        1470        1480        1490

GGT GCT GGC ACC AAG CTG GAG CTG AAA CGG GCg gcc GCA GAC AAA ACT CAC ACA TGC CCA CCG TGC CCA GCA CCT GAA CTC CTG GGG GGA ...
 G   A   G   T   K   L   E   L   K   R   A   A   A   D   K   T   H   T   C   P   P   C   P   A   P   E   L   L   G   G ...
            1510        1520        1530        1540        1550        1560        1570        1580        1590
```

scFv-scCLCH1-Fc

```
ATG GAG ACA GAC ACA CTC CTG CTA TGG GTA CTG CTG CTC TGG GTT CCA GGT TCC ACT GGT GAC GCG GCC CAG CCG GCC ATG GCC CAG GTG AAA CTG CAG C  < 100
 M   E   T   D   T   L   L   L   W   V   L   L   L   W   V   P   G   S   T   G   D   A   A   Q   P   A   M   A   Q   V   K   L   Q
            10          20          30          40          50          60          70          80          90

AG TCT GGG GCA GAA CTT GTG AGG TCA GGG ACC TCA GTC AAG TTG TCC TGC ACA GCT TCT GGC TTC AAC ATT AAA GAC TCC TAT ATG CAC TGG TTG AGG CA  < 200
Q   S   G   A   E   L   V   R   S   G   T   S   V   K   L   S   C   T   A   S   G   F   N   I   K   D   S   Y   M   H   W   L   R   Q
            110         120         130         140         150         160         170         180         190

G GGG CCT GAA CAG GGC CTG GAG TGG ATT GGA TGG ATT GAT CCT GAG AAT GGT GAT ACT GAA TAT GCC CCG AAG TTC CAG GGC AAG GCC ACT TTT ACT ACA  < 300
  G   P   E   Q   G   L   E   W   I   G   W   I   D   P   E   N   G   D   T   E   Y   A   P   K   F   Q   G   K   A   T   F   T   T
            210         220         230         240         250         260         270         280         290

GAC ACA TCC TCC AAC ACA GCC TAC CTG CAG CTC AGC AGC CTG ACA TCT GAG GAC ACT GCC GTC TAT TAT TGT AAT GAG GGG ACT CCG ACT GGG CCG TAC T  < 400
 D   T   S   S   N   T   A   Y   L   Q   L   S   S   L   T   S   E   D   T   A   V   Y   Y   C   N   E   G   T   P   T   G   P   Y
            310         320         330         340         350         360         370         380         390

AC TTT GAC TAC TGG GGC CAA GGG ACC ACG GTC ACC GTC TCC TCA GGT GGA GGC GGT TCA GGG GGA GGT GGA TCC GGT GGA GGC GGT TCA GAC ATC GAG CT  < 500
Y   F   D   Y   W   G   Q   G   T   T   V   T   V   S   S   G   G   G   G   S   G   G   G   G   S   G   G   G   G   S   D   I   E   L
            410         420         430         440         450         460         470         480         490

C ACC CAG TCT CCA GCA ATC ATG TCT GCA TCT CCA GGG GAG AAA GTC ACC ATA ACC TGC AGT GCC AGC TCA AGT GTA AGT TAC ATG CAC TGG TTC CAG CAG  < 600
  T   Q   S   P   A   I   M   S   A   S   P   G   E   K   V   T   I   T   C   S   A   S   S   S   V   S   Y   M   H   W   F   Q   Q
            510         520         530         540         550         560         570         580         590

AAG CCA GGC ACT TCT CCC AAA CTC TGG ATT TAT AGC ACA TCC AAC CTG GCT TCT GGA GTC CCT GCT CGC TTC AGT GGC AGT GGA TCT GGG ACC TCT TAC T  < 700
 K   P   G   T   S   P   K   L   W   I   Y   S   T   S   N   L   A   S   G   V   P   A   R   F   S   G   S   G   S   G   T   S   Y
            610         620         630         640         650         660         670         680         690

CT CTC ACA ATC AGC CGA ATG GAG GCT GAA GAT GCT GCC ACT TAT TAC TGC CAG CAA AGG AGT AGT TAC CCA CTC ACG TTC GGT GCT GGC ACC AAG CTG GA  < 800
S   L   T   I   S   R   M   E   A   E   D   A   A   T   Y   Y   C   Q   Q   R   S   S   Y   P   L   T   F   G   A   G   T   K   L   E
            710         720         730         740         750         760         770         780         790

G CTG AAA Cgt acG GTG GCA GCG CCA TCT GTC TTC ATC TTC CCG CCA TCT GAT GAG CAG TTG AAA TCT GGA ACT GCC TCT GTT GTG TGC CTG CTG AAT AAC  < 900
  L   K   R   T   V   A   A   P   S   V   F   I   F   P   P   S   D   E   Q   L   K   S   G   T   A   S   V   V   C   L   L   N   N
            810         820         830         840         850         860         870         880         890

TTC TAT CCC AGA GAG GCC AAA GTA CAG TGG AAG GTG GAT AAC GCC CTC CAA TCG GGT AAC TCC CAG GAG AGT GTC ACA GAG CAG GAC AGC AAG GAC AGC A  < 1000
 F   Y   P   R   E   A   K   V   Q   W   K   V   D   N   A   L   Q   S   G   N   S   Q   E   S   V   T   E   Q   D   S   K   D   S
            910         920         930         940         950         960         970         980         990

CC TAC AGC CTC AGC AGC ACC CTG ACG CTG AGC AAA GCA GAC TAC GAG AAA CAC AAA GTC TAC GCC TGC GAA GTC ACC CAT CAG GGC CTG AGC TCG CCC GT  < 1100
T   Y   S   L   S   S   T   L   T   L   S   K   A   D   Y   E   K   H   K   V   Y   A   C   E   V   T   H   Q   G   L   S   S   P   V
            1010        1020        1030        1040        1050        1060        1070        1080        1090

C ACA AAG AGC TTC AAC AGG GGA GAG TGT GGA GGC GGT GGG TCA GGG GGC GGT GGA TCC GGG GGA GGC GGT TCA GGA GGC GGT GGG AGT GCC TCC ACC AAG  < 1200
  T   K   S   F   N   R   G   E   C   G   G   G   G   S   G   G   G   G   S   G   G   G   G   S   G   G   G   G   S   A   S   T   K
            1110        1120        1130        1140        1150        1160        1170        1180        1190

GGC CCA TCG GTC TTC CCC CTG GCA CCC TCC TCC AAG AGC ACC TCT GGG GGC ACA GCG GCC CTG GGC TGC CTG GTC AAG GAC TAC TTC CCC GAA CCG GTG A  < 1300
 G   P   S   V   F   P   L   A   P   S   S   K   S   T   S   G   G   T   A   A   L   G   C   L   V   K   D   Y   F   P   E   P   V
            1210        1220        1230        1240        1250        1260        1270        1280        1290

CG GTG TCG TGG AAC TCA GGC GCC CTG ACC AGC GGC GTG CAC ACC TTC CCG GCT GTC CTA CAG TCC TCA GGA CTC TAC TCC CTC AGC AGC GTG GTG ACC GT  < 1400
T   V   S   W   N   S   G   A   L   T   S   G   V   H   T   F   P   A   V   L   Q   S   S   G   L   Y   S   L   S   S   V   V   T   V
            1310        1320        1330        1340        1350        1360        1370        1380        1390

G CCC TCC AGC AGC TTG GGC ACC CAG ACC TAC ATC TGC AAC GTG AAT CAC AAG CCC AGC AAC ACC AAG GTG GAC AAA CGC GTT GAG CCC AAA TCT TGT GCg  < 1500
  P   S   S   S   L   G   T   Q   T   Y   I   C   N   V   N   H   K   P   S   N   T   K   V   D   K   R   V   E   P   K   S   C   A
            1410        1420        1430        1440        1450        1460        1470        1480        1490

gcc GCA GAC AAA ACT CAC ACA TGC CCA CCG TGC CCA GCA CCT GAA CTC CTG GGG GGA ...
 A   A   D   K   T   H   T   C   P   P   C   P   A   P   E   L   L   G   G ...
            1510        1520        1530        1540        1550
```

Acknowledgements

First of all, I want to thank Prof Roland Kontermann for the excellent supervision of my thesis and for always sparing time for the discussion of news or troubles.

I also would like to thank Prof Klaus Pfizenmaier for giving me the opportunity to work at the IZI and for being second reviewer of this thesis.

I am very grateful to Prof Oliver Kohlbacher and his team from the University of Tübingen, in particular Magdalena Feldhahn and Pierre Dönnes, for performing the *in silico* investigation of the deimmunization in this project.

Special thanks go to all former and present members of the Kontermann lab group, especially Aline, Nadine, Dafne and Ronny for all the support and generation of great atmosphere in the lab and during our other activities. Thanks are also due to the girls from the animal facility, in particular to Alex. I owe extraordinary gratitude to my dear friends Meike, Sina, Fabi and Oli for sharing thoughts, bursts of laughter, equipment, drinks and much more during the lab time and far beyond.

My deepest thanks to my parents, my sister and the rest of my family for the continuous support and care, not only during the time of my thesis. Most important, I want to thank Jasmin for her love, affection and patience during the whole time.

Declaration

I hereby declare that this work has been prepared exclusively by me without any illegitimate help. All sources used have been quoted adequately.

Felix Unverdorben

Tuesday, August 25, 2015

Curriculum vitae

Name:	Felix Unverdorben
Address:	Immenhofer Straße 53, 70180 Stuttgart, Germany
Birthday:	January 24, 1986
Birthplace:	Immenstadt im Allgäu, Germany
Nationality:	German
E-mail:	Felix.Unverdorben@gmail.com

Professional career and education

Since 07/2015	Scientist at *immatics* biotechnologies GmbH, Tübingen
07/2011 – 12/2014	PhD student at the University of Stuttgart, Institute of Cell Biology and Immunology in the Biomedical Engineering laboratory of Prof Roland Kontermann: Immunoglobulin-based strategies for half-life extension of recombinant proteins: Affinity maturation, deimmunization and application.
03/2011 – 04/2011	TEXUS-49 mission in Kiruna/Sweden: Signal transduction in immune cells during microgravity (SITI-1)
10/2005 – 03/2011	Diploma in Technical Biology at the University of Stuttgart Main subject: Antibody Engineering and Immunology Final grade: 1.0
03/2010 – 03/2011	Diploma thesis at the University of Stuttgart, Biomedical engineering group of Prof Roland Kontermann concerning the half-life extension of recombinant antibody molecules
11/2010	Internship at the University of Zurich (Switzerland) at the Institute of Anatomy in the laboratory for Space Biotechnology of Prof Oliver Ullrich for the 16th DLR Parabolic Flight Campaign
06/2010 – 07/2010	Training for the handling of laboratory animals
03/2009 – 09/2009	Research project at the University of California – San Francisco (USA), Department of Microbiology and Immunology in the laboratory of Prof Philipp Coffino
01/2008 – 03/2009	Industrial internship at TSE-Labor GmbH & Co.KG. in Kornwestheim preparing tissue samples for ELISA based bovine spongiform encephalopathy (BSE) and scrapie tests (Biosafety level S2) according to GLP requirements
09/1996 – 07/2005	Abitur at Gymnasium Immenstadt Final grade: 1.8